Investigations on anti-IGF-1R therapy response in a colorectal cancer cell line panel

Jens Puschhof

Lady Margaret Hall

Submitted as final thesis for the Master of Science by Research in Oncology programme at the University of Oxford

Trinity Term 2016

Word count: 19,778

Abstract

Jens Puschhof
Lady Margaret Hall

Submitted as final thesis for the Master of Science by Research in Oncology
Trinity Term 2016

Investigations on anti-IGF-1R therapy response in a colorectal cancer cell line panel

Therapies targeting the type 1 insulin like growth factor receptor (IGF-1R) have so far failed to show significant benefit for colorectal cancer (CRC) patients in large clinical trials, emphasising the importance of identifying biomarkers for therapy response and developing rational combination therapies.

In this thesis, a large panel of 82 colorectal cancer cell lines was used to discover and validate associations between anti-IGF-1R therapy response, gene mutations and gene expression.

Mutations in *PIK3CA* exon 9 and 20 were found to be associated with resistance to inhibition with the tyrosine kinase inhibitor OSI-906 and the monoclonal antibody figitumumab. In a number of *PIK3CA* wild type cell lines, combination therapy with OSI-906 and the pan-Akt inhibitor GSK690693 yielded synergistic effects. *PIK3CA* wild type cell lines resistant to this combination therapy are characterised by *KRAS* mutations, a low expression of the cell surface protein CD24, and Akt-independent GSK-3β phosphorylation.

In summary, the findings of this thesis indicate an important role of the PI3K/Akt signalling pathway in anti-IGF-1R response in CRC. We have identified *PIK3CA* mutations as a biomarker for anti-IGF-1R therapy resistance in CRC. Furthermore, our study demonstrates a synergistic effect of the combination of OSI-906 with a pan-Akt inhibitor in a molecularly defined subgroup of CRC cell lines.

Acknowledgements

I would like to express my gratitude to Sir Walter Bodmer for making my work in his group possible and contributing continuously to the development of this project.

My special thanks go to Dr. Djamila Ouaret, who was the leading researcher in the design and execution of the IGF-1R project in the Bodmer laboratory before I joined the group. Her sustained and competent supervision have enabled me to grow with this project. I am grateful to Dr. Bodmer and Dr. Ouaret for extensive discussion and valuable input concerning the scientific content and shape of this thesis.

Furthermore, I would like to acknowledge the current and previous members of the Bodmer lab for providing a very enjoyable and productive working environment and helping me on a scientific, experimental and personal level at all times. I am especially grateful to the researchers and students involved in generating the anti-IGF-1R therapy response data and collecting mutation and expression data over the years.

I would like to also acknowledge the Studienstiftung des Deutschen Volkes, which has supported me for the time of my studies and without which my Master's studies in Oxford would not have been possible.

Finally, I want to express my deep gratitude to my parents, my sister and Maria, whose support and encouragement has helped me throughout my studies.

Author's declaration

The work presented in this thesis was performed in the Cancer and Immunogenetics laboratory in the Weatherall Institute of Molecular Medicine, Oxford. It is entirely my own work, except for the cases where acknowledgement is made, and has not been submitted for another degree at this or another university.

Table of contents

Abstract ..... **i**

Acknowledgements ..... **ii**

Author's declaration ..... **iii**

Table of contents ..... **iv**

List of figures ..... **vii**

List of tables ..... **viii**

Abbreviations ..... **ix**

CHAPTER 1: INTRODUCTION **1**

1.1. Colorectal cancer **1**

1.1.1 Pathogenesis and classification of colorectal cancer 1

1.1.2 Treatment of colorectal cancer 3

1.2. IGF-1R **5**

1.2.1. IGF-1R signalling 6

1.2.2. IGF-1R in cancer 9

1.2.3. Therapeutic strategies targeted at IGF-1R 10

1.3. Project motivation and concept **13**

1.3.1. The Bodmer Cell Line panel 13

1.3.2. Work on IGF-1R in the Bodmer group 15

1.3.3. Project concept 15

CHAPTER 2: MATERIALS AND METHODS **17**

2.1. Materials **17**

2.1.1. Colorectal cancer cell line panel 17

2.1.2. Microarray dataset 21
2.1.3. Mutation dataset 21
2.1.4. Antibodies 22
2.1.5. Laboratory reagents 23
2.1.6. Instruments and Software 25

2.2. Methods 26
2.2.1. Cell culture 26
2.2.2. Cell counting 27
2.2.3. Drug treatments 27
2.2.4. SRB assay 28
2.2.5. Sensitivity and drug interaction analysis 29
2.2.6. Apoptosis induction studies using flow cytometry 30
2.2.7. Protein extraction and Western Blot 31
2.2.8. Surface staining and FACS 33
2.2.9. Colony formation assay 34
2.2.10. siRNA knockdown 34
2.2.11. Statistical tests 35

CHAPTER 3: RESULTS 36

3.1. Characterisation of response to IGF-1R inhibitors across the cell line panel 36

3.2. Identification of genetic factors in anti-IGF-1R resistance 39
3.2.1. *PIK3CA* mutations in exon 9 or 20 are associated with resistance to anti-IGF-1R therapy 39
3.2.2. Differential expression of single genes cannot explain resistance to anti-IGF-1R therapy 43

3.3. Anti-IGF-1R/Akt combination therapy in *PIK3CA* wild type cell lines 44

3.4. Characterisation of anti-IGF-1R/Akt combination therapy sensitive and resistant cell lines 50

3.4.1. *KRAS* mutations are associated with resistance to anti-IGF-1R/Akt combination therapy 51

3.4.2. The signalling effects following inhibition of IGF-1R and Akt 53

3.4.3. CD24 is expressed at lower level on both the mRNA and protein levels in combination therapy resistant *PIK3CA* wild type cell lines 58

3.5. Functional implications of CD24 in IGF-1R-directed therapy response 61

3.6. Knockdown of individual Akt isoforms in combination with anti-IGF-1R therapy 64

CHAPTER 4: DISCUSSION 67

4.1. Anti-IGF-1R response-based classification of cell lines 67

4.2. Predictive factors of anti-IGF-1R response 70

4.3. Sensitisation to anti-IGF-1R therapy by adding an Akt inhibitor 73

4.4. Signalling response to combined anti-IGF-1R/Akt therapy 76

4.5. The role of CD24 in anti-IGF-1R therapy response in CRC 79

4.6. The role of Akt isoforms in anti-IGF-1R therapy response 84

4.7. Conclusion 85

REFERENCES I

SUPPLEMENTARY FIGURES XI

SUPPLEMENTARY TABLES XVI

List of figures

FIGURE 1: THE STRUCTURE OF THE IGF-1R. 5
FIGURE 2: IGF-1R SIGNALLING. 8
FIGURE 3: PROJECT WORKFLOW. 16
FIGURE 4: WORKFLOW OF DRUG INTERACTION ANALYSIS. 30
FIGURE 5: RESPONSE TO ANTI-IGF-1R THERAPEUTICS. 37
FIGURE 6: SENSITIVITY TO FIGITUMUMAB AND OSI-906 IS CORRELATED ACROSS THE CELL LINE PANEL 38
FIGURE 7: ANTI-IGF-1R RESISTANCE IS ASSOCIATED WITH *PIK3CA* MUTATIONS. 41
FIGURE 8: A SUBGROUP OF *PIK3CA* WILD TYPE CELL LINES DISPLAYS SYNERGY OF ANTI-IGF-1R/AKT THERAPY.. 46
FIGURE 9: INHIBITION OF AKT SENSITISES A SUBSET OF CELL LINES TO ANTI-IGF-1R THERAPY.. 48
FIGURE 10: STRONG INDUCTION OF APOPTOSIS AFTER DRUG COMBINATION IS OBSERVED IN SENSITISED, BUT NOT NON-SENSITISED CELL LINES. 50
FIGURE 11: *KRAS* MUTATION IS ASSOCIATED WITH RESISTANCE TO ANTI-IGF-1R/AKT COMBINATION THERAPY 52
FIGURE 12: BASELINE PROTEIN EXPRESSION ACROSS 5 COMBINATION THERAPY RESISTANT AND 5 COMBINATION THERAPY SENSITIVE CELL LINES. 55
FIGURE 13: EFFECTS OF IGF-1R AND AKT INHIBITION ON PI3K AND MAPK SIGNALLING.. .. 57
FIGURE 14: CD24 MRNA IS EXPRESSED AT LOWER LEVEL IN *PIK3CA* WILD TYPE CELL LINES RESISTANT TO COMBINATION TREATMENT. 59
FIGURE 15: CD24 PROTEIN IS EXPRESSED AT LOWER LEVEL IN *PIK3CA* WILD TYPE CELL LINES RESISTANT TO COMBINATION TREATMENT. 60
FIGURE 16: CD24-SORTED SUBPOPULATIONS OF CELL LINES VARY IN RESPONSE TO COMBINATION TREATMENT.. 63
FIGURE 17: KNOCKDOWN OF INDIVIDUAL AKT ISOFORMS INDUCES HETEROGENEOUS SENSITISATION TO OSI-906.. 66
FIGURE 18: CLASSIFICATION OF CRC CELL LINES BASED ON THE FINDINGS OF THIS THESIS. 85

List of tables

TABLE 1: CELL LINES AND SOURCES 17

TABLE 2: ANTIBODIES 22

TABLE 3: LIST OF REAGENTS 23

TABLE 4: INSTRUMENTS 25

TABLE 5: SOFTWARE 26

TABLE 6: *PIK3CA* MUTATION IS ASSOCIATED WITH RESISTANCE TO IGF-1R INHIBITION. 42

TABLE 7: *KRAS* MUTATIONS ARE ASSOCIATED WITH ANTI-IGF-1R/AKT COMBINATION THERAPY RESISTANCE IN *PIK3CA* WILD TYPE CELL LINES. 53

Abbreviations

µM	Micromolar
CIMP	CpG island methylator phenotype
CIN	Chromosomal instability
CO_2	Carbon dioxide
CRC	Colorectal cancer
CST	Cell signalling technologies
EGFR	Epidermal growth factor receptor
FAP	Familial adenomatous polyposis
GSK-3β	Glycogen synthase kinase-3 beta
HNPCC	Heritable nonpolyposis colorectal cancer
IGF-1	Insulin like growth factor 1
IGF-1R	Type 1 insulin like growth factor receptor
IGF-2	Insulin like growth factor 2
IGF-2R	Type 2 insulin like growth factor receptor
IGFBP	IGF binding protein
IR	Insulin receptor
KD	Knock down
mA	Milliampere
mAb	Monoclonal antibody
MAPK	Mitogen-activated protein kinase
MMR	DNA mismatch repair
MSI	Microsatellite instability
PBS	Phosphate buffered saline
PI3K	Phosphoinositide 3-kinase
PIP_3	Phosphatidylinositol-3,4,5-trisphosphate
siRNA	Small interfering RNA
SRB	Sulphorhodamine B
TKI	Tyrosine kinase inhibitor
V	Volt

Chapter 1: Introduction

1.1. Colorectal cancer

Colorectal cancer (CRC) is among the most abundant types of cancer with more than 1.3 million newly diagnosed cases worldwide in 2012 and a mortality of nearly 700,000 in the same year[1]. In this section, the pathogenesis of CRC as well as established and novel treatment approaches for this disease are introduced.

1.1.1 Pathogenesis and classification of colorectal cancer

The development of CRC is characterised by a progression from healthy epithelium over stages of initially benign adenoma to carcinoma[2]. The molecular mechanisms of CRC initiation and progression have been studied extensively, resulting in the identification of a complex pattern of genetic predispositions, somatic mutations, and epigenetic changes, the most important of which are summarised below.

There are two known major inherited conditions leading to a highly increased risk of CRC. In Familial adenomatous polyposis (FAP), a germline mutation in the *APC* gene causes the formation of more than 100 adenomatous polyps, inevitably resulting in development of CRC. This condition is responsible for about 0.5% of all CRC cases[3].

Heritable nonpolyposis colorectal cancer (HNPCC or Lynch syndrome) can be caused by germline mutations in several genes associated with DNA mismatch repair (MMR), contributing 1-3% of CRC cases[4].

The majority of cases of CRC, however, occur sporadically and are classified traditionally through microsatellite instability (MSI) or chromosomal instability (CIN).

Microsatellite instability is defined by variations in repeat numbers of short nucleotide sequences (microsatellites) throughout the genome. It is caused by lacking MMR function as a result of either mutation or epigenetic silencing of MMR genes and is observed in 10-20% of CRC cases[5–7]. The majority of MSI CRC cases have been shown to be associated with a CpG island methylator phenotype (CIMP) and *BRAF* mutations[8].

Chromosomal instability is observed in 50-85% of CRC cases[5,9]. While a variety of mutations can be found in CIN, common patterns of sequential mutations can be observed in the majority of CIN CRCs[2]. Somatic mutation of *APC* represents a key event in colorectal cell transformation[10], leading to an accumulation of β-catenin and thereby an deregulated activation of the Wnt pathway. Mutations in *KRAS* are thought to represent the next step involved in colorectal cancer progression. However, the fact that only about 50% of CRC harbour a *KRAS* mutations[11] indicates that alternative mechanisms exist for this step. Mutation in and chromosomal loss of the regions of tumour suppressor genes such as *TP53*, *SMAD2* and *SMAD4* represents another crucial event in the progression from adenoma to carcinoma[11].

Several aspects should be considered when studying CRC:

Despite many shared features between CRCs of different aetiology, the molecular pathways to CRC are more than alternative causes for the same phenotype. Much more, they are also reflected in cellular and morphological features, such as differentiation[12], shape of adenomatous polyps[5], and treatment response[6,7,13].

However, none of the events described above can be considered necessary or sufficient for the development of CRC. Sets of other mutations which can act both alternatively to and cooperatively with the major events in the pathways of CRC development are found in each case of CRC, overlapping between MSI and CIN. To predict the treatment response of a tumour, it may therefore make sense to consider mutations in relevant signalling proteins rather than the pathway of development[14–16].

Finally, it should be noted that for staging of tumours and many clinical trials, CRC is treated as a single entity irrespective of pathway of development or gene mutation profile. While this facilitates patient recruitment and clinical decisions on choice of treatment, identifying molecular biomarkers holds great promise for better patient selection and treatment design.

In this thesis, this will be approached by investigating drug responses in molecularly defined subsets of cell lines from a large panel of CRC cell lines representing the heterogeneity found in colorectal tumours[17].

1.1.2 Treatment of colorectal cancer

Treatment of colorectal cancer is still mainly based on the three pillars of cancer therapy, making use of combinations of surgery, radiation therapy and conventional chemotherapy. However, drugs targeted at surface receptors of cancer cells have also shown success in the treatment of advanced colorectal cancer[18].

Surgical resection of the primary tumour is the standard treatment for colorectal cancer, exhibiting curative potential in early stages of CRC.

This can be combined with different regimens of chemotherapy, typically comprised of combinations of 5-Fluorouracil, Capecitabine, Oxaliplatin, and Irinotecan. Radiotherapy is an option of particular importance in the treatment of rectal cancer, where it is commonly applied either before or after surgery[19].

Recently, a number of targeted drugs have been approved for use in CRC. Many of these are monoclonal antibodies (mAbs) which block receptors at the surface of CRC cells to interfere with pro-tumorigenic signalling or recruitment of vasculature to the tumour. Notably, it has been suggested that the effect of mAbs in cancer treatment is not only due to inhibition of receptor signalling, but also based on immune-mediated effects through antibody-dependent cellular cytotoxicity (ADCC)[14,20]. mAbs blocking the epidermal growth factor receptor (EGFR), such as cetuximab[15] and panitumumab[21], have shown clinical efficacy. Importantly, these mAbs have been demonstrated to work only in patients wild type for the proto-oncogene *KRAS*, underlining the predictive potential of tumour genetics for treatment response. Other drugs, such as the mAb Bevacizumab and the fusion protein Aflibercept, interfere with the recruitment of vasculature to the tumour through vascular endothelial growth factor (VEGF) action. Regorafenib, on the other hand, is a tyrosine kinase inhibitor (TKI) displaying similar activity as the VEGF-blocking biological.

Numerous compounds targeting a plethora of molecular targets in CRC are in preclinical and clinical development. Significant attention has been paid to the type 1 insulin like growth factor receptor (IGF-1R) as a target for both mAbs and TKIs to treat cancer. Function and signalling of the IGF-1R as well as its role in CRC are introduced in the following section.

1.2. IGF-1R

The IGF-1R is a heterotetrameric cell surface tyrosine kinase receptor consisting of 2 α- and 2 β-subunits (see Figure 1)[22,23]. It is expressed on most cells of the body, with the exception of some cell types such as hepatocytes and mature B-cells[24].

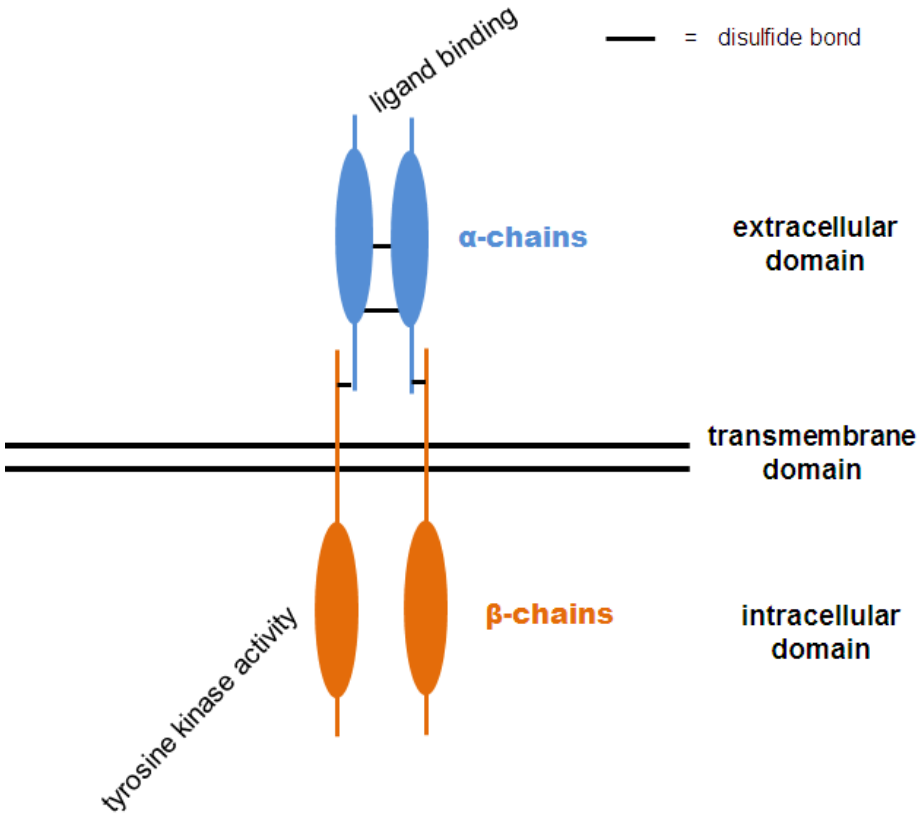

Figure 1: The structure of the IGF-1R.
The IGF-1R is a heterotetrameric complex, consisting of two extracellular α-chains and two partly intracellular and transmembrane β-chains, connected by disulfide bonds. While ligand binding occurs at the alpha chains, the beta chains are responsible the tyrosine kinase activity initiating downstream signalling.

Its structure and binding partners are closely related to two other cell surface receptors: the insulin receptor (IR) and the type 2 insulin like growth factor receptor (IGF-2R). Importantly, IGF-1R is able to bind not only the insulin like growth factor 1 (IGF-1), but also IGF-2 and insulin itself[22]. It therefore competes for insulin with the

IR and for IGF-2 with the IGF-2R and the IR. In contrast to the other two receptors, IGF-1R has been demonstrated to induce a strong mitogenic signal upon ligand binding[23,25]. The presence of the stimulating growth factors is regulated through a number of extracellularly active IGF binding proteins (IGFBPs), but also through IGF-2R, which binds IGF-2 without inducing a mitogenic signal[22]. The action of IGFBPs is in turn regulated through IGFBP proteases[23].

1.2.1. IGF-1R signalling

Activation of the IGF-1R is induced through binding of a ligand to the extracellular α-subunits. This promotes autophosphorylation of tyrosine residues in the kinase domain of the intracellular part of the β-subunits[26], which in turn promotes recruitment of factors to the binding sites in the β-subunits. The major signalling molecules directly downstream of IGF-1R which have been identified are IRS-1, IRS-2 and Shc[26]. While other molecules, such as Grb10, have been described as downstream factors of IGF-1R[22], I am going to focus on the role of the previously mentioned ß-subunit binders in IGF-1R downstream signalling.

IRS-1 and IRS-2 are considered to activate the PI3K pathway by binding the regulatory 85kD subunit of the phosphoinositide 3-kinase (PI3K) and thereby initiating signalling through this axis[22]. Activated PI3K increases the levels of phosphatidylinositol-3,4,5-trisphosphate (PIP_3), which triggers recruitment of the Protein Kinase B (PKB, also commonly referred to as Akt) to the plasma membrane. There, Akt is activated through phosphorylation, primarily conveyed by PDK1 and mTORC2[23]. The activity of Akt is dependent on phosphorylation of two residues, which are Thr308 in the kinase domain and Ser473 in the C-terminal

domain of the protein[27]. Upon recruitment to the cell membrane, the Thr308 residue gets exposed and phosphorylated through PDK1[28], leading to partial activity of Akt. For Akt to reach complete activity, additional phosphorylation of the Ser473 residue by either mTOR or DNA-PK is required[29,30].

Akt in turn phosphorylates a plethora of downstream targets[23]. The effects of activated Akt include inactivation of pro-apoptotic proteins (such as Bad and FOXO family proteins), increased expression of anti-apoptotic proteins (such as NFκB, BCL-xLandBCL2), and regulation of glucose metabolism and protein synthesis (e.g. through TORC). Inhibitory phosphorylation of the glycogen synthase kinase-3 beta (GSK-3β) by Akt is involved in many of the functions described above, such as prevention of apoptosis and glucose metabolism[31].

There are three isoforms of Akt (Akt1, Akt2 and Akt3), which have been demonstrated to play non-redundant roles in healthy cells and cancers[32]. While establishing a clear picture of Akt isoform function is hindered by the multitude of processes triggered by these proteins, mouse knockout studies hint at predominant roles of Akt1 in apoptosis prevention[33], Akt2 in glucose metabolism[34], and Akt3 in brain development[35]. All three isoforms are expressed in both healthy and cancerous colonic tissue[36]. Akt1 and Akt2 have been linked to colorectal tumorigenesis and metastasis[37,38], underlining the importance of isoform specific studies on Akt.

Alternatively to the IRS-mediated PI3K pathway signalling described above, SHC initiates signalling through the mitogen-activated protein kinase (MAPK) pathway upon binding to the phosphorylated ß-subunit of the IGF-1R. This pathway, which signals through Ras, Raf, Mek, Erk and Elk1, is reviewed in[39].

A schematic overview of IGF-1R signalling with a particular focus on the PI3K pathway and proteins of importance in this thesis is depicted in Figure 2.

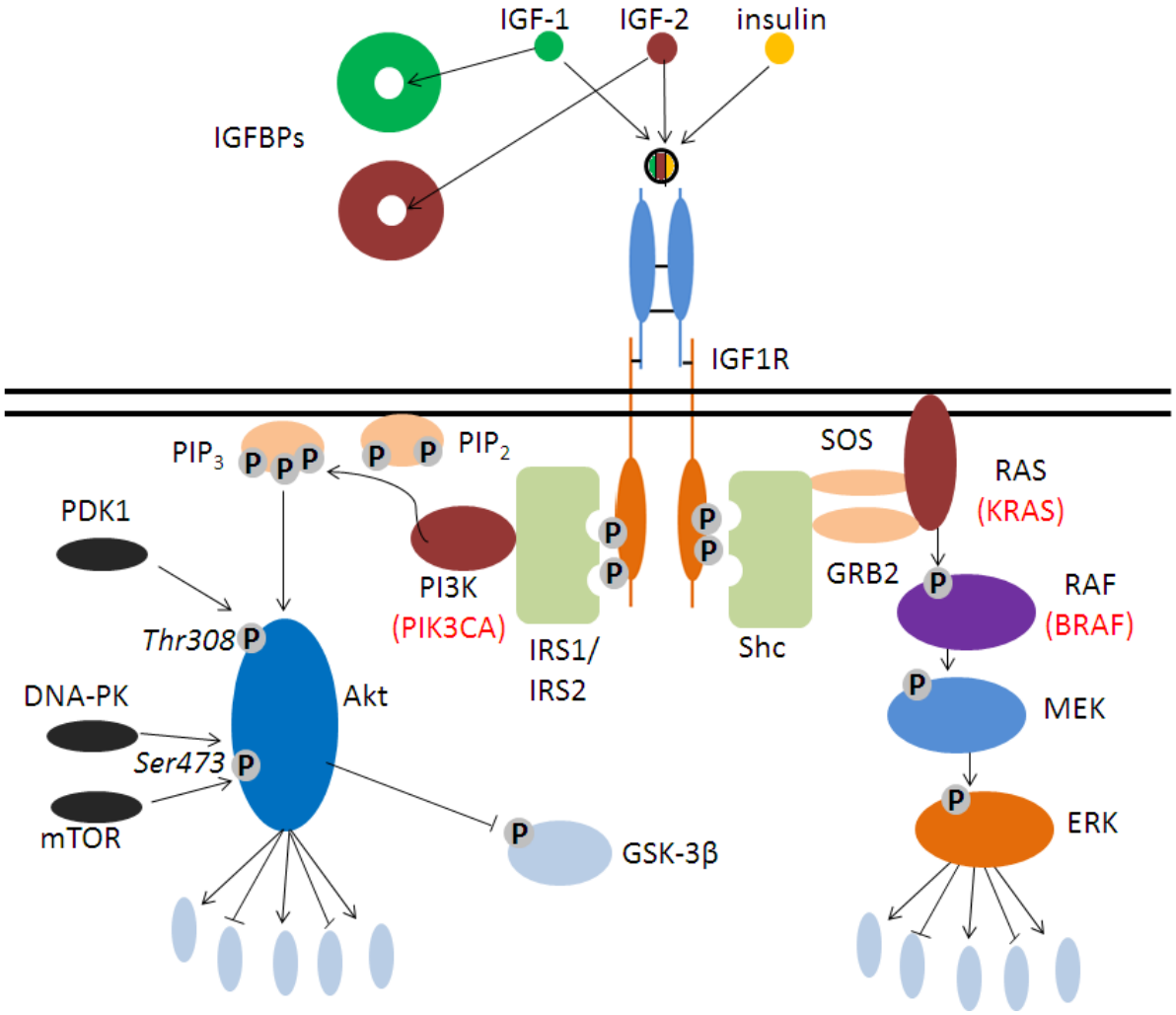

Figure 2: IGF-1R signalling.
Important signalling molecules upstream and downstream of IGF-1R are displayed. Genes commonly mutated in CRC are indicated in red under the corresponding protein, specific phosphorylation sites are depicted in italics. Upon binding of extracellular ligands, to IGF-1R, autophosphorylation of residues in the β-chain triggers binding of adapter proteins to IGF-1R. Binding of Shc to the IGF-1R induces signalling through the Ras/MAPK pathway, which signals through Ras, Raf, and Mek to Erk, which exerts effects on various downstream targets. Recruitment of IRS1/IRS2 to IGF-1R represents the first step to PI3K pathway signalling. Upon binding of PI3K to IRS1 or IRS2, the catalytic subunit of PI3K phosphorylates PIP_2 to PIP_3, triggering recruitment of Akt to the membrane. Akt is in turn activated by phosphorylation of its Thr308 and Ser473 residues, resulting in activating and inhibitory phosphorylation of a plethora of downstream targets, including GSK-3β. *Adapted from* [23].

1.2.2. IGF-1R in cancer

In the light of its involvement in anti-apoptotic and pro-proliferative signalling, it is not surprising that IGF-1R has been studied extensively as to its involvement in cancer initiation and progression. In the following paragraph, the main associations between IGF-1R expression levels and function and cancer are summarised with a particular focus on colorectal cancer.

Seminal studies have demonstrated that the presence of IGF-1R is necessary for the transformation of mouse embryonic fibroblasts through various oncogenes, including but not limited to the Simian Virus 40 T antigen, activated Ras and a variety of growth factor receptors[22,40,41]. This suggests a role for IGF-1R in the early steps of transformation. Indeed, overexpression of IGF1R on fibroblasts has been demonstrated to lead to transformation in both murine and human cells[42]. It is, however, highly questionable if this observation holds true for CRC carcinogenesis, as the mutational profile found in CRC implies the importance of other events in this process.

Furthermore, overexpression of IGF-1R has been described in a variety of cancers, including prostate[43], pancreas[44], melanoma[45], breast[46] and small cell lung cancer[47]. In CRC, the majority of cases (66-96%) show increased expression levels of IGF-1R[48–50] as compared to healthy mucosal tissue. The expression levels tend to increase with disease progression[48] and increasing tumour size[50]. On the other hand, increased levels of circulating IGF-1R ligands have also been found to be associated with colorectal cancer risk and progression[23,51,52].

Beyond its possible involvement in CRC initiation and progression, IGF-1R expression and signalling has been linked to the resistance to therapeutics in CRC

and other cancers[53]. For example, IGF-1R silencing has been demonstrated to lead to increased sensitivity to standard chemotherapeutics in CRC cells, with the multidrug-resistance-associated protein 2 (MRP-2) suggested as a downstream target of IGF-1R signalling[54]. Blockade of the anti-apoptotic effects of IGF-1R signalling provides another possible mechanism of synergy when adding IGF-1R inhibitors to cytotoxic therapies[26]. Furthermore, the epidermal growth factor receptor (EGFR) and IGF-1R share downstream signalling pathways and exhibit significant crosstalk[55,56], suggesting IGF-1R signalling as a resistance mechanism to anti-EGFR therapy[57]. As introduced above, therapeutics targeted at the EGFR are currently in use for treatment of metastatic CRC, which inspired clinical trials of combinations of anti-IGF1R and anti-EGFR therapeutics to overcome anti-EGFR therapy resistance. These are briefly introduced in the context of anti-IGF-1R therapeutical approaches below.

1.2.3. Therapeutic strategies targeted at IGF-1R

The involvement of IGF-1R signalling in cancer initiation, progression and treatment response yielded a rationale for targeted drug development by several groups and companies. Below, a brief summary is given of employed strategies to target IGF-1R, the compounds investigated in this thesis and clinical characteristics of these drugs.

In order to interfere with IGF-1R signalling, two major strategies are available[58]: Firstly, IGF-1R/ligand interaction can be targeted at several stages. Secondly, the downstream signalling of IGF-1R can be inhibited.

For the first strategy, up-regulation of IGFBPs[59] or blocking IGF-1R using IGF-1 analogues without activating properties[60] represent reasonable approaches. In clinical trials, however, monoclonal antibodies (mAbs) interfering with ligand-receptor binding play the most important role. These, in turn, can either target IGFs or IGF-1R complex. In the introductory and experimental part of this thesis, a monoclonal antibody targeted at IGF-1R will be of major interest.

As a second strategy, tyrosine kinase inhibitors (TKIs) interfering with the receptor autophosphorylation have been assessed in numerous clinical trials[61]. In contrast to mAbs, it proves difficult to generate TKIs with specificity for IGF-1R due to highly conserved regions, especially in the commonly targeted ATP binding pocket, between IGF-1R and IR. Although inhibitors not targeting the ATP binding pocket are being developed and recently entered clinical investigation[62], ATP-competitive TKIs have played a major role in clinical trials and are at the centre of this study.

Clinical trials have been performed in a multitude of cancers using several anti-IGF-1R therapeutics, both as monotherapies and in combination with other drugs. The most encouraging results of anti-IGF-1R therapy were obtained in early stage clinical trials in Ewing's sarcoma[63,64] and non-small cell lung cancer[65]. However, large scale clinical trials are yet to prove significant patient benefit and drugs were discontinued from development after disappointing results from late stage clinical trials (reviewed and evaluated in [58,66]).

In this study, the anti-IGF-1R monoclonal antibody figitumumab (CP-751,871) and the ATP-competitive tyrosine kinase inhibitor OSI-906 (Linsitinib) are investigated. Figitumumab is a human IgG2 mAb against IGF-1R which blocks IGF binding (with an IC_{50} of 1.8 nM[67]) and leads to receptor internalisation and degradation upon

binding[68]. It has been tested in several large clinical trials in various tumour entities, including non-small cell lung cancer (NSCLC)[69,70] and colorectal cancer[63]. While initial clinical results sparked intense interest in this compound, development of it has been discontinued after disappointing phase 3 results. It should also be noted that initially reported biomarker results, linking IRS-1 and circulating IGF-1 levels to figitumumab response in NSCLC, should be handled carefully after three retractions of papers due to improper analysis and collection of clinical trial data[71–73].

The TKI OSI-906 inhibits ligand binding induced autophosphorylation of both IGF-1R and IR in a highly specific manner ($IC50_{IGF\text{-}1R} \approx 35$ nM; $IC50_{IR} \approx 75$ nM)[74]. While it has been demonstrated to have no significant inhibitory effect on other kinases, reduced levels of activation of downstream factors such as Akt and Erk have been described[74]. While frequently used in in-vitro studies, only recently clinical trials of OSI-906 in colorectal cancer and other advanced malignancies have shown promising results[75,76].

In summary, there appears to be a contrast between promising preclinical and early clinical data and disappointing performance of anti-IGF-1R drugs in clinical trials in unselected patient populations. As a result, it has been proposed to return to studying the underlying biology of anti-IGF-1R therapy response more thoroughly[58,66,77]. Considering the clinical trials in unselected patients, biomarkers may facilitate identification of patients who may benefit from anti-IGF-1R therapeutics[26]. On the other hand, rational combination therapies including anti-IGF-1R drugs are already being assessed in clinical trials, but preclinical studies will help design the most effective combination regimens.

1.3. Project motivation and concept

The considerations concerning biomarkers and combination therapies are at the basis of this thesis, in which the effects of anti-IGF-1R therapeutics in a colorectal cancer cell line panel are investigated. Making use of large datasets on gene mutations, expression levels and drug response in 82 cell lines, the factors determining anti-IGF-1R sensitivity are analysed and used as starting points for investigations into the mechanisms of drug response and resistance.

Below, the features of working with large cell line panels are introduced alongside a summary of previous work in the Bodmer group and an outline of this thesis.

1.3.1. The Bodmer Cell Line panel

Cell lines represent a valuable tool for preclinical studies on cancer, as they are easy to handle, usable for high-throughput experiments, comparatively cheap and available for many cancer entities. While these features have fostered the use of cancer cell lines in many studies to date, the predictive potential regarding patient benefit and correct representation of original tumour features has been questioned, as reviewed in[78,79,80].

2D cancer tissue cultures have inherent limitations, such as the lack of the tumour microenvironment and of intra-tumour heterogeneity. However, the full predictive potential of cancer cell lines is also not always reached due to insufficient number of cell lines used and therefore lack of representation of molecular subtypes of a cancer entity[17]. While large screening efforts such as the cancer cell line encyclopedia[81] and a study of the Sanger Institute[82] are addressing this issue

across a variety of cancer types, the number of cell lines per cancer remains too low to pick up effects in a rare molecular subgroup in a particular type of cancer.

The Bodmer cell line panel, in contrast, comprises more than 120 cell lines of a single cancer entity, which is colorectal cancer. This number of cell lines leads to a better representation of the variety of molecular profiles and pathways of development introduced above[17]. In the past, these cell lines have been characterised extensively with respect to the mutational status of key genes of CRC, mismatch repair proficiency, mRNA levels through a microarray whole genome gene expression analysis, as well as other features such as sensitivity to selected therapeutics (for more details please refer to 2.1.1-3).

This cell line panel has been used previously for drug response studies[14,83] in the Bodmer group. In essence, the cell lines were classified according to their responsiveness to a set of drugs and investigated for differential gene mutation and expression patterns between the sensitive and resistant subgroups of cell lines.

The studies underline the approach which becomes feasible by using this large cell line panel: By performing drug screenings in a large, well-characterised population of cancer cell lines with good representation of the clinically relevant subtypes and mutational profiles, characteristics associated with drug response can easily be identified. Then, the identified biomarkers can be used to select suitable cell lines for functional studies and validation of the findings.

1.3.2. Work on IGF-1R in the Bodmer group

A total of 82 cell lines had previously been screened in the Bodmer lab for response to two anti-IGF-1R drugs: the TKI OSI-906 and the mAb figitumumab. Preliminary analyses of subsets of cell lines implied the involvement of key molecules of the PI3K pathway, such as PI3K and Akt3, in resistance to anti-IGF-1R drugs. In consideration of these initial observations, a particular focus of this thesis is laid on the role of the PI3K pathway in response to IGF1R inhibition.

1.3.3. Project concept

Based on the need for biomarkers for patient selection and insights into the most effective combination therapies including anti-IGF-1R drugs, the Bodmer cell line panel was used to study the factors involved in anti-IGF-1R therapy response.

As a first step, datasets on anti-IGF-1R therapy response generated by previous members of the Bodmer group were to be assembled and analysed in a coherent manner. Afterwards, correlations between anti-IGF-1R sensitivity and gene mutation and expression levels were to be investigated to gain insights into potential biomarkers and starting points for further investigations.

Categorisation of the cell lines according to their anti-IGF-1R therapy response and molecular profiles was to be used to study the associated factors and mechanisms of resistance in subgroups of CRC cell lines. For this purpose, drug combination studies with various functional readouts should be combined with continued molecular and signalling profiling in defined subgroups.

An overview of the project concept is depicted in Figure 3.

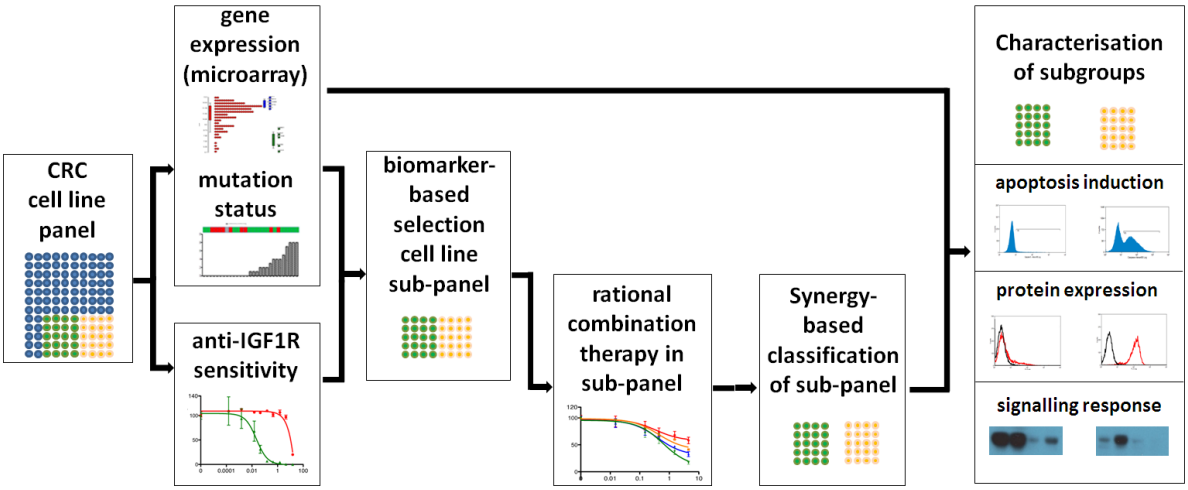

Figure 3: Project workflow.
Combining large datasets on anti-IGF-1R therapy response, mutations and gene expression levels in a CRC cell line panel, associations between molecular profiles and drug response should be investigated. Using the insights derived from these studies, smaller subsets of cell lines were to be characterised as to their sensitivity to rational drug combinations, signalling response to IGF-1R inhibition, expression of key proteins and apoptotic response to anti-IGF-1R based therapeutic regimens.

Chapter 2: Materials and Methods

2.1. Materials

2.1.1. Colorectal cancer cell line panel

The names and sources of the 82 cell lines used in this study are indicated in Table 1. Cell lines derived from the same patient are indicated by identical indices behind the cell line name. C10, C106, C125PM, C32, C80 and C99 cell lines have been established in the Cancer Immunogenetics Laboratory (Walter Bodmer) and have been deposited at the European Collection of Cell Cultures (ECACC).

Table 1: Cell lines and sources

Cell lines	Catalogue number, Source
C10[1]	ECACC: 12022901
C106	ECACC:12022906
C125PM	ECACC: 12022909
C2BBe1[2]	ATCC® CRL-2102™
C32	ECACC: 12022908
C80	ECACC: 12022904
C99	ECACC: 12022905
CACO2[2]	ATCC® HTB-37™
CAR1	JCRB0207
CC20	Kind gift from Dr. Anne R. Kinsella, Paterson Laboratories, Manchester M20 9BX, UK
CCK81	JCRB0208
CCO7	JT Immunotech, USA
CL11	DSMZ: ACC-467

Cell lines	Catalogue number, Source
CL40	DSMZ: ACC-535
COCM1	JCRB0257
COLO201[3]	ATCC® CCL-224™
COLO206[3]	DSMZ: ACC-21
COLO320DM[4]	ATCC® CCL-220™
COLO678	DSMZ: ACC-194
CW2	RCB0778
CX1[5]	DSMZ: ACC-129
DLD1[6]	ATCC® CCL-221™
GP2d[7]	ECACC: 95090714
GP5d[7]	ECACC: 95090715
HCA46	Kind gift from Dr. S.Kirkland, Royal Postgrad School, London
HCA7	Kind gift from Dr. S.Kirkland, Royal Postgrad School, London
HCC2998	Obtained from NCI-FREDERICK CANCER DCTD tumor/cell line repository, vial designation: 0507244
HCC56	JCRB1037
HCT116	ATCC® CCL-247™
HCT15[6]	ATCC® CCL-225™
HDC111	Obtained from Prof. Manfred Schwab under an MTA, DKFZ, Heidelberg, Germany
HDC114	Obtained from Prof. Manfred Schwab under an MTA, DKFZ, Heidelberg, Germany
HDC135	Obtained from Prof. Manfred Schwab under an MTA, DKFZ, Heidelberg, Germany
HDC142	Obtained from Prof. Manfred Schwab under an MTA, DKFZ, Heidelberg, Germany
HDC54[8]	Obtained from Prof. Manfred Schwab under an MTA, DKFZ, Heidelberg, Germany

Cell lines	Catalogue number, Source
HDC57[8]	Obtained from Prof. Manfred Schwab under an MTA, DKFZ, Heidelberg, Germany
HDC73	Obtained from Prof. Manfred Schwab under an MTA, DKFZ, Heidelberg, Germany
HDC8	Obtained from Prof. Manfred Schwab under an MTA, DKFZ, Heidelberg, Germany
HDC82	Obtained from Prof. Manfred Schwab under an MTA, DKFZ, Heidelberg, Germany
HDC9	Obtained from Prof. Manfred Schwab under an MTA, DKFZ, Heidelberg, Germany
HRA19	Kind gift from Dr. S.Kirkland, Royal Postgrad School, London
HT29[5]	ATCC® HTB-38™
HT55	ECACC: 85061105
LIM1863	R.Whitehead, Australia
LOVO	ATCC® CCL-229™
LS1034	Kind gift from Dr. Laurent Suardet, ISCRE, Switzerland
LS123	ATCC® CCL-255™
LS174T[9]	Kind gift from B.H.Tom, NW Uni Med Centre, Chicago
LS180[9]	Kind gift from B.H.Tom, NW Uni Med Centre, Chicago
LS411	Kind gift from Dr. Laurent Suardet, ISCRE, Switzerland
LS513	ATCC® CRL-2134™
NCIH508	ATCC® CCL-253™
NCIH548[3]	ATCC® CCL-249™
NCIH716	ATCC® CCL-251™
NCIH747	ATCC® CCL-252™
OUMS23	JCRB1022
OXCO1	Kind gift from Prof. Vincenzo Cerundolo, Weatherall Institute of Molecular Medicine, University of Oxford, Oxford OX3 9DS

Cell lines	Catalogue number, Source
OXCO2	Kind gift from Prof. Vincenzo Cerundolo, Weatherall Institute of Molecular Medicine, University of Oxford, Oxford OX3 9DS
PCJW	Kind gift from Prof. Christos Paraskeva, Department of Pathology and Microbiology, University of Bristol, UK
PMFKO14	RCB1426
RCM1	JCRB0256
RKO	ATCC® CRL-2577™
SKCO1	ATCC® HTB-39™
SNUC1	ATCC® CRL-5972™
SNUC2B	ATCC® CCL-250™
SW1116	ATCC® CCL-233™
SW1222	Kind gift from Meenhard Herlyn, Wistar Institute, Philadelphia, PA, USA.
SW1417	ATCC® CCL-238™
SW403	ATCC® CCL-230™
SW48	ATCC® CCL-231™
SW480[10]	ATCC® CCL-228™
SW620[10]	ATCC® CCL-227™
SW837	ATCC® CCL-235™
SW948	ATCC® CCL-237™
T84	ATCC® CCL-248™
TT1TKB	RCB1185
VACO10MS	Kind gift from J.McBain, VA Res.Ser. Madison, Wisconsin
VACO400	Obtained from Dr Elizabeth Zborowska under an MTA, Case Western reserve University, Cleveland, Ohio
VACO429	Obtained from Dr Elizabeth Zborowska under an MTA, Case Western reserve University, Cleveland, Ohio

Cell lines	Catalogue number, Source
VACO4A[11]	Kind gift from J.McBain, VA Res.Ser. Madison, Wisconsin
VACO4S[11]	Kind gift from J.McBain, VA Res.Ser. Madison, Wisconsin
VACO5	Kind gift from J.McBain, VA Res.Ser. Madison, Wisconsin

2.1.2. Microarray dataset

Microarray data of mRNA expression levels in the cell line panel were obtained in the Bodmer group by sending RNA samples to the Molecular Biology Core Facility of the Paterson Institute for Cancer Research in Manchester for gene expression microarray analysis. The Affymetrix GeneChip system v2.0 was used to determine expression levels of 54,675 probe sets (covering 20,741 unique genes). The detailed protocol can be accessed at http://www.affymetrix.com/support/technical/manuals.affx.

2.1.3. Mutation dataset

The mutational states of key genes in colorectal cancer (*PIK3CA, APC, TP53, CTNNB1, KRAS, BRAF, FBXW7*) and the replication error (RER) status for each cell line of the panel had previously been assembled in the Bodmer group. The indicated mutations are based on consensus of sequencing data generated in the Bodmer group and in collaborations[84] and publicly available datasets on cell line mutational states from the cancer cell line encyclopaedia[81] and a study of the Sanger institute[82].

2.1.4. Antibodies

The antibodies used in this thesis are depicted in Table 2.

Table 2: Antibodies

Target (species/clonality)	Supplier	Ref #	Application (dilution)
Akt (pan) (Rb, mAb)	Cell signalling technologies (CST)	#4685	Primary, WB (1:500)
Cleaved Caspase-8	CST	#9496	Primary, FACS (1:100)
GSK-3β (Ms, mAb)	BD Biosciences	610201	Primary, WB (1:500)
p44/42 MAPK (Erk1/2) (Rb, mAb)	CST	#9102	Primary, WB (1:500)
P-Akt (S473) (Rb, mAb)	CST	#4058	Primary, WB (1:500)
P-Akt (T308) (Rb, mAb)	CST	#9275	Primary, WB (1:500)
P-GSK-3β (S9) (Rb, mAb)	CST	#9323	Primary, WB (1:500)
P-p44/42 MAPK (T202/Y204) (Erk, Rb, mAb)	CST	#9101	Primary, WB (1:500)
β-Actin (Ms mAb)	Sigma	A5541	Primary, WB (1:10,000)
Goat anti Mouse (HRP-conjugated, polyclonal)	Dako	P0447	Secondary, WB (1:10,000)
Swine anti Rabbit (HRP-conjugated, polyclonal)	Dako	P0217	Secondary, WB (1:10,000)
CD24 (R-PE conjugate, mAb)	Life Technologies	MHCD2404	Conjugated primary, FC (1:20)
Goat anti Rabbit (Alexa 488-conjugated, polyclonal)	Thermo Fisher	A-11034	Secondary, FC (1:200)

2.1.5. Laboratory reagents

The used reagents used are depicted in Table 3.

Table 3: List of reagents

Reagent	Supplier
BCA Protein Assay Kit	Pierce
Cell Counting Chambers	Nexcelcom
Cryovials	Corning Incorporated
Crystal violet	Sigma-Aldrich
DAPI	Invitrogen
DMEM (Dulbecco's Modified Eagle Medium) (+ 4.5 g L-D-glucose, + L-glutamine, + puruvate)	Life Technologies
DMSO (dimethyl sulfoxide)	AppliChem
Dry milk powder	The Co-operative
ECL (Clarity Western ECL Substrate)	Bio-Rad
EDTA (Cell Dissociation Solution Non-enzymatic, 1X)	Sigma-Aldrich
Ethanol (100 %)	Fisher Scientific
Falcon (15 mL)	Corning Incorporated
Falcon (50 mL)	Corning Incorporated
FBS (foetal bovine serum)	Source BioScience
Figitumumab	Pfizer
Flow cytometry tubes	Becton Dickinson
GSK690693	Sigma
IMDM (Iscoves Modified Dulbecco Medium) (+ L-glutamine, + 25 mM HEPES)	Life Technologies

Reagent	Supplier
Lipofectamine (RNAiMAX Reagent)	Invitrogen
Methanol (100 %)	Fisher Scientific
M-PER (Mammalian Protein Extraction Reagent)	Thermo Scientific
MycoAlert Assay Kit	Lonza
NuPAGE Novex 4-12% Bis-Tris gels	Life Technologies
Opti-MEM (Reduced serum medium) (+ L-glutamine, + HEPES, - Phenol red)	Invitrogen
OSI-906	Cambridge Bioscience Ltd
PBS (absolute phosphate buffered saline)	In house
Pen/Strep (Penicillin/Streptomycin)	Gibco, Invitrogen
Phosphatase inhibitor (PhosSTOP)	Roche
Precision Plus Protein marker	Bio-Rad
Protease inhibitor (Complete Mini)	Roche
PVDF membrane (0.45 µm Amersham Hybond)	GE Healthcare
RPMI (Roswell Park Memorial Institute) Medium 1640 (+ L-glutamine)	Life Technologies
siRNA SMART pool (Akt1)	Dharmacon
siRNA SMART pool (Akt2)	Dharmacon
siRNA SMART pool (Akt3)	Dharmacon
siRNA SMART pool (Scramble)	Dharmacon
TCA (Trichloroacetic acid)	Sigma-Aldrich
Tissue culture flask 25 cm^2	BD Biosciences
Tissue culture flask 75 cm^2	BD Biosciences
Tissue culture petri dish (100 mm)	Corning Incorporated

Reagent	Supplier
Tissue culture petri dish (60 mm)	Corning Incorporated
Tissue culture plate (6 wells)	Corning Incorporated
Tissue culture plate (96 wells)	Corning Incorporated
Tris/Glycine buffer (10X)	BioRad
Trypsin-EDTA (10X)	Lonza
X-Ray films	Fujifilm

2.1.6. Instruments and Software

The instruments and software used in this thesis are depicted in Table 4 and Table 5.

Table 4: Instruments

Instrument	Type	Manufacturer
Cell sorter	MoFlo	Dako
Centrifuge (cell culture)	Allegra 6R	Beckman Coulter
Centrifuge (table top)	5417R	Eppendorf
Cell counter	Cellometer Auto T4	Nexelcom Biosciences
Flow cytometer	Cyan	Beckman Coulter CyAn Analyzer
Colony Counter	GelCount	Oxford Optronix
Heat block (Ori-Block)	OB-1	Techne
Incubator	Hera Cell 150	Heraeus
Plate shaker		Heidolph
Power Supply	1000/500	Bio-Rad
Spectrophotometer	µQuant	BioTek
Vortex	Vortex Genie 2	Scientific Industries

Table 5: Software

Name	Version	Supplier
Cellometer software		Nexelcom
GelCount software	v1.4	Oxford Optronix
GraphPad Prism	v5.0a	GraphPad
Partek Genomics Suite	v6.6	Partek Inc.
Summit	v2.0	Beckman Coulter

2.2. Methods

2.2.1. Cell culture

All cell lines used in this study were regularly screened for mycoplasma infection using the MycoAlert Assay kit. Cells were grown in either DMEM, RPMI or Iscove's medium with 10% (v/v) FBS and Penicillin(2 IU/ml)/Streptomycin (2 µg/ml) at 37°C and 5% CO_2 in either 25 cm^2 or 75 cm^2 tissue culture flasks.

For long term storage, $1*10^6$ cells were kept in FBS+10% DMSO (v/v) in liquid nitrogen. As cells were seeded from cryovials, the content of the vial was thawed, topped up with 7 ml of medium (+10 %FBS; + 1x Pen/Strep) before centrifugation at 1000 rpm for 5 minutes. The supernatant was poured to remove the DMSO and cells were resuspended in medium (+10 %FBS; + 1x Pen/Strep) for seeding. Upon reaching 60-80% confluency, the cells were split by a ratio between 1:3 and 1:20, depending on cell doubling time. For splitting, cells were washed with PBS and

incubated with 1x Trypsin-EDTA or EDTA for 3–15 minutes under repeated manual rocking of the plates. Trypsin activity was stopped by addition of an excess volume of medium containing 10% FBS and removed through centrifugation for 5 minutes at 1000 rpm in 15 mL falcon tubes. The obtained pellets were resuspended in media and seeded for further culturing.

2.2.2. Cell counting

Cell counting was performed using a Cellometer Auto T4 instrument and disposable counting chambers, which were loaded with 20 µl of cell suspension.

2.2.3. Drug treatments

Drug dilution rows were prepared freshly for each experiment from aliquot stock solutions of figitumumab (6 mg/ml in diH_2O), OSI-906 (20 mmol/l in DMSO) and GSK690693 (20 mmol/l in DMSO). For OSI-906 and GSK690693, each dilution step was adjusted to equal concentration of DMSO.

Cells in their exponential growth phase were harvested by trypsinisation from tissue culture flasks and counted as described above. Alternatively, cells were seeded from cryovials and counted after resuspendation in medium. The following seeding and treatment for the different experimental approaches of this thesis are briefly described below.

To study the effect of drugs in monotherapy or in combination on **cell viability**, 100 µL of cell suspension, containing 2,000–4,000 cells freshly thawed from cryo-storage, were seeded in each well of a 96-well plate, sparing the outer layer of wells

which was filled with PBS to avoid heterogeneous condensation. Cells were incubated for their lag time before drug treatment, when 100 µL of drug dilution were added to each well, covering each dose point in triplicates. After incubation with the drugs for 3 doubling times, cells were fixed by adding TCA and analysed using the SRB assay as described below. At the time of treatment, 3 wells per cell line were fixed by adding TCA and later used as a day 0 control.

To study the effect of drug combinations on **apoptosis induction**, 400,000 cells were harvested by trypsinisation and seeded in 4 ml medium in 60 mm diameter tissue culture (TC) treated petri dishes and incubated for their lag time. After this period, cells were treated with different drug dilutions for 72h. Subsequently, cells were harvested and ethanol fixed as described in the flow cytometry analysis Section 2.2.6.

The treatment of cells for protein extraction and subsequent **western blot** assessment was performed in the same way as for flow cytometry sample preparation until the step of harvesting.

Treatment of cells in colony formation assays is described in 2.2.9.

2.2.4. SRB assay

Cells were fixed by adding 12 µl of cold trichloroacetic acid (TCA, 50%) to each well and incubated at 4 °C overnight. The next day, plates were washed three times by adding 200 µl of water per well, dried by flicking of the plates and stored for further processing as all plates from an experiment reached this stage. As the next step, 100 µl of sulphorhodamine B (SRB) solution (0.04% SRB in 1% acetic acid) were

added to each well and incubated for 30 minutes at room temperature. The cells were washed subsequently four times with 200 µl of 1% acetic acid, flicked thoroughly and left to dry overnight. To dissolve the SRB stain, 200 µl of Tris solution (10mM, pH 9.5) were added. Plates were rocked on a plate shaker until all SRB stain was dissolved and the plates were subsequently read for absorbance at a wavelength of 520 nm using the µQuant microplate spectrophotometer.

2.2.5. Sensitivity and drug interaction analysis

Based on the absorbance values obtained from the SRB assay, relative cell viability was calculated by averaging the measured values from technical triplicates, subtracting the appropriate day 0 value from all measurements and normalising the obtained value to an untreated control (see first 2 steps in Figure 4).

To determine the sensitivity of cell lines to treatment with figitumumab or OSI-906, the relative viability was plotted over the dose of drug using the software GraphPad Prism. A sigmoidal curve was fitted over the data to determine the GI50 of OSI-906, while the relative growth inhibition at 10 µg/ml of figitumumab was used as a measure for sensitivity to the monoclonal antibody.

For analysis of drug interaction, the coefficient of drug interaction (CDI) was calculated across a dose range of OSI-906 and GSK690693 as reported in the literature[85,86]. The workflow for this analysis is exemplarily depicted for one cell line in Figure 4. Based on a treatment matrix of 4 doses of GSK690693 and 6 doses of OSI-906, each including a DMSO control, the coefficient of drug interaction was calculated for 15 combinations according to the formula given in Figure 4, bottom right corner. The CDI estimates the effect of a drug combination relative to the

effect of both drugs in monotherapy, with lower CDI values indicating stronger effects than expected from additional action of the compounds. As a CDI < 0.7 is commonly considered an indicator of potential synergy, the CDI values were colour coded as green representing potentially synergistic drug interaction at the applied doses. The two main measures applied for classifying cell lines as to their sensitivity to combination treatment are the number of dose points with a CDI below 0.7 and the lower quartile of CDI, also determined from the 15 CDI values characterising each cell line.

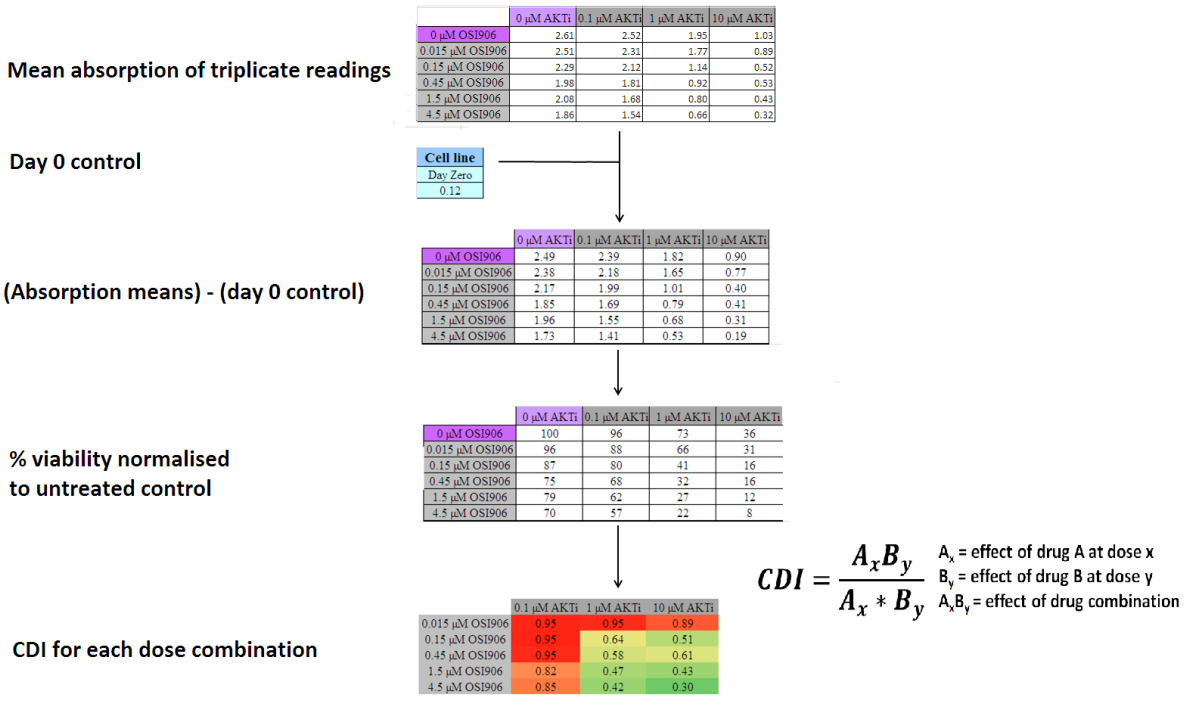

	0 µM AKTi	0.1 µM AKTi	1 µM AKTi	10 µM AKTi
0 µM OSI906	2.61	2.52	1.95	1.03
0.015 µM OSI906	2.51	2.31	1.77	0.89
0.15 µM OSI906	2.29	2.12	1.14	0.52
0.45 µM OSI906	1.98	1.81	0.92	0.53
1.5 µM OSI906	2.08	1.68	0.80	0.43
4.5 µM OSI906	1.86	1.54	0.66	0.32

	0 µM AKTi	0.1 µM AKTi	1 µM AKTi	10 µM AKTi
0 µM OSI906	2.49	2.39	1.82	0.90
0.015 µM OSI906	2.38	2.18	1.65	0.77
0.15 µM OSI906	2.17	1.99	1.01	0.40
0.45 µM OSI906	1.85	1.69	0.79	0.41
1.5 µM OSI906	1.96	1.55	0.68	0.31
4.5 µM OSI906	1.73	1.41	0.53	0.19

	0 µM AKTi	0.1 µM AKTi	1 µM AKTi	10 µM AKTi
0 µM OSI906	100	96	73	36
0.015 µM OSI906	96	88	66	31
0.15 µM OSI906	87	80	41	16
0.45 µM OSI906	75	68	32	16
1.5 µM OSI906	79	62	27	12
4.5 µM OSI906	70	57	22	8

	0.1 µM AKTi	1 µM AKTi	10 µM AKTi
0.015 µM OSI906	0.95	0.95	0.89
0.15 µM OSI906	0.95	0.64	0.51
0.45 µM OSI906	0.95	0.58	0.61
1.5 µM OSI906	0.82	0.47	0.43
4.5 µM OSI906	0.85	0.42	0.30

Figure 4: Workflow of drug interaction analysis.

2.2.6. Apoptosis induction studies using flow cytometry

After 72h of drug treatment, cells were harvested using trypsinisation and counted as described above. Cells from the supernatant and the first PBS washing step

were collected, pooled and pelleted in the same falcon tube as the trypsinised cells. The obtained cell pellets were washed with ice cold PBS through resuspending and centrifugation. For fixation, 70% ethanol was added dropwise to the pelleted cells under constant flicking of the falcon tubes. The fixed samples were incubated at 4°C overnight and stored at -20°C until analysis.

For the immunostaining, the samples were washed with and resuspended in PBS+2%FBS before approximately $1*10^6$ cells were transferred in 100 µl to a flow cytometry tube per staining condition. Subsequently, an anti-cleaved caspase 8 antibody was added in a 1:100 dilution to one set of samples. After overnight incubation at 4°C, samples were washed with and resuspended in 100 µl PBS+2%FBS before and Alexa-488 conjugated secondary anti-rabbit antibody was added in a 1:200 dilution. The isotype control consisted of an untreated sample incubated with the Alexa-488 conjugated secondary antibody only. The samples were then incubated for 1h at room temperature in the dark and under regular shaking to secure proper access of the antibody to each cell. As a final step, the samples were washed with PBS+2%FBS again and resuspended in 500 µl of the same solution for analysis at the Cyan flow cytometer.

A threshold for negative staining was set using the isotype control for each cell line and the percentage of cleaved caspase 8 positive cells from each treatment condition was used to assess apoptosis induction.

2.2.7. Protein extraction and Western Blot

After 72h of drug treatment as described above, cells were washed with ice cold PBS in their plates and stored at -80°C until further sample processing. M-PER

buffer supplemented with protease and phosphatase inhibitors was used for isolation of proteins on ice. Cells were collected through scraping into 150 µl of M-PER buffer and incubated for 30 min on ice with repeated vortexing to support lysis of cells. After this incubation, the samples were centrifuged at 4°C for 20 minutes at 14,000 rpm and the supernatant was collected and transferred to a new eppendorf tube.

The protein concentration in the obtained supernatant was determined by BCA assay in 96-well plates. Protein lysates were diluted in further M-PER buffer and mixed with 5x denaturating SDS sample buffer to obtain samples of 25 µg of protein. These samples were boiled at 100°C for 10 minutes before being loaded on NuPAGE Novex 4-12% Bis-Tris gels. The gels were run for ~1.5h at 100 V in MOPS running buffer using a Novex Mini-Cell running chamber to separate proteins by molecular weight. Subsequently, proteins were transferred to a PVDF membrane using the BioRad wet transfer system with BioRad Tris/Glycine buffer. The membrane was activated in methanol for 20 seconds before being immersed in wet transfer buffer with the gel. Proteins were transferred for 2 h at a constant current of 250 mA, with the success of the transfer being confirmed by Ponceau staining.

Membranes were subsequently blocked with 5% (w/v) dry milk powder in TBS-T at room temperature for 1h. Primary antibodies were diluted to 1:500 in the milk solution – unless indicated as different – in table 2 and incubated on the membranes at 4°C overnight in a humidified chamber. The membranes were then washed 3 times with TBS-T for 10 minutes each before HRP-coupled secondary antibodies were added at a dilution of 1:10.000. Secondary antibodies were incubated for 1h at room temperature under constant gentle rocking on a plate shaker. After another three 10 minute washing steps in TBS-T, membranes were

developed using the ECL protein detection kit and X-Ray films. The membranes were then stripped using self-made stripping buffer (1.5% w/v glycine, 0.1% v/v Tween-20; pH 2.5) for 20 minutes, so that other antibodies could be assessed according to the same protocol, starting with the blocking step.

2.2.8. Surface staining and FACS

Cells were grown in 100 mm diameter tissue culture treated petri dishes and harvested by trypsinisation upon reaching ~80% confluency. Harvested cells were counted, washed twice with ice cold PBS+2%FBS and transferred to flow cytometry tubes so that about $1*10^6$ cells were distributed to each tube in 100 µl of liquid. A volume of 5uL of anti-CD24 antibody conjugated to Phycoerythrin (PE) was added to each tube and incubated in the dark for 1h on ice. Isotype control antibodies conjugated to the same dyes added to one sample each to determine the level of background signal. After another washing and resuspension step in 500 µl PBS+2%FBS, DAPI solution was added in a 1:10.000 dilution and the samples were taken to analysis at a Cyan flow cytometer, using the software Summit. Live cells were selected for DAPI negativity. The signal level from the isotype control samples was used to set the threshold for positivity.

For live cell sorting, the same protocol was applied, with each step being performed under sterile conditions for this purpose. Cell sorting was performed at a Dako cell sorter, with the top 10% and bottom 10% CD24 expressing cells being sorted into separate FACS tubes containing growth media with 10% FBS. An unsorted sample of cells was also collected as a control for these experiments. Sorted cells were used for the colony formation assay described below.

2.2.9. Colony formation assay

Cells were harvested by trypsinisation and seeded in 60 mm diameter TC treated petri dishes or 6-well plates at low densities of 500-1,500 cells per well. After incubating for 48h to allow attachment of cells, drug dilutions were added to the wells. The cells were observed every other day to evaluate colony growth and distance. Upon reaching appropriate colony size and density, cells were washed gently in their wells twice with ice cold PBS. A volume of 2 mL ice cold methanol (100%) was added to the wells and incubated for 10 minutes, before another 10 minute incubation with self-made crystal violet solution (0.5% crystal violet in 25% methanol). Plates were then washed repeatedly immersing them in water. After drying overnight and storage at room temperature, plates were read on a gel count instrument.

Colonies were automatically detected using the instrument's software to the instrument, with appropriate recognition settings established for each cell line and kept constant amongst samples from the same cell line.

2.2.10. siRNA knockdown

Reverse transfection of cells with different siRNAs was performed in 6-well plates. 6 µl of 10 µM siRNA was diluted in 100 µl of Opti-MEM transfection medium and mixed thoroughly with 6 µl of Lipofectamine reagent diluted in 100 µl Opti-MEM. The mixture was incubated for 7 minutes and added to an empty well of a 6-well plate. Subsequently, 300,000 cells in 2 ml antibiotics-free medium with 10% FBS were added to the well and mixed by gently moving the plate. After 24h of

incubation at 37°C and 5% CO_2, the supernatant was removed and replaced by culture media with 10% FBS and 1% Penicillin/Streptomycin.

For subsequent culturing, cells were harvested by trypsinising and counted after an additional 24h. In case of drug sensitivity screenings, 3,000 cells were seeded per well of a 96-well plate and treated as described above in Section 2.2.3.

2.2.11. Statistical tests

Statistical analysis was performed using the software GraphPad Prism. For categorical data, χ^2 or two-tailed Fisher's exact test were used. To analyse correlation of drug responses to each other or gene expression levels, Spearman's rank correlation coefficient (spearman's r for further reference) was used. A threshold of p values < 0.05 was applied for evaluation of significance.

Chapter 3: Results

3.1. Characterisation of response to IGF-1R inhibitors across the cell line panel

As previously demonstrated in the Bodmer group[14,83], the CRC cell line panel can be used to identify subgroups of cell lines with respect to drug response. In this project, two IGF-1R inhibitors – the monoclonal antibody figitumumab and the tyrosine kinase inhibitor OSI-906 – were investigated. Therefore, a first step comprised assembling drug sensitivity data for these two compounds previously generated in the group and characterisation of the response across the cell line panel.

The contrast between a sensitive and a resistant cell line in responses to the two therapeutics is depicted in Figure 5. Importantly, only the direct, but not the immune-mediated effects, of the monoclonal antibody were investigated. As Figitumumab is an IgG2 mAb, no antibody-dependent cell-mediated cytotoxicity (ADCC) is expected, rendering direct effects of the antibody the only relevant mode of action. While the response characteristics to the mAb figitumumab and the TKI OSI-906 are comparable for the sensitive cell line SKCO1 (green curves), the resistant cell line CC20 (red curves) illustrates a key difference in response to the therapeutics observed in all resistant cell lines: In the case of OSI-906, a viability decrease of more than 50% is reached within the applied dose range of up to 15 µM, whereas figitumumab does not induce a striking decrease of viability at any dose applied in the screen. Hence, the GI50, which indicates the drug concentration inducing 50% growth inhibition, could only be calculated for OSI-906 ($GI50_{OSI-906}$), but not figitumumab, in the resistant cell lines. As an alternative to this measure of

sensitivity, the relative growth inhibition at 10 µg/ml figitumumab ($GI_{[Figitumumab]10µg/ml}$)was used as an indicator of responsiveness to figitumumab treatment (with greater growth inhibition indicating more sensitivity).

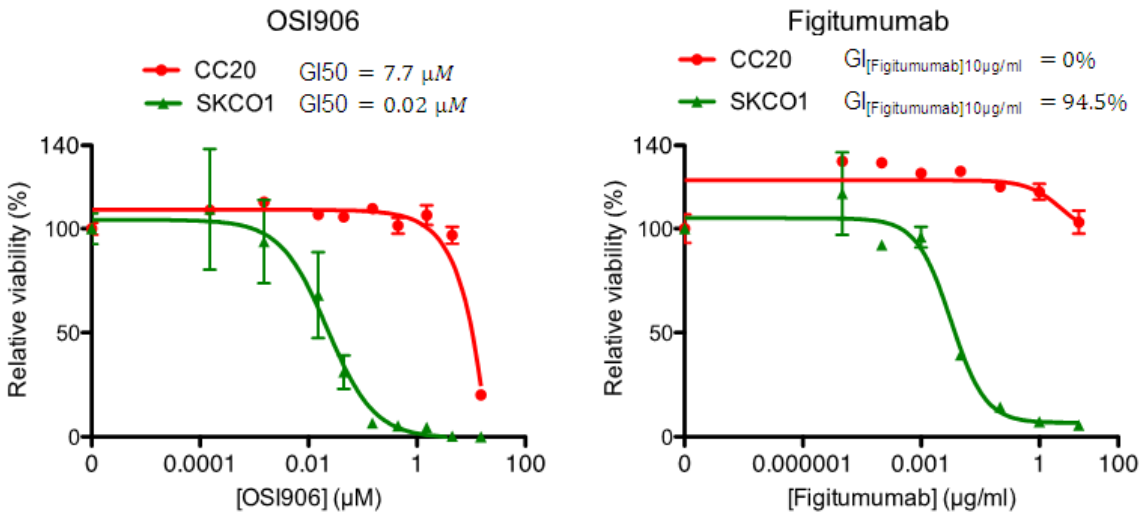

Figure 5: Response to anti-IGF-1R therapeutics.
A resistant (CC20, red) and sensitive (SKCO1, green) cell line were treated with a dose range of anti-IGF-1R drugs for 3 doubling times before assessing the cell viability. The cell lines show distinct response characteristics to the TKI OSI-906 (left graph) and the mAb figitumumab (right graph). While the drugs induce similar responses in SKCO1, the mAb does not lead to marked viability decrease in CC20 at the applied doses.

To compare the response to figitumumab and OSI-906 across the cell line panel, the $GI50_{OSI-906}$ and $GI_{[Figitumumab]10µg/ml}$ values were assembled from data previously generated in the Bodmer group. In total, data for 82 cell lines were available, including 9 pairs of duplicate cell lines. In general, the sensitivity to both drugs was found to be in agreement within the pairs of duplicate cell lines (see Figure S 1 and Figure S 2). To avoid bias from oversampling of these and justified by the good agreement within the cell line pairs, the data of one cell line from each pair were omitted from the dataset, resulting in 73 cell lines for the analysis.

For an evaluation of the agreement between sensitivity to OSI-906 and figitumumab, the responsiveness to the drugs is plotted in Figure 6. The sensitivity across the 73 cell lines shows a positive correlation with high confidence (Spearman r =-0.7277; p-value < 0.0001). This finding strengthens the notion that the observed drug effects are likely to be due to IGF-1R signalling inhibition and not to off-target effects.

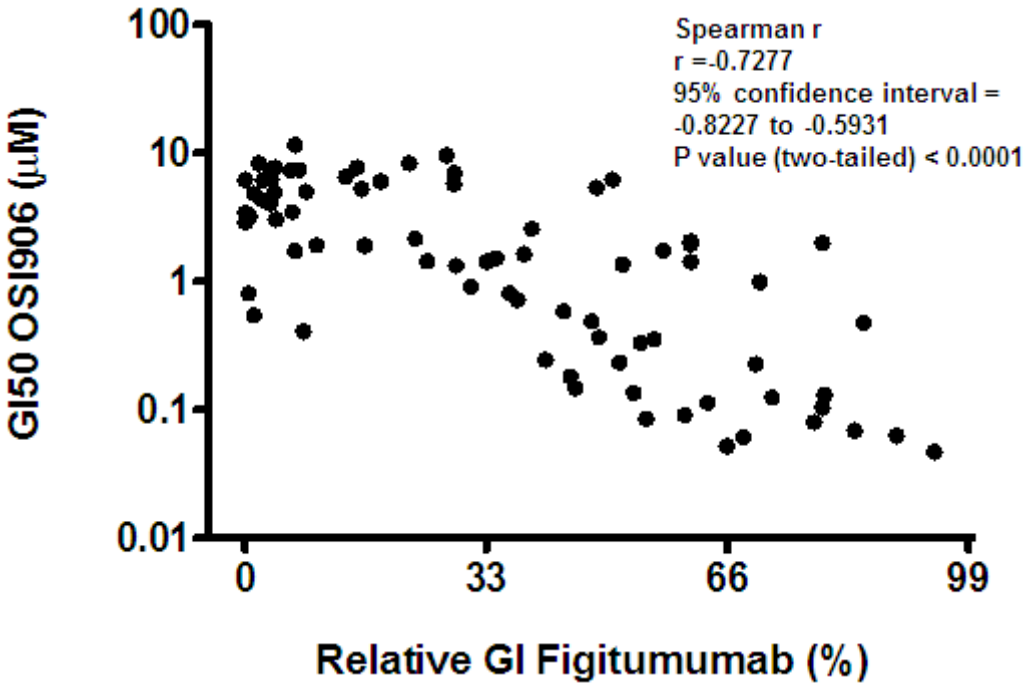

Figure 6: Sensitivity to figitumumab and OSI-906 is correlated across the cell line panel. The sensitivity of 73 cell lines to OSI-906 (GI50) is plotted against the sensitivity to figitumumab (% growth inhibition at 10 µg/ml). A strong positive correlation is observed (Spearman r ≈ -0.7277; p < 0.0001). *(Data courtesy of Dr. Djamila Ouaret)*

Notably, the sensitivity to OSI-906 ($GI50_{OSI\text{-}906}$) and figitumumab ($GI_{[Figitumumab]10\mu g/ml}$) vary significantly across the cell line panel ($GI50_{OSI\text{-}906}$: 0.0047 µM – 11.68 µM; $GI_{[Figitumumab]10\mu g/ml}$: 0 % – 94.3%).

The differential drug responses and the good agreement between sensitivity to figitumumab and OSI-906 observed across the cell line panel allow classification of

the cell lines for the analysis of factors contributing to anti-IGF-1R resistance performed below.

3.2. Identification of genetic factors in anti-IGF-1R resistance

While the response to the anti-IGF1R drugs figitumumab and OSI-906 is generally consistent within cell lines, marked differences between cell lines can be observed in Figure 5 and Figure 6. These differences could potentially be explained by mutations in the downstream pathways of IGF1R, differential expression of IGF-1R or related proteins or the signalling response to treatment.

As introduced in Section 1.3.1 and 2.1.1-3, the Bodmer laboratory has assembled datasets on the mutation status of key genes of CRC and nearly exome-wide mRNA expression levels. The way in which these 2 datasets were analysed in the light of the anti-IGF-1R response data and the most informative findings are presented below.

3.2.1. *PIK3CA* mutations in exon 9 or 20 are associated with resistance to anti-IGF-1R therapy

As a first approach, the mutation status of 7 key genes of CRC and replication error status was investigated for correlation with responsiveness to anti-IGF-1R therapy. The mutation and replication error status of each cell line had previously been assembled by members of the group as described in Section 2.1.3.

The 73 cell lines were assigned to categories according to their responsiveness to IGF-1R inhibition. For this purpose, a classification system based on sensitivity terciles to both OSI-906 and figitumumab was applied: If a cell line was in the most sensitive tercile of 73 cell lines (i.e. belonging to the 24 most sensitive cell lines) to both OSI-906 and figitumumab, it was classified as sensitive. Cell lines falling in the most resistant tercile to both drugs were classified as resistant. If neither of the criteria for sensitivity or resistant was fulfilled, cell lines were judged to be partially responsive.

This classification and correlation with mutation status is exemplarily depicted for *PIK3CA* mutations in Figure 7. Colour coding cell lines harbouring the activating mutations in *PIK3CA* in exon 9 or 20 as red, wild type cell lines as green and cell lines with unknown *PIK3CA* mutation as grey permits an overview of the distribution of these cell lines in the drug response chart. In the case of *PIK3CA*, mutant cell lines cluster in the top left corner, indicating resistance to both figitumumab and OSI-906.

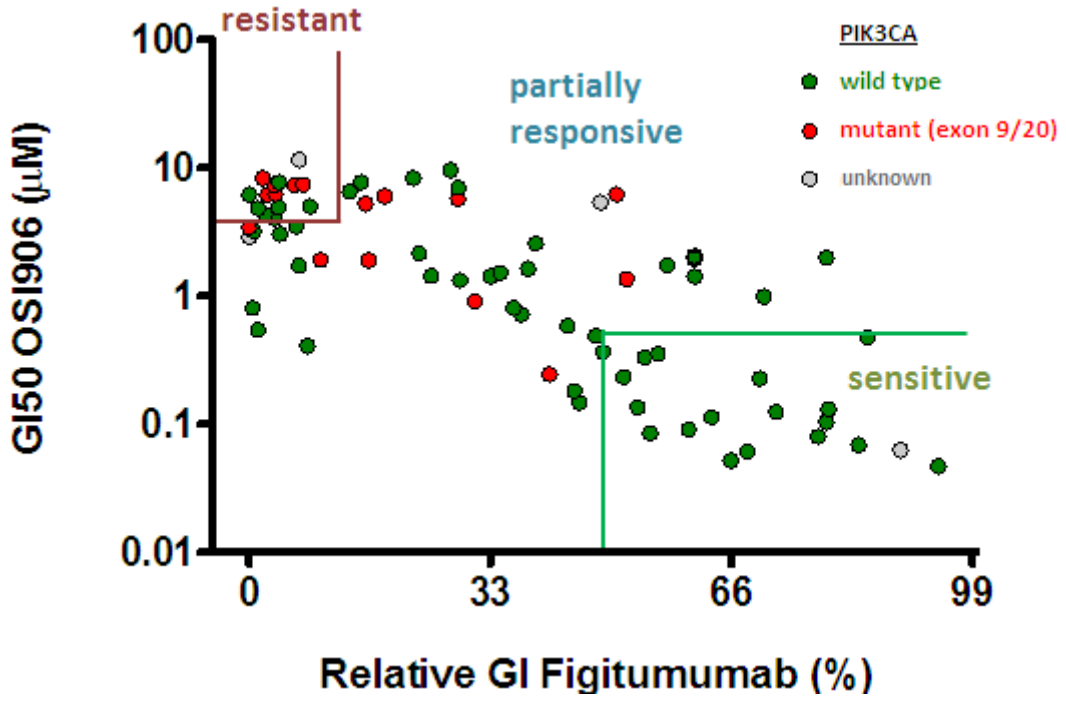

Figure 7: Anti-IGF-1R resistance is associated with *PIK3CA* mutations.
The GI50 to OSI-906 treatment was plotted against the relative growth inhibition at 10 µg/ml figitumumab. *PIK3CA* mutant cell lines are depicted as red dots, while *PIK3CA* wild type cell lines are displayed green and unknown *PIK3CA* mutation status is colour coded grey. Classification into resistant, partially responsive and sensitive is indicated by coloured boundaries. 6 out of 16 *PIK3CA* mutant cell lines fall in the resistant category, while the remaining 10 *PIK3CA* mutants are classified as partially responsive, indicating an association of *PIK3CA* mutation with anti-IGF-1R resistance. *(Data courtesy of Dr. Djamila Ouaret)*

To analyse the correlation between *PIK3CA* mutations and anti-IGF-1R sensitivity, a 3-by-2 table (Table 6) was set up using the drug response categories outlined above and indicated by coloured boundaries in Figure 7. Analysis using a χ^2 test for trend yields $p \approx 0.003$, indicating a significant association of *PIK3CA* mutation to anti-IGF-1R resistance, even after correcting for testing of 8 characteristics (corrected $p \approx 0.022$).

Table 6: *PIK3CA* mutation is associated with resistance to IGF-1R inhibition.
Classification of cell lines according to anti-IGF-1R sensitivity and correlation to *PIK3CA* mutational status (in exon 9 and 20) reveals a significant correlation between anti-IGF-1R resistance and *PIK3CA* mutations (p = 0.003).

PIK3CA mutation and anti-IGF-1R sensitivity			
	anti-IGF-1R response		
p = 0.003	sensitive	partially responsive	resistant
PIK3CA			
wild type	15	25	6
mutant	0	10	6

In accordance with this approach, correlation analysis for each of 6 other mutations (*APC, TP53, CTNNB1, KRAS, BRAF, FBXW7*) and replication error (RER) status was performed using 3-by-2 tables and a χ^2 for trend test, the results of which are depicted in Tables S 1-7.

While replication error status reached the second highest significance in this analysis ($p \approx 0.154$ before correction), only *PIK3CA* mutations were found to be strongly associated with anti-IGF-1R resistance. This is in line with a previous analysis of a set of CRC cell lines in the Bodmer group, which found *PIK3CA* mutations to be associated with resistance IGF-1R inhibition.

As PI3K is a central signalling molecule downstream of IGF-1R (see introduction), activating mutations in the gene encoding its catalytic subunit (*PIK3CA*) could conceivably contribute to IGF-1R signalling independence and thereby resistance to IGF-1R-directed drugs. Based on these findings and considerations, a particular focus was laid on *PIK3CA* mutation status and the PI3K signalling axis in further investigations.

3.2.2. Differential expression of single genes cannot explain resistance to anti-IGF-1R therapy

To investigate whether differential expression of single genes contributes to anti-IGF-1R resistance, the microarray dataset of mRNA expression levels across the cell line panel (see Section 2.1.2) was correlated to the drug response data.

In a first approach, the expression of all 54,675 probe sets (covering 20,741 unique genes) was analysed for differences between the 10 most resistant and most sensitive cell lines to OSI-906 using the software Partek Genomics Suite. To assess which candidate genes were of interest for further investigation, the corrected p-value for multiple hypotheses testing, the fold-change in expression, and biological plausibility were considered. Using these criteria, no clear hits could be found when looking at the cell lines irrespective of mutation status.

As another approach, a list of candidate genes – for which there was an priori reason to suspect they might be involved in anti-IGF-1R/PI3K response – was assembled from the literature and analysed for correlation of expression with the response to OSI-906 and figitumumab separately (the list of genes is depicted in Table S 8). None of the gene expression levels was significantly associated with sensitivity to OSI-906 after correction for multiple hypothesis testing. The findings of this analysis therefore provided no actionable experimental avenues, yet are put into context and contrasted with other reports from the literature in Section 4.2.

A particular focus was laid on the observation that *PIK3CA* mutations are associated with anti-IGF-1R resistance in the cell line panel, yet 31 cell lines are resistant or only partially responsive although being *PIK3CA* wild type.

To address if specific gene expression patterns confer resistance in *PIK3CA* wild type cell lines, this population of cell lines was again analysed separately from *PIK3CA* mutant cell lines. As depicted in Table 6, the *PIK3CA* wild type population comprises 6 sensitive, 25 partially responsive and 15 resistant cell lines. To investigate if differential expression of single genes can serve as an explanation for this varying responsiveness to anti-IGF-1R therapies, the analytical approaches outlined above were repeated, this time only considering the 46 *PIK3CA* wild type cell lines.

A previous analysis of CRC cell lines in the Bodmer group had indicated Akt3 overexpression to be associated with anti-IGF-1R resistance in *PIK3CA* wild type cell lines. However, this finding did not reach significance in this larger dataset.

In summary, the differential expression of single genes cannot clearly distinguish responding from non-responding cell lines in the *PIK3CA* wild type population. Taken together with the mutation analysis, however, components of the PI3K/Akt pathway represent the targets most prominently mutated and overexpressed in anti-IGF-1R resistant cell lines, yielding a rationale to study the involvement of this pathway in anti-IGF-1R therapy response.

3.3. Anti-IGF-1R/Akt combination therapy in *PIK3CA* wild type cell lines

While mutations in *PIK3CA* reliably predict resistance to anti-IGF-1R therapy in the cell line panel, a number of cell lines are resistant or partially responsive to IGF-1R inhibition despite being *PIK3CA* wt.

As the relevance of the PI3K pathway in anti-IGF-1R response was further strengthened by this first finding, Akt represented a readily druggable target to interfere with this pathway.

Furthermore, a preliminary analysis indicated overexpression of Akt3 as a potential resistance mechanism in *PIK3CA* wild type cell lines, though the differential expression did not reach significance in the final analysis (see 3.2.2). It was hypothesised that targeting Akt could sensitise the *PIK3CA* wild type cell lines to IGF1R inhibition.

To address this hypothesis, the 33 most OSI-906-resistant *PIK3CA* wild type cell lines were subjected to treatment with OSI-906 and the pan-Akt inhibitor GSK690693. Based on the data obtained using the SRB assay, 25 cell lines were selected for in-depth analysis. Exclusion criteria were low absorbance values and duplication of cell lines, which again showed good agreement in this screen.

As a first step of the analysis, the coefficient of drug interaction (CDI) was calculated for each dose combination as described in Section 2.2.5. As a means to classify cell lines, the number of dose points at which the CDI yielded a value below 0.7, which is widely considered an indicator of potential synergy, was calculated for each cell line. The number of dose points with a CDI < 0.7 for each of the 25 cell lines is depicted in Figure 8.

A heterogeneous response of the cell lines to combined IGF-1R and Akt inhibition can be observed: Of the 25 cell lines, 12 do not reach a CDI below 0.7 at a single dose point, while 7 cell lines exhibit at least 4 dose points indicating synergy, each.

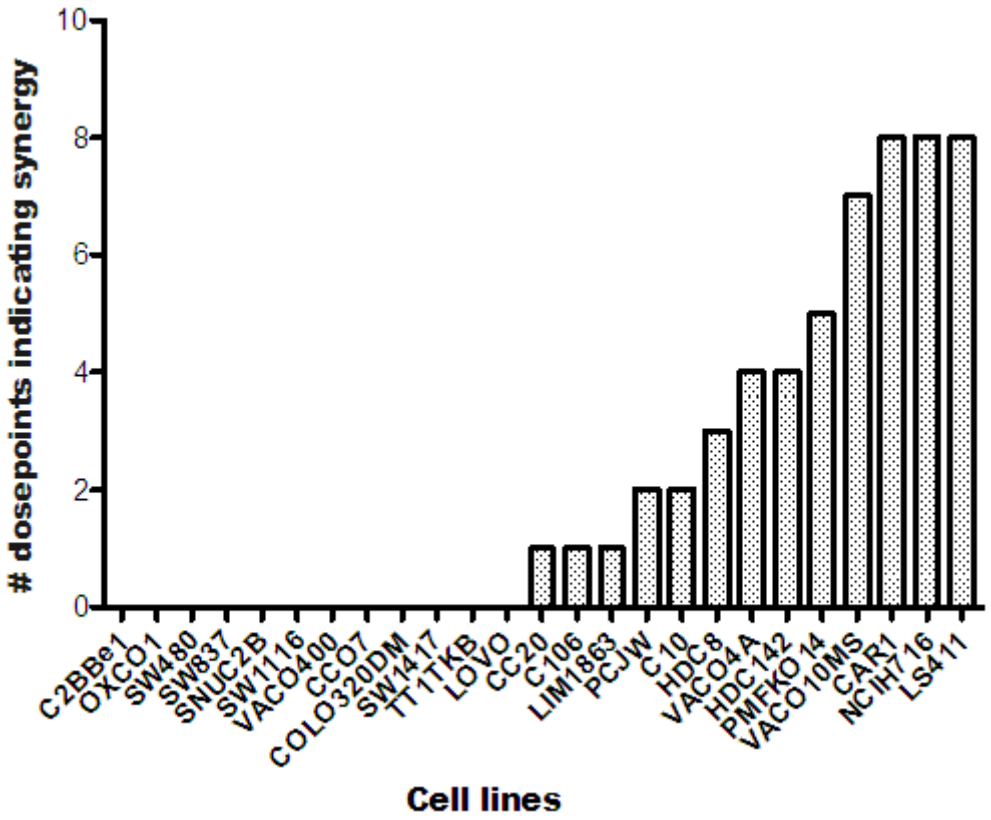

Figure 8: A subgroup of *PIK3CA* wild type cell lines displays synergy of anti-IGF-1R/Akt therapy.
The coefficient of drug interaction (CDI) was calculated at 15 dose combinations of OSI-906 and GSK690693. The number of dose points with CDI < 0.7 was calculated for each cell line and used to rank 25 *PIK3CA* wild type cell lines. To rank cell lines exhibiting the same number of dose points with CDI < 0.7, the lower quartile of the 15 CDIs per cell line was used. 7 cell lines display synergy at more than 4 dose points, while 12 cell lines have no dose point indicating synergy.

For validation of the observed synergy in a subset of CRC cell lines from the panel, the 5 most and the 5 least sensitised cell lines were selected for further analysis based on the data depicted in Figure 8. As several cell lines exhibit no dose point with CDI < 0.7, the lower quartile of CDIs was used to rank these cell lines and determine the 5 cell lines showing the least synergy (see 2.2.5).

The differential response to anti-IGF-1R/Akt combination therapy is underlined by the data depicted in Figure 9. The dose response curves to OSI-906 at varying

levels of GSK690693 indicate substantial synergy over a broad dose range in a subset of cell lines (sensitised, left panel), while the drug combination induces no synergistic effect at all in other cell lines (non-sensitised, right panel). Notably, an antagonistic effect is present in 3 of the 5 non-sensitised cell lines (SW837, C2BBe1, OXCO-1), indicating that different subsets of cell lines might be classified together as non-sensitised in this analysis. The response patterns of smaller subsets of cell lines were validated in several repeat experiments, with varying drug dosage and treatment time, strengthening anti-IGF-1R/Akt synergy as a robust marker for classification of the CRC cell line panel.

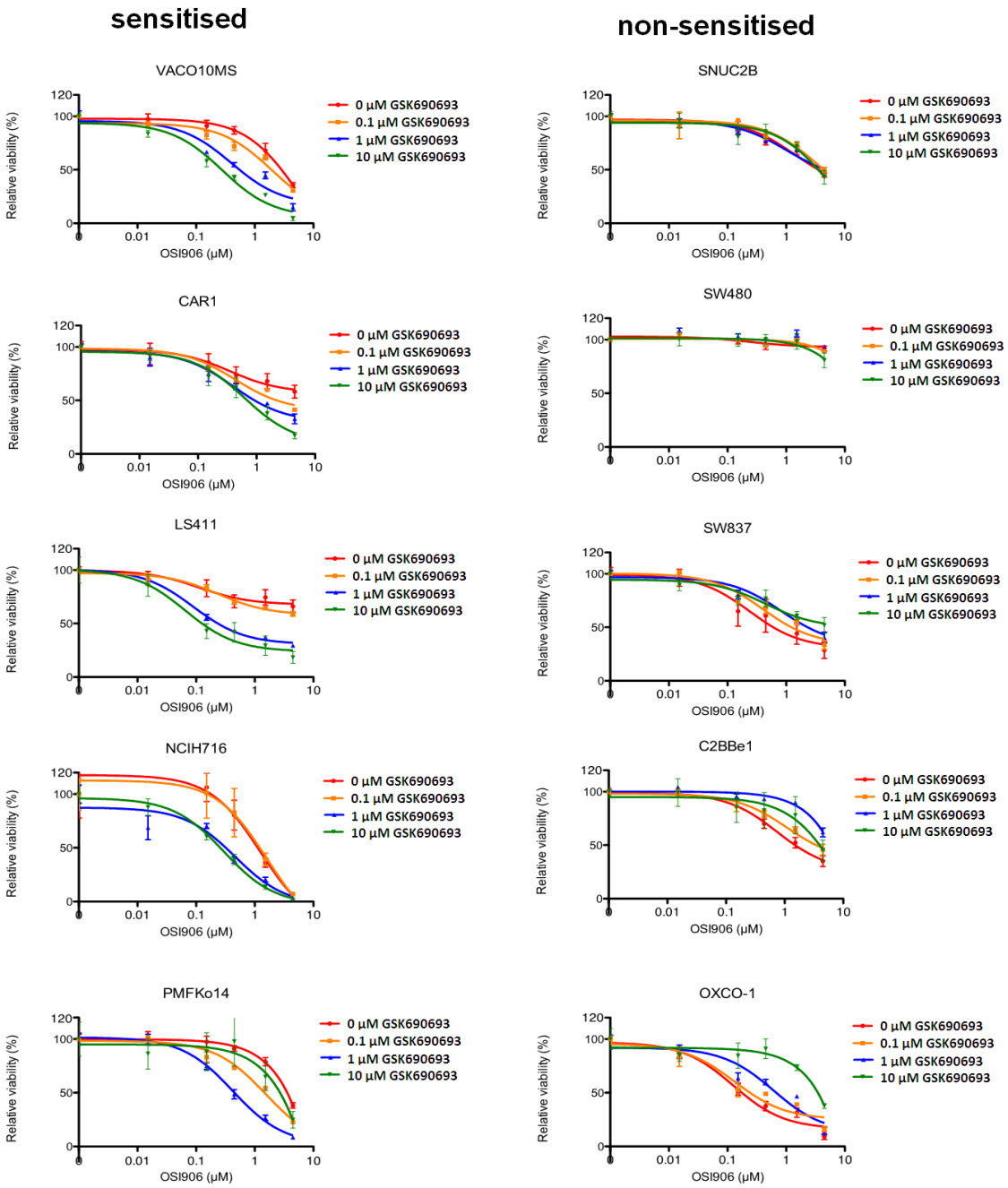

Figure 9: Inhibition of Akt sensitises a subset of cell lines to anti-IGF-1R therapy. Dose-response curves to OSI-906 were recorded at 3 different levels of the pan-Akt inhibitor GSK690693 (orange, blue, green) and for a DMSO control (red). In the sensitised cell lines (left panel), a GSK690693-dose-dependent increase in sensitivity to OSI-906 can be observed, while the non-sensitised cell lines (right panel) do not get sensitised or even show antagonism of the drugs (SW837, C2BBe1, OXCO-1).

To further validate the observed synergy, apoptosis induction by the drugs in monotherapy and combination was investigated. Two non-sensitised (SW837, SW480) and two sensitised (VACO10MS, PMFKo14) cell lines were chosen from the SRB-synergy screen and treated with GSK690693 (1 µM) and OSI-906 (4.5 µM) for 72h, both as monotherapy and in combination. The induction of apoptosis was assessed by flow cytometry after staining with an anti-cleaved caspase 8 antibody. As shown in Figure 10, a strong induction of apoptosis can be observed for both sensitised cell lines under combination therapy conditions.

While in case of PMFKo14 a synergistic pattern of drug interaction can be observed, VACO10MS displays an additional effect of the drugs. Nevertheless, for each cell the combination therapy markedly exceeds apoptosis induction of both monotherapies in the sensitised cell lines, as is depicted in Figure S 3.

In contrast, none of the treatment conditions induces significant apoptosis in the non-sensitised cell lines, which is further considered in Section 4.3. Overall, the strong induction of apoptosis after combination treatment in cell lines classified as combination therapy sensitive based on SRB data strengthens the classification of cell lines according to this criterion.

Figure 10: Strong induction of apoptosis after drug combination is observed in sensitised, but not non-sensitised cell lines.
Two non-sensitised (left panel) and two sensitised (right panel) cell lines were subjected to treatment with OSI-906 and GSK690693, both as monotherapy and combination with each other, for 72h. Depicted are histograms of cleaved caspase-8 levels with the percentage of cells considered apoptotic indicated in the top right corner of each histogram. A strong induction of apoptosis can be observed for both combination therapy sensitive cell lines after combination therapy.

3.4. Characterisation of anti-IGF-1R/Akt combination therapy sensitive and resistant cell lines

To characterise the subgroup of *PIK3CA* wild type cell lines that benefit from combined IGF-1R- and Akt-inhibition, the 5 most sensitised and 5 least sensitised cell lines from the drug combination screen (see Figure 8) were selected for further investigations. Analogous to the characterisation of anti-IGF-1R sensitive cell lines in 3.2, gene mutations and differential expression of genes were analysed for

correlation with drug combination sensitivity. Furthermore, the signalling response to treatment with mono- and combination therapy of the drugs was investigated.

3.4.1. *KRAS* mutations are associated with resistance to anti-IGF-1R/Akt combination therapy

Analysis of the mutation status of the genes introduced in Section 2.1.3 was performed to investigate distinguishing features between the *PIK3CA* wild type cell lines sensitive to the anti-IGF-1R/Akt combination and those resistant. For this purpose, cell lines were assigned to the categories “not sensitised” (no CDI < 0.7 across all dose points) and “sensitised” (at least 1 CDI < 0.7), as indicated by the grey bar in Figure 11.

KRAS, a central protein upstream of the MAPK pathway, turned up as a striking hit in this analysis (see Figure 11). 7 out of 9 *KRAS* mutant cell lines show no sensitisation by adding the Akt inhibitor GSK690693 to OSI-906, suggesting *KRAS* mutations as a potential predictive marker for combination therapy resistance. Analysis of the association between *KRAS* mutation and combination therapy resistant yielded a significant correlation (Table 7). As the MAPK pathway has been shown to exhibit intense cross-talk with and signal in a complementary manner to the PI3K pathway[87,88] – which is targeted by GSK690693 – a constitutively activating mutation upstream of the MAPK pathway could therefore plausibly lead to combination therapy resistance.

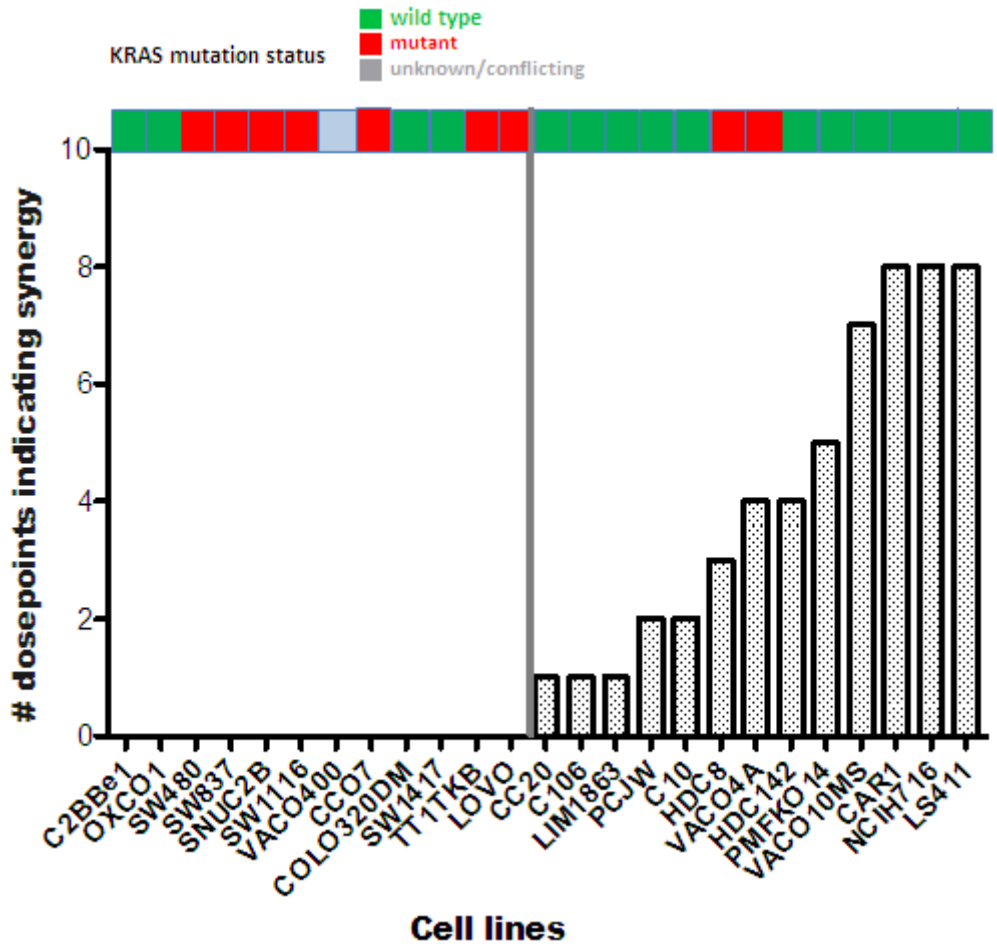

Figure 11: *KRAS* mutation is associated with resistance to anti-IGF-1R/Akt combination therapy.
Cell lines are ranked according to number of dose points with CDI < 0.7, with the *KRAS* mutation status indicated for each cell line. *KRAS* mutant cell lines are enriched in the population without any dose points with CDI < 0.7.

Table 7: *KRAS* mutations are associated with anti-IGF-1R/Akt combination therapy resistance in *PIK3CA* wild type cell lines.
Classification of *PIK3CA* wild type cell lines as combination therapy sensitive or resistant based on presence of a dose point with CDI < 0.7 and correlation analysis with *KRAS* mutation status yields a significant association between *KRAS* mutation and resistance to the combination therapy (p = 0.033, two-tailed Fisher's exact test).

KRAS mutation and anti-IGF-1R/Akt sensitivity		
	IGF1Ri/Akti synergy at ≥ 1 dose point	
p = 0.033	yes	no
KRAS		
wild type	11	4
mutant	2	7

3.4.2. The signalling effects following inhibition of IGF-1R and Akt

The association of resistance to anti-IGF-1R/Akt combination treatment with activating *KRAS* mutations raised the question as to what extent PI3K and MAPK pathway activity are involved in the response to both mono- and combination therapy.

To address this, the expression and phosphorylation states of key proteins of the PI3K and MAPK pathways were assessed, both at baseline and after mono- or combination therapy with OSI-906 and GSK690693.

The baseline protein expression and phosphorylation state, depicted in Figure 12, indicates more activation of Akt at the Ser473 and Thr308 residue among the combination therapy sensitive cell lines. This is in agreement with the hypothesis of an activated PI3K/Akt pathway leading to anti-IGF-1R resistance in some cell lines and the possibility to sensitise these by adding an Akt inhibitor. Interestingly, there

is a good agreement between phosphorylation levels of Akt at the Ser473 residue and phosphorylation of GSK-3β in combination sensitive cell lines. This suggests that the inhibitory phosphorylation at GSK-3β might indeed be conferred by Akt in these cell lines. In combination therapy resistant cell lines, however, GSK-3β phosphorylation seems to be independent of Akt activity, suggesting involvement of further pathways in GSK-3β inhibition in this group of cell lines.

In contrast to the Akt activation pattern, the MAPK pathway component Erk is more markedly activated among combination therapy resistant as compared to combination therapy sensitive cell lines. This hints at an active MAPK pathway as a potential mechanism of resistance to anti-IGF-1R/Akt combination therapy which has been described in the literature[89]. Interestingly, while 3 of the 5 most resistant cell lines are *KRAS* mutant, the highest levels of both Erk and phosphorylated Erk are found in OXCO-1, which is *KRAS* wild type yet combination therapy resistant.

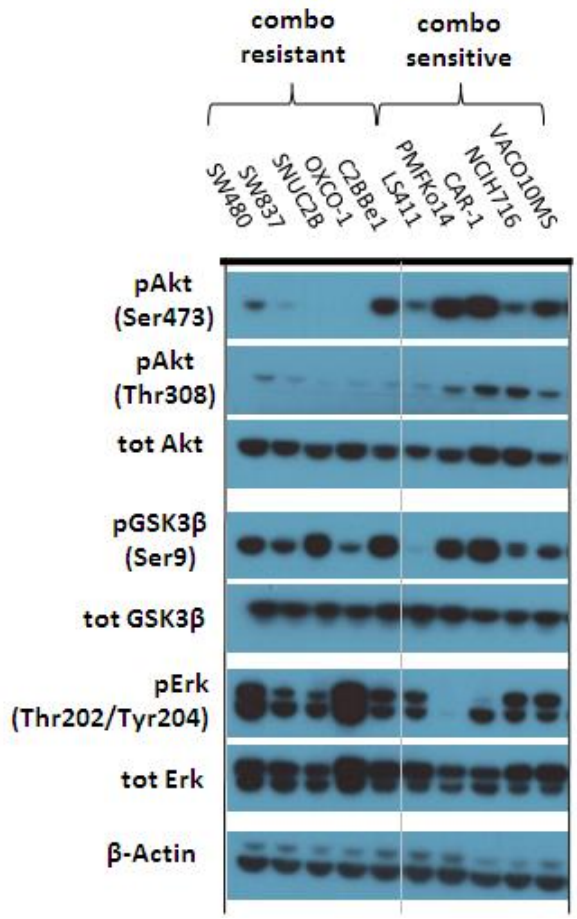

Figure 12: Baseline protein expression across 5 combination therapy resistant and 5 combination therapy sensitive cell lines.
Key PI3K and MAPK pathway proteins and their phosphorylation state were assessed after 72h of culture with 10% FBS. β-actin was probed as a housekeeping control.

As a next step, the effects of OSI-906, GSK690693 and combination treatment on the key signalling molecules were assessed in the same 10 cell lines (shown in Figure 13). The most striking effect is the increase in phosphorylation of Akt at both the Ser473 and Thr308 residue, which occurs in all cell lines after treatment with the Akt inhibitor GSK690693. Although this may seem contradictory at first glance, it is an effect commonly observed with GSK690693[90–92] and may indicate a compensatory activation of Akt while its downstream signalling activity is blocked. This interpretation is supported by the commonly observed decrease in GSK-3β phosphorylation induced by GSK690693 and combination treatment. While this

decrease in GSK-3β phosphorylation is present in both combination therapy sensitive and resistant cell lines, 4 out of 5 sensitive cell lines display barely detectable pGSK-3β levels after combination treatment. In contrast, the combination therapy resistant cell lines exhibit more residual GSK-3β activation after combination treatment.

In summary, cell lines sensitive to combination treatment generally exhibit higher baseline activation levels of Akt, which correlates well with p-GSK3 β levels, and a more pronounced inhibition of GSK-3β phosphorylation upon combination treatment. Despite these observations, the variation within each category of cell lines indicates that different signalling pathways are active in individual cell lines of a category and may well contribute to the differential response to anti-IGF-1R/Akt combination therapy.

After the insights into the role of *KRAS* mutations and Akt signalling in combination therapy response, the differential expression of genes was to be examined as a potential mediator of resistance or sensitivity.

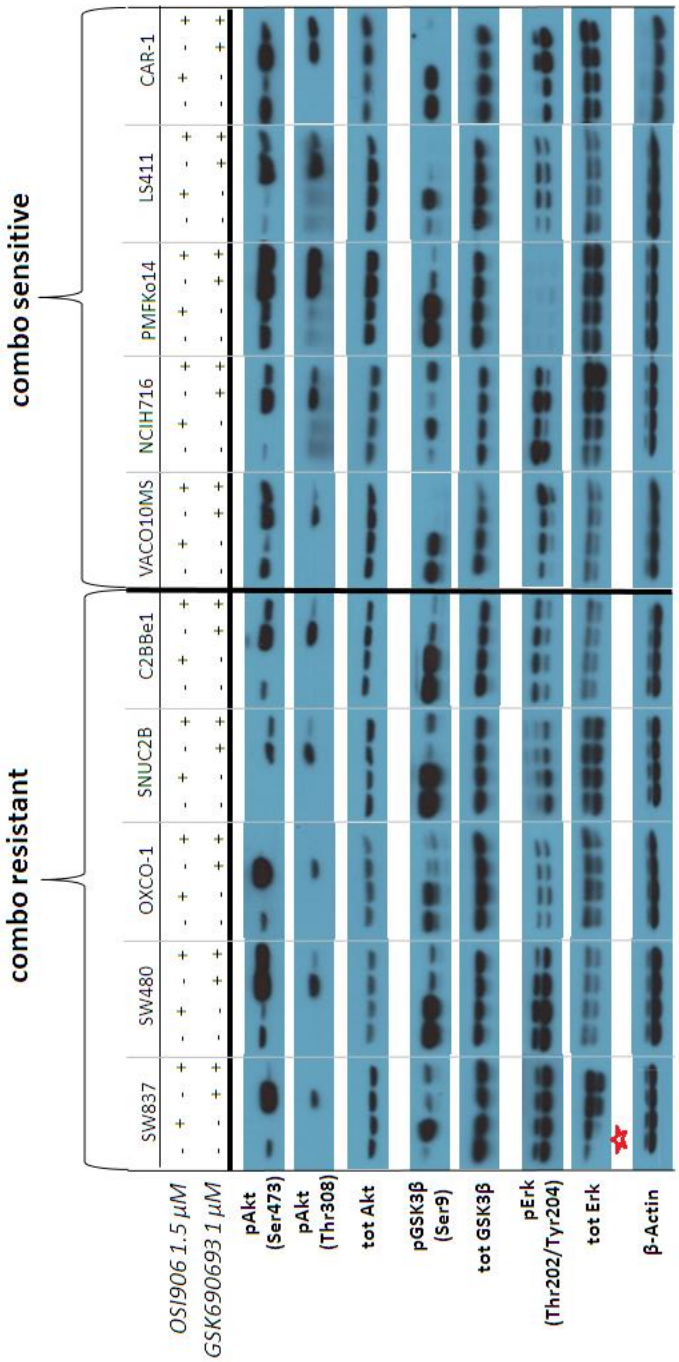

Figure 13: Effects of IGF-1R and Akt inhibition on PI3K and MAPK signalling. 5 combination therapy sensitive and 5 combination therapy resistant cell lines were treated with DMSO, OSI-906, GSK690693 or the combination of the drugs for 72h before the expression and phosphorylation state of key signalling proteins of the PI3K and MAPK pathway were assessed. β-actin was probed as a housekeeping control. The total Erk levels in SW837 (red star) were not detected properly due to a technical error in incubation with the developing solution.

3.4.3. CD24 is expressed at lower level on both the mRNA and protein levels in combination therapy resistant *PIK3CA* wild type cell lines

In a third approach to find distinguishing features between sensitised and non-sensitised cell lines, the microarray dataset on mRNA expression levels was used to analyse differential gene expression between the two groups. As depicted in Figure 14, the cell surface anchored glycoprotein CD24 is expressed at lower level in the 5 *PIK3CA* wild type cell lines that are resistant to combined Akt and IGF-1R inhibition (green) as compared to the 5 most sensitive cell lines (blue). The striking pattern of differential expression yielded a rationale to study the role of CD24 in anti-IGF-1R therapy response in CRC.

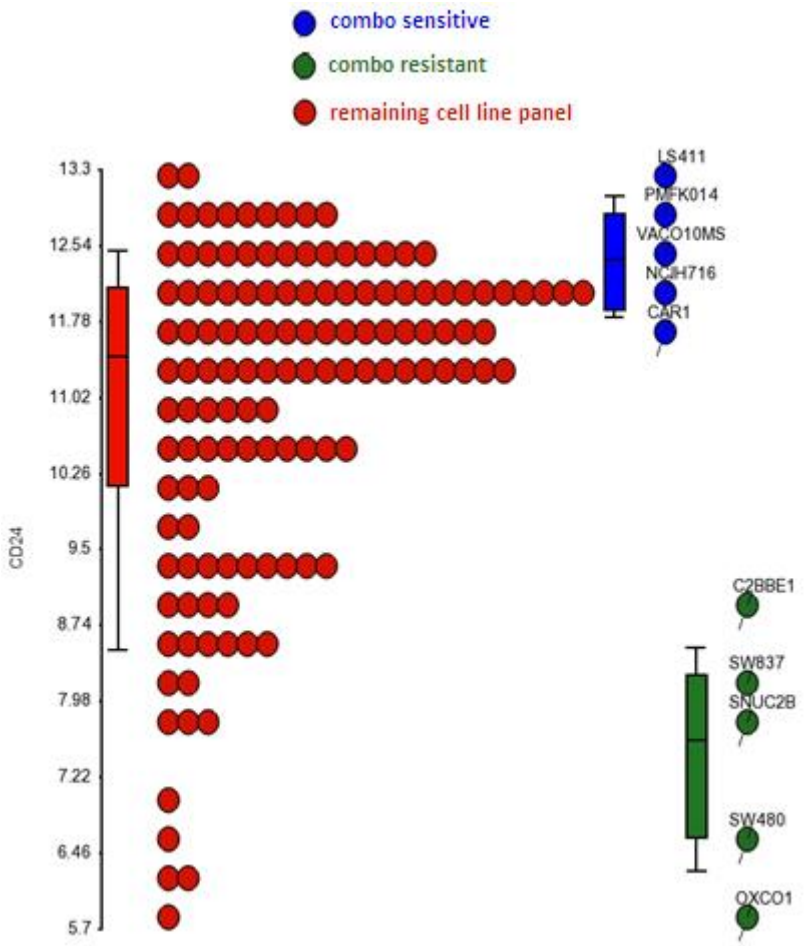

Figure 14: CD24 mRNA is expressed at lower level in *PIK3CA* wild type cell lines resistant to combination treatment.
mRNA expression levels were compared amongst *PIK3CA* wild type cell lines, differentiating between the 5 most combination therapy sensitive (blue) and combination therapy resistant (green) cell lines. The remaining cell lines are depicted in red. The cell surface anchored glycoprotein CD24 was found to be expressed lower in combination therapy resistant as compared to sensitive cell lines (32 fold, corrected p value < 0.05).

As a first step to validate CD24 as being differentially expressed between combination treatment sensitive and resistant cell lines, a flow cytometry based approach was utilised. The same 10 sensitised and non-sensitised cell lines as for the microarray analysis were stained for surface CD24 expression and analysed using flow cytometry. As shown in Figure 15, surface CD24 expression is in good agreement with the observed overexpression of CD24 mRNA in sensitised cell lines. The 5 sensitised cell lines (Figure 15, top panel) exhibit strikingly higher levels

of surface CD24 than the non-sensitised cell lines (bottom panel). Notably, some of the non-sensitised cell lines (such as SNUC2B and SW837) show CD24 expression in a subpopulation of cells, while other cell lines (such as OXCO1) appear to be completely negative for CD24 surface expression, which is in good agreement with the microarray data depicted in Figure 14.

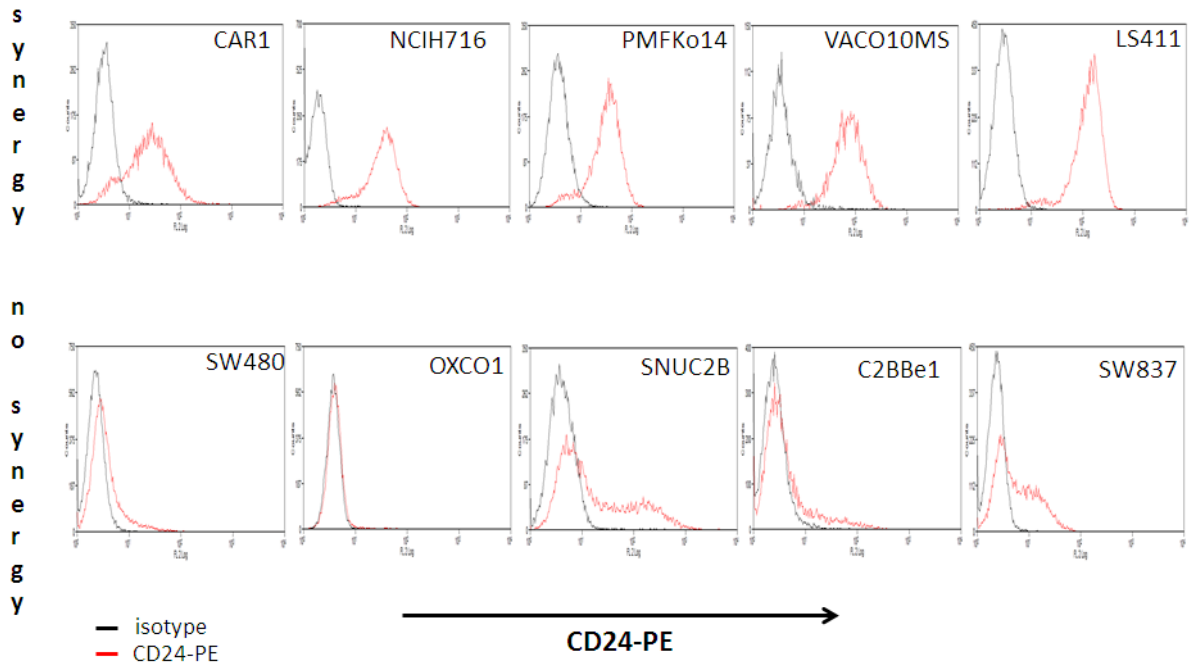

Figure 15: CD24 protein is expressed at lower level in *PIK3CA* wild type cell lines resistant to combination treatment.
The 5 sensitised and non-sensitised cell lines depicted in Figure 9 were analysed for CD24 expression using flow cytometry. In all sensitised cell lines (top panel), CD24 is highly expressed as demonstrated by the strong shift in CD24 (red line) compared to the isotype control (black line). Conversely, expression levels are lower in non-sensitised cell lines (bottom panel). Notably, while some non-sensitised cell lines are negative for CD24 surface expression (OXCO1), others exhibit a small CD24- high population (SNUC2B, SW837) indicated by the presence of a tail or shoulder in the CD24 expression histogram (red line).

Taken together, anti-IGF-1R/Akt combination therapy sensitive cell lines were demonstrated to differ from resistant cell lines in *KRAS* mutation status, Akt signalling at baseline and after treatment, and expression of the surface-anchored glycoprotein CD24. As the latter finding showed the most striking pattern and is

supported by a rapidly evolving body of literature on CD24 in cancer stem-like cell biology and response to IGF-1R-directed therapy, it was investigated in more depth.

3.5. Functional implications of CD24 in IGF-1R-directed therapy response

Having validated differential expression of CD24 at the mRNA and protein levels as a distinguishing factor between sensitised and non-sensitised cell lines, the role of CD24 in IGF-1R directed therapy response was to be investigated in more depth.

Based on the findings from 3.4., it was hypothesised that low CD24 expression predicts resistance to combined anti-IGF-1R/Akt therapy and vice versa. To address this, it was investigated how CD24 expression differences within cell lines affect treatment response. The observation that small subpopulations of CD24 high cells exist in some combination therapy resistant cell lines was exploited for this purpose:

SW480 and SNUC2B, two combination therapy resistant cell lines, were selected for the presence of a sub-population of CD24 high cells whereas CAR1, a combination therapy sensitive cell line, was chosen based on the presence of a CD24- cell population (Figure 15). These cells were sorted according to their surface CD24 levels as described in materials and methods (sorting characteristics are depicted in Figure S 6-8).

The resulting 3 subpopulations of each cell line (CD24 high, CD24 low and bulk) were subsequently analysed as to their ability to form colonies and sensitivity to mono- and combination therapy against IGF-1R and Akt.

The results from the colony formation assay depicted in Figure S 4 indicate that the sorted populations from all 3 possess the ability to form colonies in 2D. However, an inter-cell line variability in clonogenicity can be observed, with CAR-1 yielding the lowest number of colonies.

Regarding sensitivity to treatment with OSI-906 and GSK690693, the CD24 high subpopulations of SNUC2B and SW480 appear to be slightly more sensitive than the unselected and CD24 low subpopulations (Figure 16, upper two panels). This finding would support the association between CD24 expression and combination therapy sensitivity, yet it has to be treated with caution as these data stem from a single colony formation experiment. Furthermore, in the combination therapy sensitive cell line CAR-1 (Figure 16, lower panel), the CD24 low population displays most sensitivity to the drugs in mono- and combination therapy.

Taken together, the data yield an inconclusive but promising pattern and further investigations in a larger set of cell lines are warranted to obtain a clearer view of the characteristics of CD24-sorted subpopulations within a cell line. In addition to this, other approaches for investigating the role of CD24 in anti-IGF-1R therapy response, such as drug-induced induction or depletion of CD24, are outlined in Section 4.5.

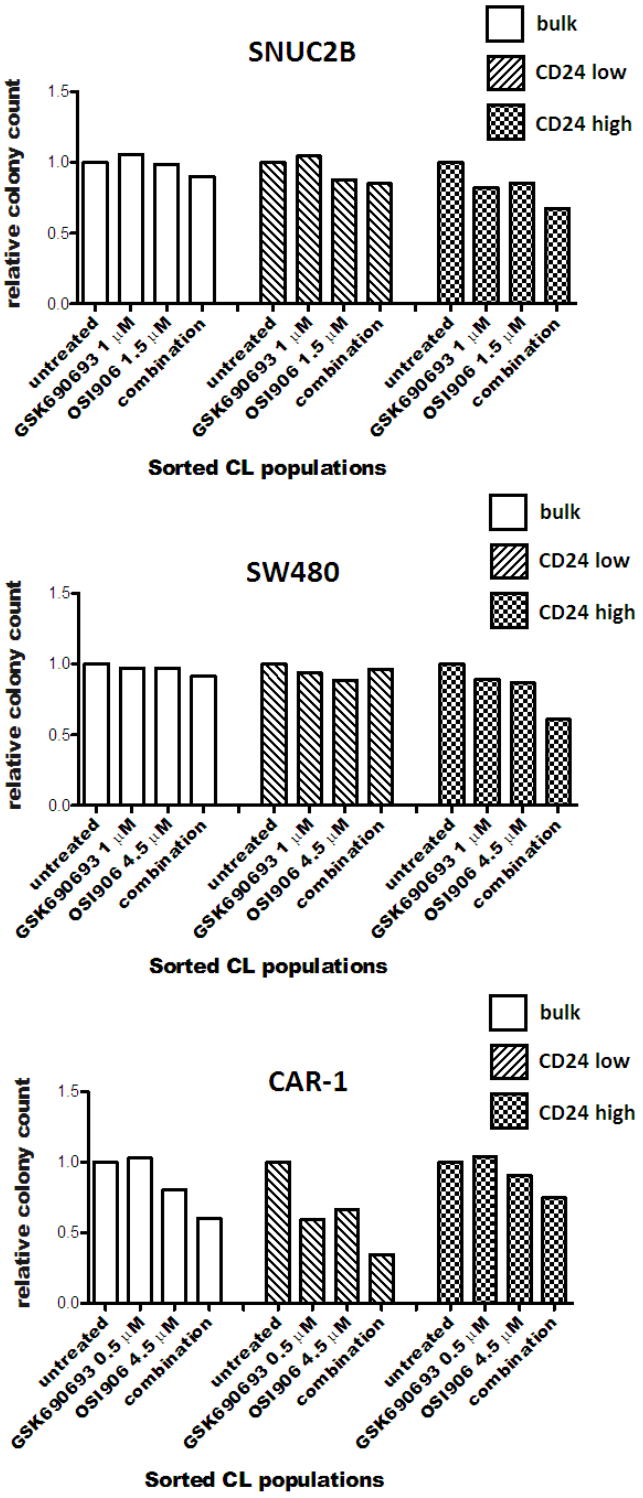

Figure 16: CD24-sorted subpopulations of cell lines vary in response to combination treatment.
CD24 low, high and unsorted cells of 2 combination therapy resistant (SNUC2B, SW480) and one combination therapy sensitive (CAR-1) cell lines were grown under DMSO, OSI-906, GSK690693 or combination conditions until sufficient colony sizes were obtained. A modest effect of the drugs can be observed for bulk and CD24 negative SNUC2B and SW480 cells, which is slightly increased in CD24 high cells. For CAR-1, the CD24 low population appears to be most sensitive to both drugs in monotherapy and in combination.

3.6. Knockdown of individual Akt isoforms in combination with anti-IGF-1R therapy

A substantial synergy was observed between OSI-906 and the pan-Akt inhibitor GSK690693 in a subset of *PIK3CA* wild type cell lines. While pan-Akt inhibition is the clinically most feasible way to interfere with Akt action, the 3 different isoforms of Akt have shown distinct functionalities in a variety of tissues and diseases (see Section 1.2.1), which contributes to a better understanding of the underlying mechanisms. Furthermore, as introduced in Section 3.2.2, a preliminary analysis had indicated Akt3 overexpression as a potential mechanism of resistance to IGF-1R inhibition in *PIK3CA* wild type cell lines. In the light of these considerations it was of interest to investigate the contribution of the individual Akt isoforms to the sensitisation of CRC cells to anti-IGF-1R therapy.

To address this, the 3 Akt isoforms were knocked down individually using siRNA in the 10 combination therapy sensitive and combination therapy resistant cell lines before treatment with OSI-906. As controls, an untreated as well as a scrambled siRNA treated sample were included. One combination therapy sensitive (VACO10MS) and one resistant (C2BBe1) cell line were excluded from the analysis due to high deviations in drug response in the control sample.

The results depicted in Figure 17 indicate a general tendency towards sensitisation after knockdown of any of the 3 isoforms of Akt in the combination therapy sensitive cell lines (left panel, A). Akt1 knockdown induces the strongest sensitisation in 3 out of 4 combination therapy sensitive cell lines, while Akt3 does so in 1 (PMFKo14). In the combination therapy resistant cell lines (right panel, B), less or no sensitisation can be observed after knockdown of the Akt isoforms. In case of most cell lines,

however, deriving reliable conclusions is rendered impossible due to variations between the untreated and scrambled control.

Taking into consideration the Akt isoform mRNA expression levels from the microarray dataset, no clear association between initial expression level and sensitisation after knockdown can be confirmed. The only emerging patterns are higher expression levels of Akt1 in the combination therapy resistant as compared to the combination therapy sensitive cell lines.

In summary, the data indicate a tendency towards sensitisation of the combination therapy sensitive cell lines after Akt isoform knockdown, while they do not allow identification of a single isoform of Akt as responsible for synergy when combined with anti-IGF-1R therapy.

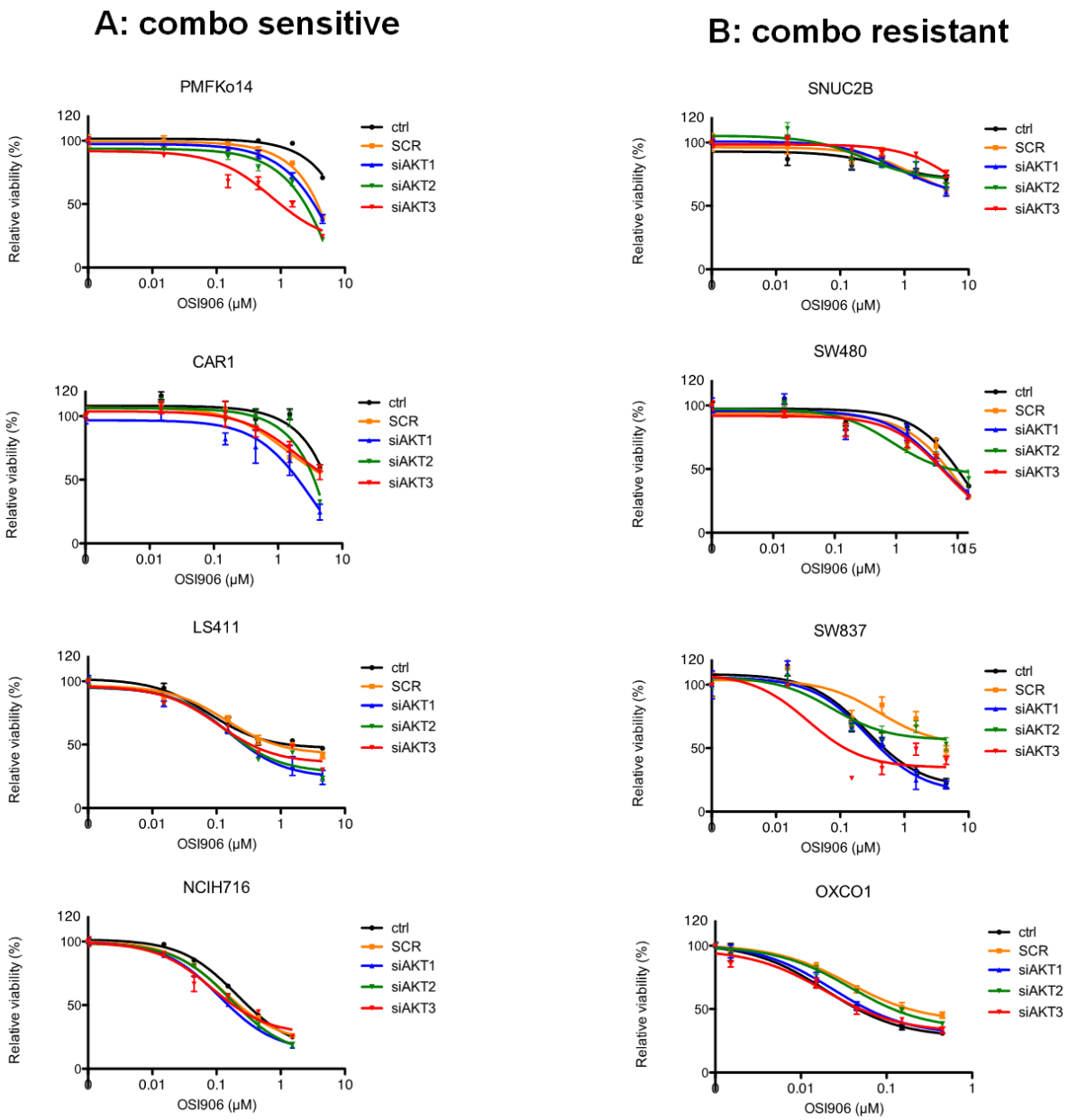

Figure 17: Knockdown of individual Akt isoforms induces heterogeneous sensitisation to OSI-906.

The 3 Akt isoforms (Akt1: blue; Akt2: green; Akt3: red) were knocked down using siRNA in 8 combination therapy sensitive or resistant cell lines. Untreated (black) and scrambled siRNA treated (orange) samples were used as controls. After 24h of siRNA knockdown, cells were split into 96-well plates and treated with OSI-906 to determine the sensitising effect of single isoform knockdown on IGF-1R inhibition. Generally, more sensitisation for each individual Akt isoform can be observed in the combination therapy sensitive (A, left panel) than in the combination therapy resistant (B, right panel) cell lines.

Chapter 4: Discussion

The results of this thesis are discussed in the context of previous findings below. I also consider potential next steps and the limitations of the study at hand. A summary of the most relevant results is provided at the end of this chapter.

4.1. Anti-IGF-1R response-based classification of cell lines

As a first step of my research, the sensitivity profile of a cell line panel to anti-IGF-1R was analysed to confirm in-vitro efficacy of the drugs used and lay the basis for later association studies. Sensitivity to figitumumab and OSI-906 in 82 cell lines was analysed based on data previously generated in the laboratory. The good correlation between response to figitumumab and OSI-906 was previously observed in the analysis of subsets of these cell lines in the group and represents a previously unreported finding in large cell line panels. Considering the different mechanisms of action of the therapeutics outlined in Section 1.2.3, this finding supports the interpretation that cell line sensitivity to figitumumab and OSI-906 is due to functional inhibition of IGF-1R and not off-target or primarily IR-mediated effects. It also justifies combining sensitivity to both figitumumab and OSI-906 for classification of cell lines.

While this thesis for the first time brings together response to figitumumab and OSI-906 in a large CRC cell line panel, studies have been performed on both compounds in smaller cell line populations:

For OSI-906, two studies are available, one screening 27 CRC cell lines for OSI-906 sensitivity (Pitts study)[89] and the other investigating sensitivity and the

involvement of the MAPK pathway in 13 CRC cell lines (Flanigan study)[93]. As the Flanigan study investigated a subset of the cell lines characterised in the Pitts study, the drug response of this thesis will be compared to the latter, while the former provides context for the and drug combination experiments performed in this thesis. Figitumumab has been studied in a panel of 93 NSCLC, breast and colorectal cancer, comprising 21 CRC cell lines (Pavlicek study)[67].

Comparing the overlapping cell lines from this thesis and the aforementioned studies yields valuable insights into experimental reproducibility and data analysis.

After removing duplicate and non-overlapping cell lines from the Pitts study, 4 sensitive and 12 resistant cell lines are represented in the panel used in this thesis. When looking at these cell lines based on the GI_{50} values from the thesis dataset, 4 of 4 sensitive cell lines would have been classified the same, which holds true only for 5 of the 12 resistant cell lines. However, this comparison has limited significance since the treatment was performed for 3 doubling times in this thesis, whereas all cell lines were treated for 72h in the Pitts study.

In the Pavlicek study[67], the GI50 value of Figitumumab was determined in 21 CRC cell lines using the CellTiter-Glo assay. Cell lines with a GI50 < 100 nM (corresponding to 50% growth inhibition at a dose of 14.6 µg/ml, for comparison with this thesis) were classified as sensitive, while all other cell lines were considered to have a GI50 > 1 µM, and therefore resistant. After proceeding in the same way as for the Pitts study, 7 sensitive and 10 resistant cell lines could be compared to the dataset of this thesis. Of 7 sensitive cell lines, 6 reached a GI > 50% at 10 µg/ml figitumumab, supporting their sensitivity. 8 of the 10 cell lines considered resistant in the Pavlicek study displayed a GI < 50% at this dose point,

although proper comparison was not possible due to the Pavlicek study omitting IC50 values between 100 nM and 1 µM from its study and lack of response data above 10 µg/ml from the dataset of this thesis. Again, the treatment was performed for 72h irrespective of cell line-specific doubling time and using a different assay system, which highlights the limited comparability of the datasets. Overall, classification agreement was better for figitumumab than for OSI-906, which might be at least partially attributable to the almost complete lack of response in resistant cell lines discussed in Section 3.1 and Figure 5.

Combining the Pitts and Pavlicek studies, there are 13 cell lines for which data are available from both studies. Of 5 cell lines considered sensitive to figitumumab, 3 are classified as sensitive and 2 as partially responsive to OSI-906. 7 out of 8 cell lines resistant to figitumumab are regarded as resistant to OSI-906, with the remaining cell line reaching borderline resistance. This agreement between sensitivity to the two therapeutics further supports the IGF-1R-inhibition-based nature of therapy resistance.

Using the criteria of this thesis, 4 cell lines are classified in disagreement with the two other studies: LS123, T84, LS1034, and C2BBe1, which are consistently considered either resistant or sensitive by both studies, are classified as partially responsive based on figitumumab and OSI-906 response in this thesis' analysis. As each of these cell lines is reaching borderline sensitivity/resistance, the differing classification can be attributed mainly to the different thresholds, treatment duration and assay system applied in this thesis.

In summary, using the large CRC cell line panel and the $GI_{[Figitumumab]10\mu g/ml}$ measure instead of a GI50-based classification resulted in a more nuanced picture of anti-

IGF-1R response in CRC cell lines. Based on the extensive datasets on drug response in a large cell line panel, a measure for classification was introduced, combining responsiveness to both OSI-906 and figitumumab. This comprehensive way of classifying cell lines is supported by the good agreement with monotherapy-based classification from two independent studies.

4.2. Predictive factors of anti-IGF-1R response

The search for biomarkers of anti-IGF-1R therapy response in colorectal cancer using the cell line panel was of central interest in this thesis. Mutations in *PIK3CA* exons 9 and 20 were identified as the most powerful predictors of anti-IGF-1R therapy resistance. Considering the importance of the PI3K pathway downstream of IGF-1R introduced in Section 1.2.1, this finding could well be interpreted as a constitutive action of the PI3K resulting In IGF-1R independence. In fact, activation of PI3K/Akt signalling has been demonstrated to be able to confer resistance to anti-IGF-1R therapy in rhabdomyosarcoma[94].

Considering the finding of *PIK3CA* as a potentially predictive marker of anti-IGF-1R resistance in colorectal cancer in the light of other studies on biomarkers for this purpose, an interesting pattern emerges. In the Pitts study[89], the mutational status of *KRAS*, *BRAF* and *PIK3CA* was investigated for association with sensitivity to OSI-906 in a panel of 27 CRC cell lines. While none of the correlations reached significance, an association of *KRAS* wild type with OSI-906 sensitivity was observed, which does not hold true in the larger cell line panel used in this thesis (Table S 5). The assessment of *PIK3CA* mutation association epitomises the relevance of sufficient population size to pick up correlations: In the panel of 27 cell

lines, 6 are considered sensitive to OSI-906, 1 of which is *PIK3CA* mutant. These small numbers make the analysis quite vulnerable to the particular selection of cell lines since, for example, exclusion of a single cell line would have resulted in a strikingly different conclusion in this case. The results reported in the Pavlicek study[67] underline the relevance of large cell line panels for a single cancer entity to discover molecularly defined subgroups of cell lines with regard to treatment response. While a panel of 93 cell lines characterised for 19 mutations represents a valuable tool to perform mutation/drug-response association studies, the analysis performed by Pavlicek and colleagues highlights the differences between colorectal cancer and lung or breast cancer. In a pooled analysis of all cell lines from different tissues, mutations in *APC* and *CTNNB1* (β-catenin) are associated with sensitivity to figitumumab. This, however, does not hold true for a sub-analysis of CRC cell lines alone, which is in line with the analysis of this thesis (see Table S 1, Table S 6). Importantly, the authors noted that the increased prevalence of these mutations in colorectal cancer cell lines, which also tend to be more sensitive to figitumumab treatment than other cancer cell lines, can therefore explain the observed correlation in the pooled analysis.

In summary, the use of a large CRC cell line panel allowed identification of an association between *PIK3CA* mutations in exon 9 or 20 and resistance to anti-IGF-1R therapy. This was not previously detected in cell line panel screenings with anti-IGF-1R therapeutics, potentially due to insufficient panel size.

Considering mRNA expression associations with anti-IGF-1R response, no promising candidate gene turned up as significant in expression comparisons

between the 10 most sensitive and 10 most resistant cell lines to either OSI-906 or figitumumab after correction for testing 54,675 probe sets. Based on reported associations from the literature, a small panel of candidate genes was assembled and assessed for correlation with anti-IGF-1R sensitivity across all 73 non-duplicate cell lines.

There are conflicting reports in the literature concerning the association of IGF-1R expression and anti-IGF-1R response, though these have been generated using different therapeutics[67,89,95]. In the thesis dataset, mRNA expression levels of IGF-1R itself were not correlated significantly with therapy response to either OSI-906 or figitumumab. This behaviour is analogous to the situation for the direct effect of anti-EGFR antibodies[14] in colorectal cancer.

In the Pitts study[89], increased expression of metallothionin 2A (MT2A) was found to be associated with resistance to IGF-1R inhibition. This finding could be confirmed in the candidate gene panel ($p \approx 0.006$ before correction), though not reaching significance after correction for testing of the 35 genes in the panel. As a role of MT2A in anti-IGF-1R therapy response was validated through knockdown in both colorectal[89] and breast cancer[96] cell lines, a better understanding of the role of MT2A could result in new combination therapy strategies with anti-IGF-1R drugs. The Pitts study also reported high expression of MAP2K6, a component of the MAPK pathway, to be associated with sensitivity to IGF-1R inhibition. This finding only reached significance ($p \approx 0.03$) before correction for multiple hypotheses testing. Other potential associations reported in the Pitts study did not reach significance for association with OSI-906 even before correcting for multiple hypotheses testing.

Of the potential biomarkers for figitumumab response which were reported in the Pavlicek study[67], two reached significance only before correction for multiple hypotheses testing in the datasets of this thesis. In accordance with the Pavlicek study, low expression levels of IGFBP6 and IGF2BP3 were associated with sensitivity to Figitumumab ($p \approx 0.03$ each, before correction).

Taken together, mutations in *PIK3CA* represent the most promising predictor of anti-IGF-1R therapy resistance identified in this thesis. This finding could be validated by gene-editing-based introduction of activating *PIK3CA* mutations in *PIK3CA* wild type anti-IGF-1R sensitive cell lines to assess if it is sufficient to induce resistance. After further validation, *PIK3CA* mutational profiling could be implemented in future clinical trials in CRC patients.

4.3. Sensitisation to anti-IGF-1R therapy by adding an Akt inhibitor

Based on the association of constitutively activated PI3K/Akt pathway signalling and anti-IGF-1R resistance, described both in the literature[94,97] and this thesis, addition of the pan-Akt inhibitor GSK690693 to OSI-906 represented a rational approach that had not been investigated before in colorectal cancer. Indeed, synergistic interaction could be observed in a subset of *PIK3CA* wild type cell lines, further strengthening the importance of the PI3K pathway in IGF-1R downstream signalling in colorectal cancer.

The two compounds were combined over a broad dose range (15 nM – 4.5 µM OSI-906 and 100 nM – 10 µM GSK690693) in 33 *PIK3CA* wild type cell lines, all of which were not sensitive to OSI906 as monotherapy.

The number of dose points indicating synergy of the two drugs through a CDI < 0.7 (see Section 2.2.5 and 3.3) provided an objective and robust measure to classify the panel of cell lines. This allowed ranking of the cell lines according to drug combination sensitivity as well as identification of a subset of cell lines with especially strong synergy for further analysis.

It should be noted that this classification is based on cell viability decrease assessed using the SRB assay. Validation of these findings was approached using an apoptosis induction assay based on cleaved caspase 8 detection. The flow cytometry-based apoptosis assessment validated the classification of cell lines as it yielded increased numbers of apoptotic cells after drug combination. Apoptosis induction generally corresponded well to the viability decrease observed using the SRB assay. It should be noted, however, that the levels of apoptosis induction both with mono- and combination therapy in the 2 combination therapy resistant cell lines which were used are rather low, which was expected for SW837. Expansion of the apoptosis assessment to a 10 cell line combination therapy sensitive/resistant panel could therefore shed light on the question if this is a genuine picture in combination therapy resistant cell lines or an artefact due to small cell line number.

This thesis does not represent the first study of drug combinations in CRC involving OSI-906, as addition of a MEK inhibitor[93] and a p70S6K inhibitor[98] have previously been assessed in smaller CRC cell line panels. The studies indicated synergy of the drugs in 11 of 13 and 2 of 2 cell lines, respectively.

Importantly, OSI-906 is already being assessed in early stage clinical trials in combination with the EGFR inhibitor erlotinib in advanced solid tumours with promising first results[76]. In an early stage clinical trial in a cohort of Ewing's sarcoma, addition of the mTOR inhibitor temsirolimus to an anti-IGF-1R inhibitor yielded promising activity and manageable toxicity[99], although clinical data could not confirm efficacy of anti-IGF-1R/mTOR combination using OSI-906 and everolimus in CRC[100].

Taken together, these studies demonstrate that not only the PI3K pathway, but also signalling through other surface receptors and pathways can represent appropriate targets for combination with anti-IGF-1R therapy. In this thesis, a pan-Akt inhibitor was chosen to investigate the role of this specific pathway in anti-IGF-1R therapy response, supported by the fact that Akt represents a druggable target assessed in clinical trials[101]. The finding that *KRAS* mutations are associated with resistance to combined anti-IGF-1R/Akt therapy suggests potential for addition of a MEK inhibitor to the combination therapy. However, blockade of three major signalling proteins may lead to intolerable toxicities in patients, underlining the value of further investigations as to the optimal target to interfere with PI3K, MAPK or other signalling pathways downstream of IGF-1R. The studies on combination with mTOR and p70S6K inhibition, which represent overlapping signalling nodes of the MAPK and PI3K pathways, could well yield valuable insights on resistance mechanisms to anti-IGF-1R-based combination therapies when extended to in larger cell line panels.

4.4. Signalling response to combined anti-IGF-1R/Akt therapy

To better understand the differential response to anti-IGF-1R/Akt combination therapy amongst cell lines, the signalling response was investigated in the context of drug sensitivity and mutational profile.

While *KRAS* mutations did not correlate with overall responsiveness to anti-IGF-1R treatment (see Table S 5), they proved to be associated with resistance to combined anti-IGF-1R/Akt therapy in *PIK3CA* wild type cell lines (see Figure 11 and Table 7). A possible interpretation of this observation could be constitutive activation of the MAPK pathway rendering cell lines resistant to blockade of an upstream (IGF-1R) and alternative pathway (PI3K). This finding again highlights the importance of PI3K and MAPK signalling as interacting pathways downstream of IGF-1R as discussed above.

It also yielded a clear rationale to study the baseline and adaptive activation state of proteins from both pathways, as depicted in Figure 12 and Figure 13. While antibodies targeted at other key proteins in IGF-1R signalling did not yield western blots of sufficient quality to allow interpretation, the results depicted for the two phosphorylation sites of Akt (Ser473 and Thr308), phosphorylated Erk and GSK-3β and the respective total protein levels provide an insight into PI3K and MAPK signalling in 10 combination therapy resistant or sensitive cell lines.

The general activity of OSI-906 and GSK690693 was confirmed in the cell line panel. For GSK690693, an increased phosphorylation of Akt after treatment has been reported consistently in the literature[90–92]. This was observed in 10 out of 10 cell lines in this thesis. In the case of OSI-906, the direct effect on IGF-1R and IR phosphorylation could not be assessed due to nonspecific binding of the applied

anti-IGF-1R antibodies. However, a slight but noticeable decrease in Akt phosphorylation levels at the Ser473 residue, which is a known downstream effect, could be observed in 9 out of 10 cell lines. The remaining cell line did not display sufficient baseline Akt Ser473 phosphorylation to allow assessment.

Taking together baseline protein phosphorylation state and signalling response to treatment displayed and described in Section 3.4.2, an interesting pattern emerges: Combination therapy sensitive cell lines tend to have higher phosphorylation levels of Akt at both the Ser473 and Thr308 residues, while 4 and 5 out of 5 combination therapy resistant cell lines display low phosphorylation levels at Ser473 and Thr308. In combination therapy sensitive cell lines, the phosphorylation of Akt at the Ser473 residue corresponds well to the phosphorylation levels of GSK-3β. However, in combination therapy resistant cell lines, GSK-3β phosphorylation appears to be independent of the Akt phosphorylation state, suggesting alternative pathways to be involved in inhibition of GSK-3β in these cell lines.

The finding that both the Akt inhibitor GSK690693 and combination treatment induce a more pronounced decrease of GSK-3β phosphorylation in combination therapy sensitive cell lines is in agreement with this interpretation and also provides a potential explanation for the differential sensitivity to combination treatment: GSK-3β phosphorylation and inhibition might be dependent on Akt signalling in combination therapy sensitive cell lines, which is found at baseline, while GSK-3β is inhibited through phosphorylation by alternative pathways in combination therapy resistant cell lines. As a result, inhibition of Akt affects GSK-3β phosphorylation and cell survival in combination therapy sensitive cell lines, while alternative pathways maintain a residual GSK-3β phosphorylation in combination therapy resistant cell lines, preventing effective induction of apoptosis in these cell lines. It should be

noted that combination treatment does not deplete p-Akt levels completely in any of the combination therapy sensitive cell lines. However, the literature on GSK690693 suggests consideration of the downstream partners of Akt to assess inhibition of this pathway, as the striking increase in p-Akt after treatment does not result in pathway activation and may mask effects of the combination therapy[90–92].

Beyond these main differences between combination therapy sensitive and combination therapy resistant cell lines, the variation of signalling within each category highlights the likely presence of different molecular profiles in each category. For example, C2BBe1 is the only combination therapy resistant cell line with high p-Akt levels at baseline while SW837 and OXCO-1 are the only cell lines to display almost complete depletion of p-Akt after combination treatment. The combination therapy sensitive cell line LS411 differs from the sensitive subgroup as it displays low Akt phosphorylation at the Ser473 residue at baseline, yet in contrast to the combination therapy resistant cell lines this corresponds with low pGSK-3β levels. PMFKo14 is the only one of the 10 cell lines to display low Erk phosphorylation at baseline. Finally, NCIH716 is the only combination therapy sensitive cell line to display detectable GSK-3β phosphorylation after combination treatment. The fact that NCIH716 is the only suspension cell line in the signalling analysis and its differing signalling with respect to baseline p-Akt and responsive p-Erk and p-GSK-3β, indicate that it might be different from the other combination therapy sensitive cell lines.

Overall, the signalling studies provide hints that GSK-3β inhibition might be more dependent on Akt signalling in combination therapy sensitive cell lines, which could yield an explanation for the observed synergy. However, the differential signalling patterns within the subgroups of cell lines indicate the presence of different

molecular profiles in these and warrant further studies in more cell lines, combined with appropriate knock outs, to identify the relevant response profiles in combination therapy sensitive and combination therapy resistant cell lines.

4.5. The role of CD24 in anti-IGF-1R therapy response in CRC

In the search for characteristics differing between combination therapy resistant and combination therapy sensitive cell lines, low expression of CD24 was identified as the most striking feature of combination therapy resistant *PIK3CA* wild type cell lines.

This pattern holds true for a comparison of surface CD24 expression (see Figure 15) and CD24 mRNA levels (Figure 14) in the panel of 10 combination therapy sensitive/resistant cell lines, as well as CD24 mRNA levels across all *PIK3CA* wild type cell lines assessed for synergy ($p < 0.05$ corrected for multiple hypotheses testing from the candidate gene panel in Table S 8).

Considering the signalling across cell lines depicted in Figure 12 and the CD24 expression data shown in Figure 14, an association between CD24 expression and Akt phosphorylation at the Ser473 residue can be observed in the combination therapy resistant cell lines. While the number of cell lines does not allow generalisation of this pattern, CD24 knockdown has been shown to decrease Akt phosphorylation levels in breast cancer cells[102], which could be assessed in future studies of CRC.

The identification of CD24 low and high subpopulations within cell lines allowed sorting of these populations using FACS and assessing their sensitivity to

combination therapies in a pilot experiment. In 2 CD24 low cell lines, the CD24 high subpopulation displayed a slightly increased sensitivity to combination therapy with OSI-906 and GSK690693, which is in line with the initial observation that CD24 expression level is correlated to combination sensitivity. However, for the CD24 high cell line CAR-1, the CD24 low subpopulation appears to be most sensitive to both mono- and combination therapy. These data are fairly preliminary and require validation in repeat experiments and an expanded panel of cell lines. Furthermore, the sorting of the top and bottom 10 per cent of cells with respect to CD24 expression might not suffice to separate functionally relevant subpopulations, which could explain the observed lack of differential clonogenicity between subpopulations (Figure S 4). Selection based on expression distribution for each cell line might yield more reliable results.

While the data presented in this thesis do not suffice to establish a clear role for CD24 in anti-IGF-1R therapy response in colorectal cancer, they feed into a highly interesting picture of the involvement of CD24 in cancer stem cell characteristics and anti-RTK therapy response which has been reported in the last years and is briefly discussed below with respect to the data of this thesis and potential follow-up experiments.

A first consideration to be made is the nature of CD24 expression levels being either causally linked to combination therapy response or secondary to another characteristic differentiating combination therapy sensitive from resistant cell lines. Importantly, activating *KRAS* mutations have been demonstrated to repress CD24 expression[103,104], in a process thought to be primarily mediated through Raf

signalling. Considering the association of *KRAS* mutations and low CD24 expression to combination therapy resistance, this link should not be ignored in the analysis of the dataset in this thesis. Indeed, a correlation analysis of *KRAS* mutations and CD24 mRNA expression levels in the complete panel of cell lines revealed a 2.7-fold higher median expression of CD24 in *KRAS* wild type cell lines ($p \approx 0.008$, the pattern is depicted in Figure S 5). However, 2 of the 5 most combination therapy resistant cell lines are *KRAS* wild type and low in CD24 expression. In fact, these cell lines are lowest (OXCO-1) and third lowest (C2BBe1) in CD24 expression of all *KRAS* wild type cell lines in the 82 cell line panel, strengthening the association CD24 in anti-IGF-1R/Akt combination therapy response and indicating factors additional to activated *KRAS* to be involved in CD24 expression repression.

CD24, particularly in combination with CD44, has been described as a marker for colorectal cancer stem cells[105,106]. CD24/CD44 high cells derived from CRC cell lines were demonstrated to be highly clonogenic and able to differentiate into various cell lineages when grown in matrigel[105]. The finding of CD24 expression as a predictor of sensitivity to a therapeutic regimen in this thesis yields a rationale to develop therapeutic strategies aimed at CD24 high cells to target potential cancer stem cell in CRC. However, it should be noted that the role of CD24 in stemness and therapy response is all but understood and varies significantly between cancer types (in breast cancer, e.g. low CD24 levels are associated with tumour initiating properties[107]), which should be kept in mind in the following discussion. For future studies on anti-IGF-1R-based combination therapies in CRC stem cells, other markers such as CD44 or CD133 should be included in the sorting process to obtain a clearer picture of stem cell sensitivity to a drug combination.

Interestingly, high CD24 expression has been shown to be associated with anti-IGF-1R therapy sensitivity in mammary cancer cells[108], while IGF-1R was demonstrated to influence the capacity of CD24 high cells to act in a stem-like fashion in the same study. Among the CRC cell line panel of this study, CD24 expression levels were weakly associated with resistance to OSI-906 treatment, though not reaching significance (spearman's $r \approx 0.17$; $p \approx 0.16$ before correction).

Little information is available from the literature concerning potential mechanisms of the involvement of CD24 in combination therapy response. Two studies, however, deserve attention in this regard: In [109], an IGF-1-induced enrichment of CRC stem cells is described, which depends on Akt signalling and can be blocked through figitumumab. While CD24 is not used for stem cell classification in this study, effective treatment of stem-like cell lines appears feasible when successfully inhibiting both IGF-1R and Akt signalling. In [110], a novel role for CD24 in EGFR signalling is described in gastric cancer, which might well influence anti-IGF-1R therapy response. Briefly, CD24 is shown to support EGFR downstream signalling, potentially by stabilising EGFR at the cell surface. As EGFR and IGF-1R share many of their downstream signalling, cells with low CD24 might have developed a higher grade of RTK-signalling independence, which could explain the less pronounced drug responses in this cell line population.

To address these hypotheses, the effect of CD24 expression levels should be studied beyond the sorting-based approach applied in this thesis. While gene knockdown and editing approaches will facilitate preclinical establishment of CD24 function in anti-IGF-1R therapy response, recently reported drug-based strategies

for modulation of CD24 expression could facilitate rapid translation of these findings.

Metformin, a compound approved for the treatment for diabetes, was demonstrated to decrease CD24 expression on breast cancer cells[111]. Conversely, TGF-β was reported to augment CD24 expression in colorectal cancer cell lines[112]. Both of these findings may be viewed critically, as the decrease in CD24 expression after metformin treatment could well stem from a preferential killing of CD24 high cells based on the data presented in[111]. Furthermore, the flow cytometry analysis on which the finding of CD24 induction after TGF-β is based might not be suitable to support this statement. A pilot experiment to verify these findings could reproduce the induction of CD24 after treatment with 10 ng/ml of TGF-β for 72h in the CD24 low cell line SW837. A slight decrease in CD24 expressing cells could be achieved using 10 mM Metformin for 72h in the CD24 high cell line VACO10MS.

While these data are very preliminary, metformin and TGF-β could provide feasible means of modulating CD24 high cell populations in the clinical setting. While in-vitro combination studies of Metformin and figitumumab have indicated synergy in NSCLC[94], CD24 is not so far discussed as a factor in combination therapy response in these studies. In the light of the differences in CD24 function between different tissues, a careful evaluation of its role in CRC is warranted to assess the potential for its use as a biomarker or target in this disease.

4.6. The role of Akt isoforms in anti-IGF-1R therapy response

Knockdown of the Akt isoforms was performed as a follow-up experiment to investigate their contribution to anti-IGF-1R sensitisation in CRC cell lines. As briefly discussed in Section 3.6, knockdown of Akt1 resulted in the strongest sensitisation in 3 of 4 combination therapy sensitive cell lines, yet knockdown of the other 2 isoforms also induced sensitisation to varying degrees.

Assessing the effects of Akt isoform knockdown on signalling in combination therapy sensitive and resistant cell lines could shed more light on the role of Akt isoforms in these cell lines and in response to anti-IGF-1R therapy.

However, in summary, focusing on a particular isoform of Akt is not indicated by the data presented in this thesis. In the light of this situation, the summarising statements and outlook will focus on the previous findings concerning factors associated with anti-IGF-1R and combined anti-IGF-1R/Akt therapy response.

4.7. Conclusion

This project was designed to identify potentially predictive biomarkers and better understand the biology of anti-IGF-1R therapy response in colorectal cancer. Mutations in *PIK3CA* were identified to be associated with resistance to anti-IGF-1R therapy in the colorectal cancer cell line panel. Sensitisation by combined therapy with an Akt inhibitor was observed in a subgroup of *PIK3CA* wild type cell lines, characterised by wild type *KRAS*, high CD24 expression and active Akt signalling at baseline. The classification of CRC cell lines based on the characteristics found in this thesis is depicted in Figure 18.

Upon retrospective validation on clinical samples, clinical trials could make use of these findings by assessing combined anti-IGF-1R/Akt therapy in *PIK3CA*/*KRAS* wild type patients expressing high levels of CD24.

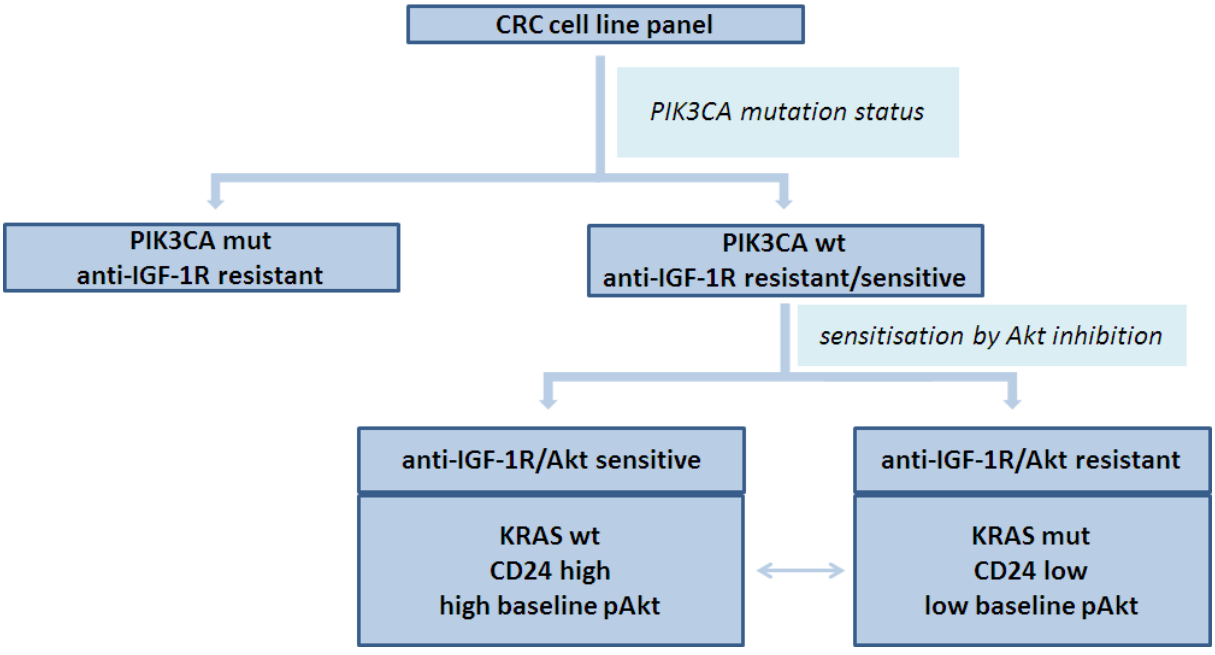

Figure 18: Classification of CRC cell lines based on the findings of this thesis.

References

1. Ferlay, Dienstmann R, Wang X, et al. Globocan. *Nat Med*. 2015;21(11):1350-1356. doi:10.1038/nm.3967.

2. Fearon ER, Vogelstein B. A genetic model for colorectal tumorigenesis. *Cell*. 1990;61(5):759-767. doi:http://dx.doi.org/10.1016/0092-8674(90)90186-I.

3. Burt RW, Samowitz WS. The adenomatous polyp and the hereditary polyposis syndromes. *Gastroenterol Clin North Am*. 1988;17(4):657-678.

4. de la Chapelle A. The incidence of Lynch syndrome. *Fam Cancer*. 2005;4(3):233-237. doi:10.1007/s10689-004-5811-3.

5. Issa J-P. Colon cancer: it's CIN or CIMP. *Clin Cancer Res*. 2008;14(19):5939-5940. doi:10.1158/1078-0432.CCR-08-1596.

6. Ribic CM, Sargent DJ, Moore MJ, et al. Tumor Microsatellite-Instability Status as a Predictor of Benefit from Fluorouracil-Based Adjuvant Chemotherapy for Colon Cancer. *N Engl J Med*. 2003;349(3):247-257. doi:10.1056/NEJMoa022289.

7. Sargent DJ, Marsoni S, Monges G, et al. Defective Mismatch Repair As a Predictive Marker for Lack of Efficacy of Fluorouracil-Based Adjuvant Therapy in Colon Cancer. *J Clin Oncol* . 2010;28 (20):3219-3226. http://jco.ascopubs.org/content/28/20/3219.abstract.

8. Weisenberger DJ, Siegmund KD, Campan M, et al. CpG island methylator phenotype underlies sporadic microsatellite instability and is tightly associated with BRAF mutation in colorectal cancer. *Nat Genet*. 2006;38(7):787-793. doi:10.1038/ng1834.

9. Worthley DL, Leggett BA. Colorectal Cancer: Molecular Features and Clinical Opportunities. *Clin Biochem Rev*. 2010;31(2):31-38. http://www.ncbi.nlm.nih.gov/pmc/articles/PMC2874430/.

10. Powell SM, Zilz N, Beazer-Barclay Y, et al. APC mutations occur early during colorectal tumorigenesis. *Nature*. 1992;359(6392):235-237. doi:10.1038/359235a0.

11. Fodde R, Smits R, Clevers H. APC, Signal transduction and genetic instability in colorectal cancer. *Nat Rev Cancer*. 2001;1(1):55-67. http://dx.doi.org/10.1038/35094067.

12. Lothe RA, Peltomäki P, Meling GI, et al. Genomic Instability in Colorectal Cancer: Relationship to Clinicopathological Variables and Family History. *Cancer Res*. 1993;53(24):5849-5852. http://cancerres.aacrjournals.org/content/53/24/5849.abstract.

13. Le DT, Uram JN, Wang H, et al. PD-1 Blockade in Tumors with Mismatch-Repair Deficiency. *N Engl J Med*. 2015;372(26):2509-2520. doi:10.1056/NEJMoa1500596.

14. Ashraf SQ, Nicholls AM, Wilding JL, Ntouroupi TG, Mortensen NJ, Bodmer WF. Direct and immune mediated antibody targeting of ERBB receptors in a colorectal cancer cell-line panel. *Proc Natl Acad Sci U S A*. 2012;109(51):21046-21051. doi:10.1073/pnas.1218750110.

15. Van Cutsem E, Kohne C-H, Lang I, et al. Cetuximab plus irinotecan, fluorouracil, and leucovorin as first-line treatment for metastatic colorectal cancer: updated analysis of overall survival according to tumor KRAS and BRAF mutation status. *J Clin Oncol*. 2011;29(15):2011-2019. doi:10.1200/JCO.2010.33.5091.

16. Hsu H-C, Thiam TK, Lu Y-J, et al. Mutations of KRAS/NRAS/BRAF predict cetuximab resistance in metastatic colorectal cancer patients. *Oncotarget*. 2016;7(16):22257-22270. doi:10.18632/oncotarget.8076.

17. Wilding JL, Bodmer WF. Cancer cell lines for drug discovery and development. *Cancer Res*. 2014;74(9):2377-2384. doi:10.1158/0008-5472.CAN-13-2971.

18. Jonker DJ, O'Callaghan CJ, Karapetis CS, et al. Cetuximab for the Treatment of Colorectal Cancer. *N Engl J Med*. 2007;357(20):2040-2048. doi:10.1056/NEJMoa071834.

19. UK CR. Which treatment for advanced bowel cancer. http://www.cancerresearchuk.org/about-cancer/type/bowel-cancer/treatment/types/which-treatment-for-advanced-bowel-cancer.

20. Yang X, Zhang X, Mortenson ED, Radkevich-Brown O, Wang Y, Fu Y-X. Cetuximab-mediated Tumor Regression Depends on Innate and Adaptive Immune Responses. *Mol Ther*. 2013;21(1):91-100. http://dx.doi.org/10.1038/mt.2012.184.

21. Douillard J-Y, Siena S, Cassidy J, et al. Randomized, phase III trial of panitumumab with infusional fluorouracil, leucovorin, and oxaliplatin (FOLFOX4) versus FOLFOX4 alone as first-line treatment in patients with previously untreated metastatic colorectal cancer: the PRIME study. *J Clin Oncol*. 2010;28(31):4697-4705. doi:10.1200/JCO.2009.27.4860.

22. Baserga R, Hongo A, Rubini M, Prisco M, Valentinis B. The IGF-I receptor in cell growth, transformation and apoptosis. *Biochim Biophys Acta*. 1997;1332(3):F105-F126.

23. Zha J, Lackner MR. Targeting the insulin-like growth factor receptor-1R pathway for cancer therapy. *Clin Cancer Res*. 2010;16(9):2512-2517. doi:10.1158/1078-0432.CCR-09-2232.

24. Valentinis B, Baserga R. IGF-I receptor signalling in transformation and differentiation. *Mol Pathol*. 2001;54(3):133-137.

25. Lammers R, Gray A, Schlessinger J, Ullrich A. Differential signalling potential of insulin- and IGF-1-receptor cytoplasmic domains. *EMBO J*. 1989;8(5):1369-1375.

26. Riedemann J, Macaulay VM. IGF1R signalling and its inhibition. *Endocr Relat Cancer*. 2006;13 Suppl 1:S33-S43. doi:10.1677/erc.1.01280.

27. Hemmings BA, Restuccia DF. PI3K-PKB/Akt Pathway. *Cold Spring Harb Perspect Biol* . 2012;4 (9). doi:10.1101/cshperspect.a011189 .

28. Alessi DR, James SR, Downes CP, et al. Characterization of a 3-phosphoinositide-dependent protein kinase which phosphorylates and activates protein kinase Balpha. *Curr Biol*. 1997;7(4):261-269.

29. Sarbassov DD, Guertin DA, Ali SM, Sabatini DM. Phosphorylation and Regulation of Akt/PKB by the Rictor-mTOR Complex. *Science (80-)*. 2005;307(5712):1098 LP - 1101. http://science.sciencemag.org/content/307/5712/1098.abstract.

30. Feng J, Park J, Cron P, Hess D, Hemmings BA. Identification of a PKB/Akt Hydrophobic Motif Ser-473 Kinase as DNA-dependent Protein Kinase. *J Biol Chem* . 2004;279 (39):41189-41196. http://www.jbc.org/content/279/39/41189.abstract.

31. Ali A, Hoeflich KP, Woodgett JR. Glycogen synthase kinase-3: properties, functions, and regulation. *Chem Rev*. 2001;101(8):2527-2540.

32. Dummler B, Hemmings BA. Physiological roles of PKB/Akt isoforms in development and disease. *Biochem Soc Trans*. 2007;35(Pt 2):231-235. doi:10.1042/BST0350231.

33. Chen WS, Xu PZ, Gottlob K, et al. Growth retardation and increased apoptosis in mice with homozygous disruption of the Akt1 gene. *Genes Dev*. 2001;15(17):2203-2208. doi:10.1101/gad.913901.

34. Garofalo RS, Orena SJ, Rafidi K, et al. Severe diabetes, age-dependent loss of adipose tissue, and mild growth deficiency in mice lacking Akt2/PKB beta. J Clin Invest. 2003;112(2):197-208. doi:10.1172/JCI16885.

35. Tschopp O, Yang Z-Z, Brodbeck D, et al. Essential role of protein kinase B gamma (PKB gamma/Akt3) in postnatal brain development but not in glucose homeostasis. *Development*. 2005;132(13):2943-2954. doi:10.1242/dev.01864.

36. Zinda MJ, Johnson MA, Paul JD, et al. AKT-1, -2, and -3 are Expressed in Both Normal and Tumor Tissues of the Lung, Breast, Prostate, and Colon. *Clin Cancer Res*. 2001;7(8):2475 LP - 2479. http://clincancerres.aacrjournals.org/content/7/8/2475.abstract.

37. Rychahou PG, Kang J, Gulhati P, et al. Akt2 overexpression plays a critical role in the establishment of colorectal cancer metastasis. *Proc Natl Acad Sci U S A*. 2008;105(51):20315-20320. doi:10.1073/pnas.0810715105.

38. Roper J. The Role of Akt Isoforms in Colorectal Cancer. *Annu rept US Army Med Res Mater Command Fort Detrick, Maryl 21702-5012*. 2014.

39. Dhillon AS, Hagan S, Rath O, Kolch W. MAP kinase signalling pathways in cancer. *Oncogene*. 26(22):3279-3290. http://dx.doi.org/10.1038/sj.onc.1210421.

40. Sell C, Rubini M, Rubin R, Liu JP, Efstratiadis A, Baserga R. Simian virus 40 large tumor antigen is unable to transform mouse embryonic fibroblasts lacking type 1 insulin-like growth factor receptor. *Proc Natl Acad Sci U S A*. 1993;90(23):11217-11221.

41. DeAngelis T, Chen J, Wu A, Prisco M, Baserga R. Transformation by the simian virus 40 T antigen is regulated by IGF-I receptor and IRS-1 signaling. *Oncogene*. 2006;25(1):32-42. doi:10.1038/sj.onc.1209013.

42. Kaleko M, Rutter WJ, Miller AD. Overexpression of the human insulinlike growth factor I receptor promotes ligand-dependent neoplastic transformation. *Mol Cell Biol*. 1990;10(2):464-473.

43. Hellawell GO, Turner GDH, Davies DR, Poulsom R, Brewster SF, Macaulay VM. Expression of the type 1 insulin-like growth factor receptor is up-regulated in primary prostate cancer and commonly persists in metastatic disease. *Cancer Res*. 2002;62(10):2942-2950.

44. Bergmann U, Funatomi H, Yokoyama M, Beger HG, Korc M. Insulin-like growth factor I overexpression in human pancreatic cancer: evidence for autocrine and paracrine roles. *Cancer Res*. 1995;55(10):2007-2011.

45. Kanter-Lewensohn L, Dricu A, Girnita L, Wejde J, Larsson O. Expression of insulin-like growth factor-1 receptor (IGF-1R) and p27Kip1 in melanocytic tumors: a potential regulatory role of IGF-1 pathway in distribution of p27Kip1 between different cyclins. *Growth Factors*. 2000;17(3):193-202.

46. Jammes H, Peyrat JP, Ban E, et al. Insulin-like growth factor 1 receptors in human breast tumour: localisation and quantification by histo-autoradiographic analysis. *Br J Cancer*. 1992;66(2):248-253.

47. Wang Z, Lu P, Liang Z, et al. Increased insulin-like growth factor 1 receptor (IGF1R) expression in small cell lung cancer and the effect of inhibition of IGF1R expression by RNAi on growth of human small cell lung cancer NCI-H446 cell. *Growth Factors*. 2015;33(5-6):337-346. doi:10.3109/08977194.2015.1088533.

48. Hakam A, Yeatman TJ, Lu L, et al. Expression of insulin-like growth factor-1 receptor in human colorectal cancer. *Hum Pathol*. 1999;30(10):1128-1133.

49. Freier S, Weiss O, Eran M, et al. Expression of the insulin-like growth factors and their receptors in adenocarcinoma of the colon. *Gut*. 1999;44(5):704-708.

50. Shiratsuchi I, Akagi Y, Kawahara A, et al. Expression of IGF-1 and IGF-1R and their relation to clinicopathological factors in colorectal cancer. *Anticancer Res*. 2011;31(7):2541-2545.

51. Furstenberger G, Senn H-J. Insulin-like growth factors and cancer. *Lancet Oncol*.

2002;3(5):298-302.

52. Cui H, Cruz-Correa M, Giardiello FM, et al. Loss of IGF2 imprinting: a potential marker of colorectal cancer risk. *Science*. 2003;299(5613):1753-1755. doi:10.1126/science.1080902.

53. Casa AJ, Dearth RK, Litzenburger BC, Lee A V, Cui X. The type I insulin-like growth factor receptor pathway: a key player in cancer therapeutic resistance. *Front Biosci*. 2008;13:3273-3287.

54. Shen K, Cui D, Sun L, Lu Y, Han M, Liu J. Inhibition of IGF-IR increases chemosensitivity in human colorectal cancer cells through MRP-2 promoter suppression. *J Cell Biochem*. 2012;113(6):2086-2097. doi:10.1002/jcb.24080.

55. Hu YP, Patil SB, Panasiewicz M, et al. Heterogeneity of receptor function in colon carcinoma cells determined by cross-talk between type I insulin-like growth factor receptor and epidermal growth factor receptor. *Cancer Res*. 2008;68(19):8004-8013. doi:10.1158/0008-5472.CAN-08-0280.

56. Adams TE, McKern NM, Ward CW. Signalling by the type 1 insulin-like growth factor receptor: interplay with the epidermal growth factor receptor. *Growth Factors*. 2004;22(2):89-95.

57. Shaib W, Mahajan R, El-Rayes B. Markers of resistance to anti-EGFR therapy in colorectal cancer. *J Gastrointest Oncol*. 2013;4(3):308-318. doi:10.3978/j.issn.2078-6891.2013.029.

58. Crudden C, Girnita A, Girnita L. Targeting the IGF-1R: The Tale of the Tortoise and the Hare. *Front Endocrinol (Lausanne)*. 2015;6:64. doi:10.3389/fendo.2015.00064.

59. Ren SG, Ezzat S, Melmed S, Braunstein GD. Somatostatin analog induces insulin-like growth factor binding protein-1 (IGFBP-1) expression in human hepatoma cells. *Endocrinology*. 1992;131(5):2479-2481. doi:10.1210/endo.131.5.1385103.

60. Pietrzkowski Z, Mulholland G, Gomella L, Jameson BA, Wernicke D, Baserga R. Inhibition of growth of prostatic cancer cell lines by peptide analogues of insulin-like growth factor 1. *Cancer Res*. 1993;53(5):1102-1106.

61. Buck E, Mulvihill M. Small molecule inhibitors of the IGF-1R/IR axis for the treatment of cancer. *Expert Opin Investig Drugs*. 2011;20(5):605-621. doi:10.1517/13543784.2011.558501.

62. Ekman S, Frodin J-E, Harmenberg J, et al. Clinical Phase I study with an Insulin-like Growth Factor-1 receptor inhibitor: experiences in patients with squamous non-small cell lung carcinoma. *Acta Oncol*. 2011;50(3):441-447. doi:10.3109/0284186X.2010.499370.

63. Olmos D, Postel-Vinay S, Molife LR, et al. Safety, pharmacokinetics, and preliminary activity of the anti-IGF-1R antibody figitumumab (CP-751,871) in patients with sarcoma and Ewing's sarcoma: a phase 1 expansion cohort study. *Lancet Oncol*. 2010;11(2):129-135.

doi:10.1016/S1470-2045(09)70354-7.

64. Tolcher AW, Sarantopoulos J, Patnaik A, et al. Phase I, pharmacokinetic, and pharmacodynamic study of AMG 479, a fully human monoclonal antibody to insulin-like growth factor receptor 1. *J Clin Oncol*. 2009;27(34):5800-5807. doi:10.1200/JCO.2009.23.6745.

65. Karp DD, Pollak MN, Cohen RB, et al. Safety, pharmacokinetics, and pharmacodynamics of the insulin-like growth factor type 1 receptor inhibitor figitumumab (CP-751,871) in combination with paclitaxel and carboplatin. *J Thorac Oncol*. 2009;4(11):1397-1403. doi:10.1097/JTO.0b013e3181ba2f1d.

66. King H, Aleksic T, Haluska P, Macaulay VM. Can we unlock the potential of IGF-1R inhibition in cancer therapy? *Cancer Treat Rev*. 2014;40(9):1096-1105. doi:10.1016/j.ctrv.2014.07.004.

67. Pavlicek A, Lira ME, Lee N V, et al. Molecular Predictors of Sensitivity to the Insulin-like Growth Factor 1 Receptor Inhibitor Figitumumab (CP-751,871). *Mol Cancer Ther*. 2013;12(12):2929 LP - 2939. http://mct.aacrjournals.org/content/12/12/2929.abstract.

68. Zheng H, Shen H, Oprea I, et al. beta-Arrestin-biased agonism as the central mechanism of action for insulin-like growth factor 1 receptor-targeting antibodies in Ewing's sarcoma. *Proc Natl Acad Sci U S A*. 2012;109(50):20620-20625. doi:10.1073/pnas.1216348110.

69. Karp DD, Paz-Ares LG, Novello S, et al. Phase II study of the anti-insulin-like growth factor type 1 receptor antibody CP-751,871 in combination with paclitaxel and carboplatin in previously untreated, locally advanced, or metastatic non-small-cell lung cancer. *J Clin Oncol*. 2009;27(15):2516-2522. doi:10.1200/JCO.2008.19.9331.

70. Scagliotti G V, Bondarenko I, Blackhall F, et al. Randomized, phase III trial of figitumumab in combination with erlotinib versus erlotinib alone in patients with nonadenocarcinoma nonsmall-cell lung cancer. *Ann Oncol*. 2015;26(3):497-504. doi:10.1093/annonc/mdu517.

71. Retraction. "Phase II study of the anti-insulin-like growth factor type 1 receptor antibody CP-751,871 in combination with paclitaxel and carboplatin in previously untreated, locally advanced, or metastatic non-small-cell lung cancer". *J Clin Oncol*. 2012;30(33):4179.

72. Gualberto A, Hixon ML, Karp DD, et al. Pre-treatment levels of circulating free IGF-1 identify NSCLC patients who derive clinical benefit from figitumumab. *Br J Cancer*. 2011;104(1):68-74. doi:10.1038/sj.bjc.6605972.

73. Gualberto A, Dolled-Filhart M, Gustavson M, et al. Molecular Analysis of Non–Small Cell Lung Cancer Identifies Subsets with Different Sensitivity to Insulin-like Growth Factor I Receptor Inhibition. *Clin Cancer Res*. 2010;16(18):4654 LP - 4665. http://clincancerres.aacrjournals.org/content/16/18/4654.abstract.

74. Mulvihill MJ, Cooke A, Rosenfeld-Franklin M, et al. Discovery of OSI-906: a selective and orally efficacious dual inhibitor of the IGF-1 receptor and insulin receptor. *Future Med Chem*. 2009;1(6):1153-1171. doi:10.4155/fmc.09.89.

75. Puzanov I, Lindsay CR, Goff L, et al. A phase I study of continuous oral dosing of OSI-906, a dual inhibitor of insulin-like growth factor-1 and insulin receptors, in patients with advanced solid tumors. *Clin Cancer Res*. 2015;21(4):701-711. doi:10.1158/1078-0432.CCR-14-0303.

76. Macaulay VM, Middleton MR, Eckhardt SG, et al. Phase I Dose-Escalation Study of Linsitinib (OSI-906) and Erlotinib in Patients with Advanced Solid Tumors. *Clin Cancer Res*. 2016;22(12):2897 LP - 2907. http://clincancerres.aacrjournals.org/content/22/12/2897.abstract.

77. Chen HX, Sharon E. IGF-1R as an anti-cancer target—trials and tribulations. *Chin J Cancer*. 2013;32(5):242-252. doi:10.5732/cjc.012.10263.

78. van Staveren WCG, Solis DYW, Hebrant A, Detours V, Dumont JE, Maenhaut C. Human cancer cell lines: Experimental models for cancer cells in situ? For cancer stem cells? *Biochim Biophys Acta*. 2009;1795(2):92-103. doi:10.1016/j.bbcan.2008.12.004.

79. Gazdar AF, Gao B, Minna JD. Lung cancer cell lines: Useless artifacts or invaluable tools for medical science? *Lung Cancer*. 2010;68(3):309-318. doi:10.1016/j.lungcan.2009.12.005.

80. Masters JRW. Human cancer cell lines: fact and fantasy. *Nat Rev Mol Cell Biol*. 2000;1(3):233-236. http://dx.doi.org/10.1038/35043102.

81. Barretina J, Caponigro G, Stransky N, et al. The Cancer Cell Line Encyclopedia enables predictive modelling of anticancer drug sensitivity. *Nature*. 2012;483(7391):307-603. http://dx.doi.org/10.1038/nature11003.

82. Garnett MJ, Edelman EJ, Heidorn SJ, et al. Systematic identification of genomic markers of drug sensitivity in cancer cells. *Nature*. 2012;483(7391):570-575. doi:10.1038/nature11005.

83. Bracht K, Nicholls AM, Liu Y, Bodmer WF. 5-Fluorouracil response in a large panel of colorectal cancer cell lines is associated with mismatch repair deficiency. *Br J Cancer*. 2010;103(3):340-346. doi:10.1038/sj.bjc.6605780.

84. Mouradov D, Sloggett C, Jorissen RN, et al. Colorectal cancer cell lines are representative models of the main molecular subtypes of primary cancer. *Cancer Res*. 2014;74(12):3238-3247. doi:10.1158/0008-5472.CAN-14-0013.

85. Xu S-P, Sun G-P, Shen Y-X, Peng W-R, Wang H, Wei W. Synergistic effect of combining paeonol and cisplatin on apoptotic induction of human hepatoma cell lines. *Acta Pharmacol Sin*. 2007;28(6):869-878. doi:10.1111/j.1745-7254.2007.00564.x.

86. Lopez-Acevedo M, Grace L, Teoh D, et al. Dasatinib (BMS-35482) potentiates the activity of gemcitabine and docetaxel in uterine leiomyosarcoma cell lines. *Gynecol Oncol Res Pract*. 2014;1(1):1-10. doi:10.1186/2053-6844-1-2.

87. Mendoza MC, Er EE, Blenis J. The Ras-ERK and PI3K-mTOR pathways: cross-talk and compensation. *Trends Biochem Sci*. 2011;36. doi:10.1016/j.tibs.2011.03.006.

88. Kuger S, Flentje M, Djuzenova CS. Simultaneous perturbation of the MAPK and the PI3K/mTOR pathways does not lead to increased radiosensitization. *Radiat Oncol*. 2015;10(1):1-16. doi:10.1186/s13014-015-0514-5.

89. Pitts TM, Tan AC, Kulikowski GN, et al. Development of an Integrated Genomic Classifier for a Novel Agent in Colorectal Cancer: Approach to Individualized Therapy in Early Development. *Clin Cancer Res*. 2010;16(12):3193-3204. doi:10.1158/1078-0432.CCR-09-3191.

90. Levy DS, Kahana JA, Kumar R. AKT inhibitor, GSK690693, induces growth inhibition and apoptosis in acute lymphoblastic leukemia cell lines. *Blood*. 2009;113(8):1723 LP - 1729. http://www.bloodjournal.org/content/113/8/1723.abstract.

91. Rhodes N, Heerding DA, Duckett DR, et al. Characterization of an Akt kinase inhibitor with potent pharmacodynamic and antitumor activity. *Cancer Res*. 2008;68(7):2366-2374. doi:10.1158/0008-5472.CAN-07-5783.

92. Cani A, Simioni C, Martelli AM, et al. Triple Akt inhibition as a new therapeutic strategy in T-cell acute lymphoblastic leukemia. *Oncotarget*. 2015;6(9):6597-6610. http://www.ncbi.nlm.nih.gov/pmc/articles/PMC4466637/.

93. Flanigan SA, Pitts TM, Newton TP, et al. Overcoming IGF1R/IR resistance through inhibition of MEK signaling in colorectal cancer models. *Clin Cancer Res*. 2013;19(22):6219-6229. doi:10.1158/1078-0432.CCR-13-0145.

94. Cao L, Yu Y, Darko I, et al. Addiction to elevated insulin-like growth factor I receptor and initial modulation of the AKT pathway define the responsiveness of rhabdomyosarcoma to the targeting antibody. *Cancer Res*. 2008;68(19):8039-8048. doi:10.1158/0008-5472.CAN-08-1712.

95. Zha J, O'Brien C, Savage H, et al. Molecular predictors of response to a humanized anti-insulin-like growth factor-I receptor monoclonal antibody in breast and colorectal cancer. *Mol Cancer Ther*. 2009;8(8):2110-2121. doi:10.1158/1535-7163.MCT-09-0381.

96. Huang F, Greer A, Hurlburt W, et al. The mechanisms of differential sensitivity to an insulin-like growth factor-1 receptor inhibitor (BMS-536924) and rationale for combining with EGFR/HER2 inhibitors. *Cancer Res*. 2009;69(1):161-170. doi:10.1158/0008-5472.CAN-08-0835.

97. Axelrod MJ, Mendez RE, Khalil A, et al. Synergistic apoptosis in head and neck squamous cell carcinoma cells by co-inhibition of insulin-like growth factor-1 receptor signaling and compensatory signaling pathways. *Head Neck*. 2015;37(12):1722-1732. doi:10.1002/hed.23822.

98. Zhang Y, Wang Q, Chen L, Yang H-S. Inhibition of p70S6K1 Activation by Pdcd4 Overcomes the Resistance to an IGF-1R/IR Inhibitor in Colon Carcinoma Cells. *Mol Cancer Ther*. 2015;14(3):799-809. doi:10.1158/1535-7163.MCT-14-0648.

99. Naing A, LoRusso P, Fu S, et al. Insulin growth factor-receptor (IGF-1R) antibody cixutumumab combined with the mTOR inhibitor temsirolimus in patients with refractory Ewing's sarcoma family tumors. *Clin Cancer Res*. 2012;18(9):2625-2631. doi:10.1158/1078-0432.CCR-12-0061.

100. Bendell JC, Jones SF, Hart L, et al. A phase Ib study of linsitinib (OSI-906), a dual inhibitor of IGF-1R and IR tyrosine kinase, in combination with everolimus as treatment for patients with refractory metastatic colorectal cancer. *Invest New Drugs*. 2015;33(1):187-193. doi:10.1007/s10637-014-0177-3.

101. Nitulescu GM, Margina D, Juzenas P, et al. Akt inhibitors in cancer treatment: The long journey from drug discovery to clinical use (Review). *Int J Oncol*. 2016;48(3):869-885. doi:10.3892/ijo.2015.3306.

102. Hosonaga M, Arima Y, Sugihara E, Kohno N, Saya H. Expression of CD24 is associated with HER2 expression and supports HER2-Akt signaling in HER2-positive breast cancer cells. *Cancer Sci*. 2014;105(7):779-787. doi:10.1111/cas.12427.

103. Morel A-P, Lievre M, Thomas C, Hinkal G, Ansieau S, Puisieux A. Generation of breast cancer stem cells through epithelial-mesenchymal transition. *PLoS One*. 2008;3(8):e2888. doi:10.1371/journal.pone.0002888.

104. Pallegar NK, Ayre DC, Christian SL. Repression of CD24 surface protein expression by oncogenic Ras is relieved by inhibition of Raf but not MEK or PI3K. *Front cell Dev Biol*. 2015;3:47. doi:10.3389/fcell.2015.00047.

105. Yeung TM, Gandhi SC, Wilding JL, Muschel R, Bodmer WF. Cancer stem cells from colorectal cancer-derived cell lines. *Proc Natl Acad Sci U S A*. 2010;107(8):3722-3727. doi:10.1073/pnas.0915135107.

106. Kemper K, Grandela C, Medema JP. Molecular identification and targeting of colorectal cancer stem cells. *Oncotarget*. 2010;1(6):387-395. doi:10.18632/oncotarget.101003.

107. So JY, Wahler J, Das Gupta S, et al. HES1-mediated inhibition of Notch1 signaling by a Gemini vitamin D analog leads to decreased CD44(+)/CD24(-/low) tumor-initiating subpopulation in basal-like breast cancer. *J Steroid Biochem Mol Biol*. 2015;148:111-121. doi:10.1016/j.jsbmb.2014.12.013.

108. Rostoker R, Ben-Shmuel S, Rashed R, Shen Orr Z, LeRoith D. CD24 cell surface expression in Mvt1 mammary cancer cells serves as a biomarker for sensitivity to anti-IGF1R therapy. *Breast Cancer Res*. 2016;18(1):51. doi:10.1186/s13058-016-0711-7.

109. Hart LS, Dolloff NG, Dicker DT, et al. Human colon cancer stem cells are enriched by insulin-like growth factor-1 and are sensitive to figitumumab. *Cell Cycle*. 2011;10(14):2331-2338. doi:10.4161/cc.10.14.16418.

110. Deng W, Gu L, Li X, et al. CD24 associates with EGFR and supports EGF/EGFR signaling via RhoA in gastric cancer cells. *J Transl Med*. 2016;14(1):1-13. doi:10.1186/s12967-016-

0787-y.

111. Vazquez-Martin A, Oliveras-Ferraros C, Cufi S, et al. The anti-diabetic drug metformin suppresses the metastasis-associated protein CD24 in MDA-MB-468 triple-negative breast cancer cells. *Oncol Rep*. 2011;25(1):135-140.

112. Okano M, Konno M, Kano Y, et al. Human colorectal CD24+ cancer stem cells are susceptible to epithelial-mesenchymal transition. *Int J Oncol*. 2014;45(2):575-580. doi:10.3892/ijo.2014.2462.

Supplementary figures

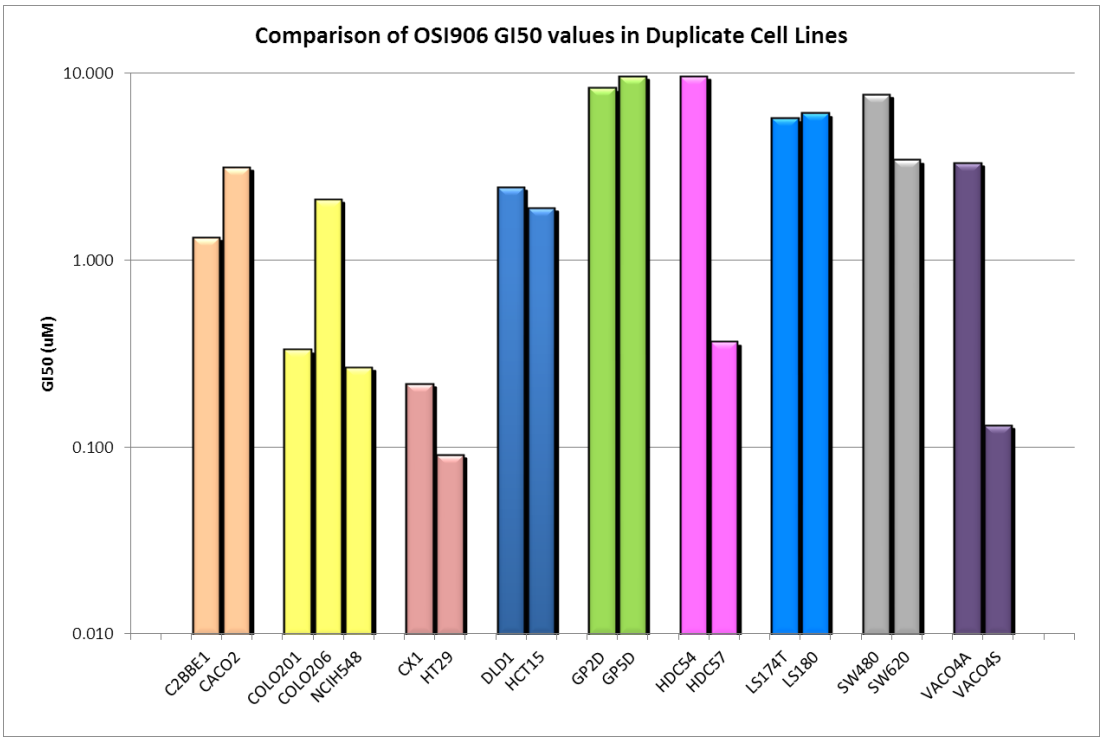

Figure S 1: Response to OSI-906 in duplicate cell lines.
The GI50 values of known duplicate cell lines in the Bodmer cell line panel are in good agreement with each other.

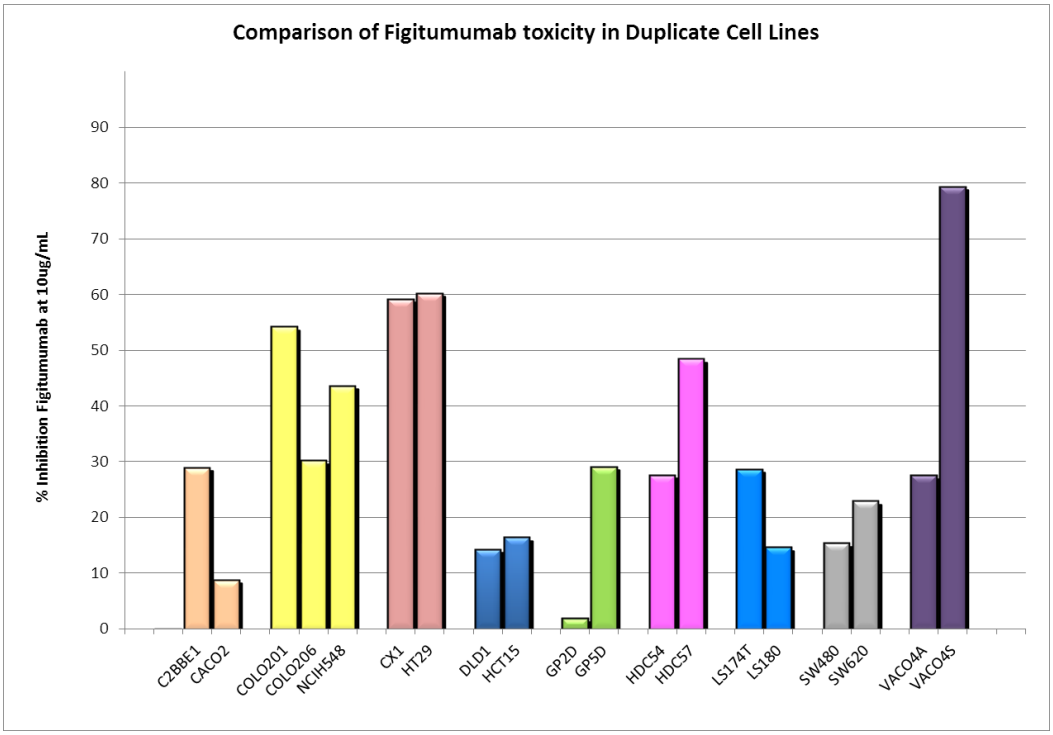

Figure S 2: Response to figitumumab in duplicate cell lines.
The relative growth inhibition at 10 µg/ml figitumumab of known duplicate cell lines in the Bodmer cell line panel is in good agreement with each other for 7 of 9 cell line groups. In case of C2BBe1/CACO2 and GP2D/GP5D, a deviation of more than 100% can be observed between the cell lines.

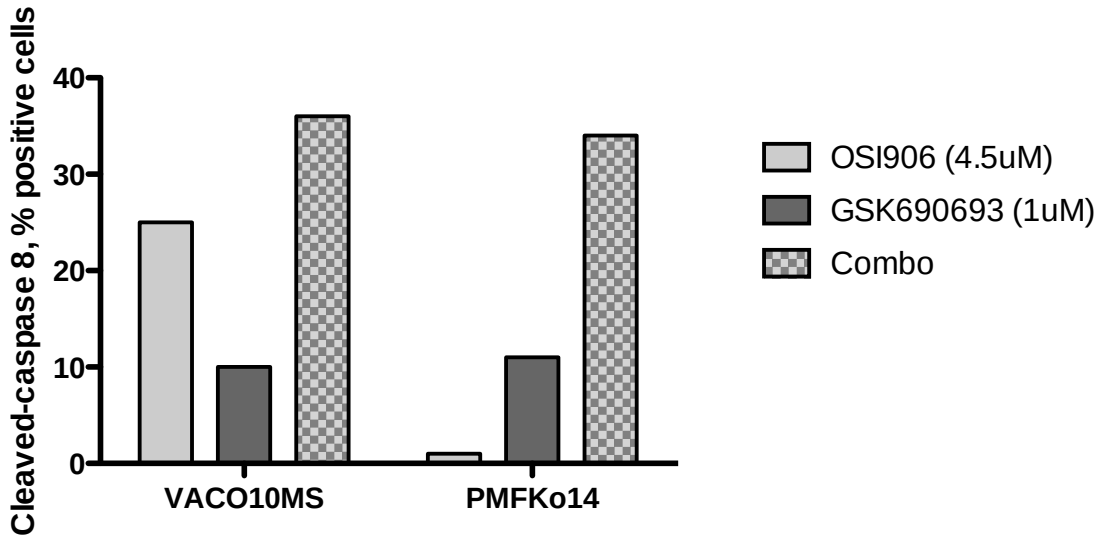

Figure S 3: Apoptosis induction in PMFKo14 and VACO10MS.
Based on the cleaved caspase 8-based flow cytometrical detection of apoptosis presented in Figure 10, the baseline fraction of apoptotic cells of the untreated sample was subtracted from the other samples to allow insights into the induction of apoptosis after each treatment. A synergistic increase after combination treatment can be observed for PMFKo14, whereas VACO10MS yields an additional drug interaction.

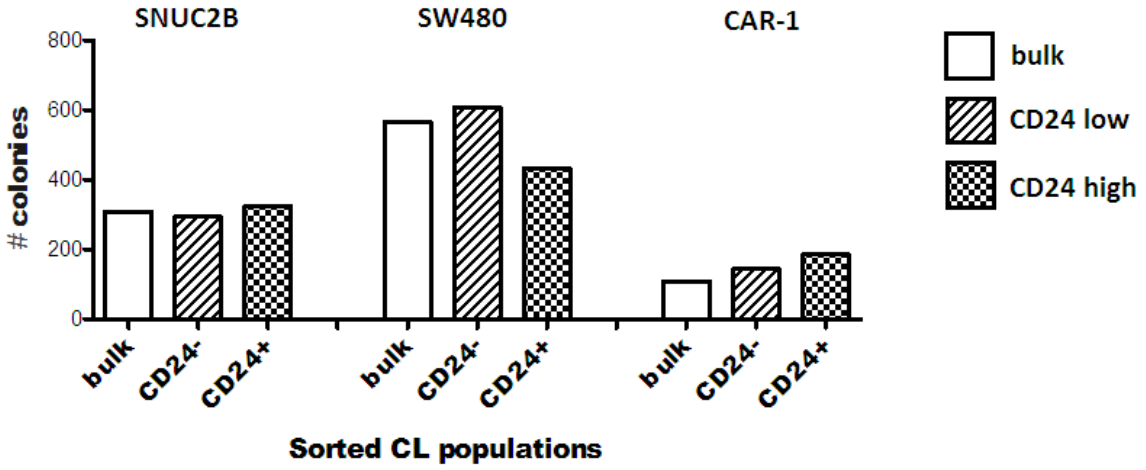

Figure S 4: Colony forming ability of CD24-sorted cell-line-subpopulations.
No striking changes in clonogenicity can be observed after sorting 3 cell lines into CD24 high, low and bulk populations and culturing them in medium with 10% FBS. The combination therapy sensitive cell line CAR-1 displays lower clonogenicity than the 2 combination therapy resistant cell lines.

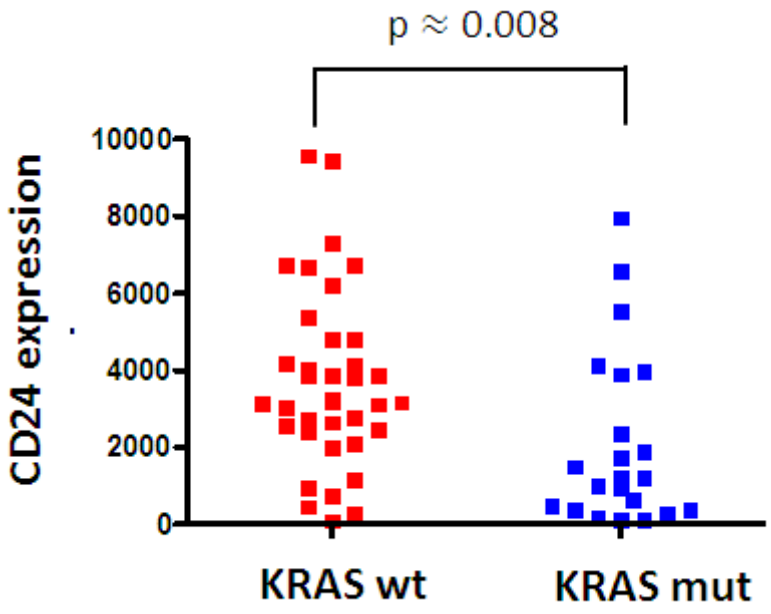

Figure S 5: CD24 expression is decreased in *KRAS* mutant cell lines.
A 2.7-fold higher CD24 expression can be observed among *KRAS* wild type cell lines in the cell line panel as compared to *KRAS* mutant cell lines (p = 0.008).

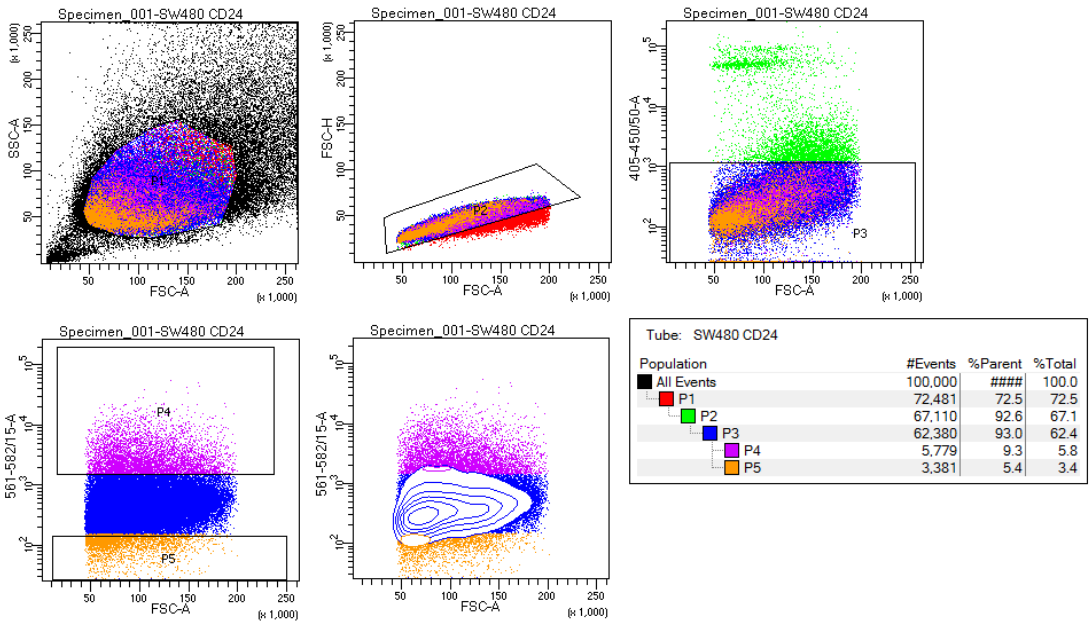

Figure S 6: FACS sorting characteristics of SW480 for CD24.
The ~10% of cells with the highest (P4) and lowest (P5) CD24 expression, respectively, were sorted for further analysis as well as the remaining viable cells (remaining P3).

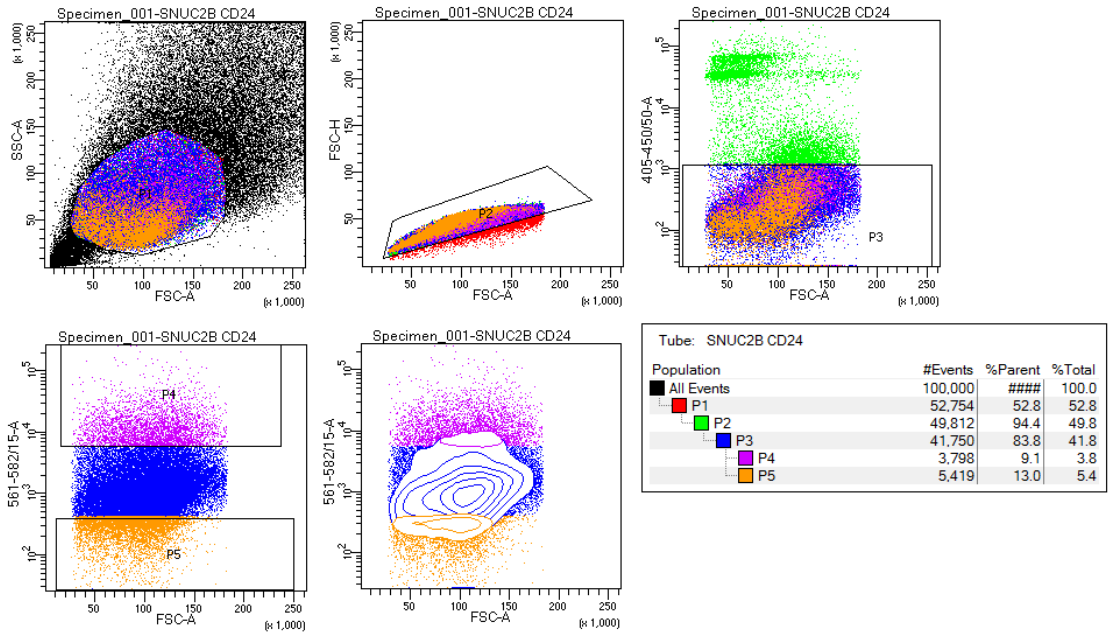

Figure S 7: FACS sorting characteristics of SNUC2B for CD24.
The ~10% of cells with the highest (P4) and lowest (P5) CD24 expression, respectively, were sorted for further analysis as well as the remaining viable cells (remaining P3).

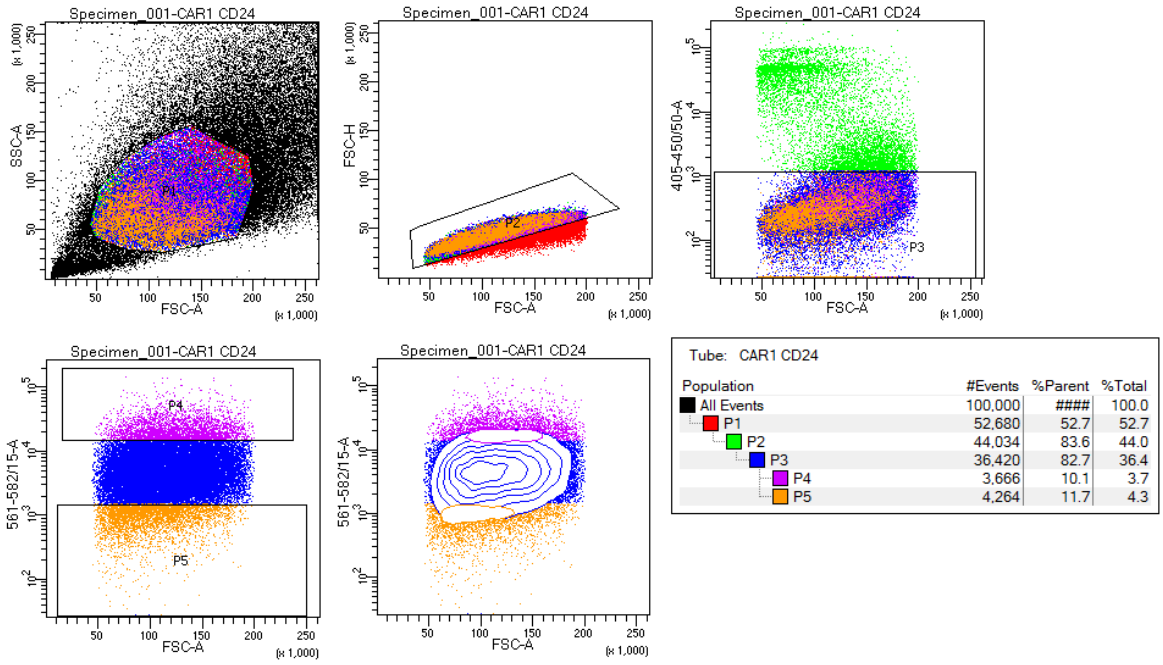

Figure S 8: FACS sorting characteristics of CAR-1 for CD24.
The ~10% of cells with the highest (P4) and lowest (P5) CD24 expression, respectively, were sorted for further analysis as well as the remaining viable cells (remaining P3).

Supplementary Tables

Table S 1: *APC* mutation and sensitivity to IGF1R inhibition.
Classification of cell lines according to anti-IGF-1R sensitivity and correlation to *APC* mutation status reveals a non-significant correlation between anti-IGF-1R resistance and *APC* mutation (p = 0.204).

APC mutation and anti-IGF-1R sensitivity			
	anti-IGF-1R response		
p = 0.204	sensitive	partially responsive	resistant
APC			
wild type	3	9	5
mutant	11	22	6

Table S 2: RER status and sensitivity to IGF1R inhibition.
Classification of cell lines according to anti-IGF-1R sensitivity and correlation to RER status reveals a non-significant correlation between anti-IGF-1R resistance and RER status (p = 0.154).

RER status and anti-IGF-1R sensitivity			
	anti-IGF-1R response		
p = 0.154	sensitive	partially responsive	resistant
RER status			
positive	12	16	2
negative	5	9	4

Table S 3: *FBXW7* mutation and sensitivity to IGF1R inhibition.
Classification of cell lines according to anti-IGF-1R sensitivity and correlation to *FBXW7* mutation status reveals a non-significant correlation between anti-IGF-1R resistance and *FBXW7* mutation ($p = 0.639$).

FBXW7 mutation and anti-IGF-1R sensitivity			
	anti-IGF-1R response		
p = 0.639	sensitive	partially responsive	resistant
FBXW7			
wild-type	15	29	7
mutant	1	2	1

Table S 4: *BRAF* mutation and sensitivity to IGF1R inhibition.
Classification of cell lines according to anti-IGF-1R sensitivity and correlation to *BRAF* mutation status reveals a non-significant correlation between anti-IGF-1R resistance and *BRAF* mutation ($p = 0.568$).

BRAF mutation and anti-IGF-1R sensitivity			
	anti-IGF-1R response		
p = 0.568	sensitive	partially responsive	resistant
BRAF			
wild type	14	33	10
mutant	4	4	2

Table S 5: *KRAS* mutation and sensitivity to IGF1R inhibition.
Classification of cell lines according to anti-IGF-1R sensitivity and correlation to *KRAS* mutation status reveals a non-significant correlation between anti-IGF-1R resistance and *KRAS* mutation ($p = 0.339$).

KRAS mutation and anti-IGF-1R sensitivity			
	anti-IGF-1R response		
p = 0.339	sensitive	partially responsive	resistant
KRAS			
wild type	12	21	7
mutant	5	14	6

Table S 6: β-catenin mutation and sensitivity to IGF1R inhibition.
Classification of cell lines according to anti-IGF-1R sensitivity and correlation to β-catenin mutation status reveals a non-significant correlation between anti-IGF-1R resistance and β-catenin mutation ($p = 0.639$).

β-catenin mutation and anti-IGF-1R sensitivity			
	anti-IGF-1R response		
p = 0.639	sensitive	partially responsive	resistant
β-catenin			
wild type	15	29	7
mutant	1	2	1

Table S 7: *TP53* mutation and sensitivity to IGF1R inhibition.
Classification of cell lines according to anti-IGF-1R sensitivity and correlation to *TP53* mutation status reveals a non-significant correlation between anti-IGF-1R resistance and *APC* mutation (p = 0.364).

P53 mutation and anti-IGF-1R sensitivity			
	anti-IGF-1R response		
p = 0.364	sensitive	partially responsive	resistant
P53			
wild type	4	5	5
mutant	14	31	8

Table S 8: List of genes-of-interest for correlation analysis with cell line characteristics.

Gene symbol	Gene name
AKT1	v-akt murine thymoma viral oncogene homolog 1
AKT2	V-akt murine thymoma viral oncogene homolog 2
AKT3	v-akt murine thymoma viral oncogene homolog 3 (protein kinase B, gamma)
ALDH1A1	aldehyde dehydrogenase 1 family, member A1
BAD	BCL2-associated agonist of cell death
BCL2L11	BCL2-like 11 (apoptosis facilitator)
CD24	CD24 molecule
CD44	CD44 molecule (Indian blood group)
CTGF	connective tissue growth factor
DVL3	dishevelled, dsh homolog 3 (Drosophila)
EGFR	epidermal growth factor receptor
GRB2	growth factor receptor-bound protein 2
IGF1	insulin-like growth factor 1 (somatomedin C)
IGF1R	insulin-like growth factor 1 receptor
IGF2	insulin-like growth factor 2 (somatomedin A) /// INS-IGF2 readthrough transcript
IGF2BP3	insulin-like growth factor 2 mRNA binding protein 3
IGF2R	insulin-like growth factor 2 receptor
IGFBP1	insulin-like growth factor binding protein 1
IGFBP2	insulin-like growth factor binding protein 2
IGFBP3	insulin-like growth factor binding protein 3
IGFBP4	insulin-like growth factor binding protein 4
IGFBP5	insulin-like growth factor binding protein 5
IGFBP6	insulin-like growth factor binding protein 6

Gene symbol	Gene name
IGFBP7	insulin-like growth factor binding protein 7
INSR	insulin receptor
IRS1	insulin receptor substrate 1
IRS2	insulin receptor substrate 2
KRAS	v-Ki-ras2 Kirsten rat sarcoma viral oncogene homolog
MAP2K1	mitogen-activated protein kinase kinase 1
MAP2K6	mitogen-activated protein kinase kinase 6
MAPK1	mitogen-activated protein kinase 1
MT2A	metallothionein 2A
MTOR	mechanistic target of rapamycin (serine/threonine kinase)
NFKB2	nuclear factor of kappa light polypeptide gene enhancer in B-cells 2
PDCD4	programmed cell death 4 (neoplastic transformation inhibitor)
PDPK1	3-phosphoinositide dependent protein kinase-1
PTEN	phosphatase and tensin homolog
RPS6KB1	ribosomal protein S6 kinase, 70kDa, polypeptide 1
SHC1	SHC (Src homology 2 domain containing) transforming protein 1
SLP1	secretory leukocyte peptidase inhibitor
SOS1	son of sevenless homolog 1 (Drosophila)